GHENT UNIVERSITY,
FACULTY OF PHARMACEUTICAL SCIENCES

SARATOV STATE UNIVERSITY,
CHEMISTRY INSTITUTE

DEVELOPMENT AND FUNCTIONALIZATION OF QUANTUM DOTS AS LUMINESCENT LABELS TOWARDS MYCOTOXIN DETECTION

Valentina Goftman, M. Sc.

2016

Thesis submitted in fulfillment of the requirements for the degree of

Doctor in Pharmaceutical Sciences

Please refer to this work as follows

Valentina Goftman (2016) Development and functionalization of quantum dots as luminescent labels towards mycotoxin detection. Thesis submitted in the fulfillment of the requirements for the degree of Doctor in Pharmaceutical Sciences, Ghent University.

Financial support

The research leading to these results has received funding from the Special Research Fund, Ghent University (Joint PhD programme), project № 01SF3012.

Members of the Jury

MEMBERS OF THE JURY

Promoter

Prof. Dr. Sarah De Saeger
Faculty of Pharmaceutical Sciences, Department of Bioanalysis , Ghent University, Belgium

Promoter

Prof. Dr. Irina Yu. Goryacheva
Chemistry Institute, Department of General and Inorganic Chemistry, Saratov State University, Russia

Promoter

Prof. Dr. ir. Zeger Hens
Faculty of Science, Department of Inorganic and Physical Chemistry, Ghent University, Belgium

Examination (reading) committee

Prof. Dr. Katrien Remaut (chair)
Faculty of Pharmaceutical Sciences, Department of Pharmaceutics, Ghent University, Belgium

Prof. Dr. Kevin Braeckmans (secretary)
Faculty of Pharmaceutical Sciences, Department of Pharmaceutics, Ghent University, Belgium

Prof. Dr. Laura Anfossi
Faculty of Sciences, Department of Analytical Chemistry, University of Turin, Italy

Prof. Dr. Andre Skirtach
Faculty of Bioscience Engineering, Department Molecular Biotechnology, Ghent University, Belgium

Dr. Mickael Tessier
Faculty of Science, Department of Inorganic and Physical Chemistry, Ghent University, Belgium

ACKNOWLEDGEMENTS

ACKNOWLEDGEMENTS

First of all, I would like to express my gratitude to my supervisors for helping me to implement my project in reality. I am very grateful to Prof. Irina Goryacheva for her endless support and positive way of thinking. 7 years ago she believed in me and my ability to do research, and then she opened countless possibilities in front of me. She taught me to analyse experimental data, to write scientific articles and projects, to take responsibilities and many other not only technical things. Thanks to Prof. Sarah De Saeger, I got the opportunity to apply for such an interesting Joint PhD program, to carry out my research study in her laboratory and overall to learn about food analysis. I am thankful to Prof. Zeger Hens for allowing me to work with the best QD-minds in his laboratory.

My PhD would not have been done without my colleagues, older and younger, with whom I have been working closely during the past 4 years. Especially, I would like to thank Dr. Elena Speranskaya for being so smart and funny in general, and interested in QDs in particular, that at some point it became contagious. Separately, I want to thank Dr. Tangi Aubert: you showed me what it is to be a bright and passionate scientist. Dr. Natalia Beloglazova, thank you for sharing your valuable experience in immunoassay.

Mijn Belgische collega's, dankjewel voor de vriendelijke attitude en ondersteuning. Jullie maakten elke dag heel interessant voor mij, omdat jullie me de echte Belgische mentaliteit toonden. Speciale dank ook aan *Esthrid*, want jullie beiden creëren een unieke atmosfeer in ons lab.

International part of the Laboratory of Food Analysis (Cynthia, Melody, Kinga, Somar, Karl, Natasha), thank you for all funny moments we shared and for your wise advices regarding survival in Belgium.

Young generation in Saratov State University, I will never forget those hours we spent together in the lab №15. We managed to deal with all challenges! I believe you will lead our laboratory to the new scientific level! Success!

I would like to thank all people from different institutes in Saratov and Gent, who helped me to perform and interpret my measurements on the very progressive equipment.

Last 4 years there were many friends around me. Thank you for the time that we have spent together outside my working hours. It was a great fun and sometimes a necessity! I am very lucky that my Gent's friends were nearby me these years. Dasha, Pieter and Alisa, visiting you always gives me positive "home" feelings. Kolya, you are the only one! I'm grateful to the Universe that I'm honoured to be your friend. I wish to save our friendship till the end of time!

I cannot imagine my life and my PhD without my family. Mama and papa, Zhenya and Katya, Dasha and babushka, thank you for sincere interest to my work, for outspoken support, for your witty feedback, and for letting me rehearse my presentations in front of you. I know, it was quite a challenge! Separately, thanks for the support you are giving me when I am in Belgium. Thank you that you are always waiting for me, ready to hear my endless stories and to tell yours. I love you all and I wish you happiness!

My beloved prof. dr. ir. Dries, accept my profound gratitude. Your input in my PhD is priceless. Your encouragement helped me to survive (figuratively and literately) on the scientific battle field. With you on my side I can accomplish much more than PhD. And together we can achieve everything we have ever dreamed of!

Valentina Goftman

August 2016

TABLE OF CONTENTS

TABLE OF CONTENTS

ACKNOWLEDGEMENTS

Table of Contents **i**

List of abbreviations **v**

Introduction and Objectives of the dissertation **1**

Part 1. Scientific Background **9**

Chapter 1. Background on Quantum Dots *11*
1.1. Quantum Confinement 11
1.2. Optical Properties of Quantum Dots 13
1.3. Structure of Quantum Dots 16
1.4. Synthesis of CdSe Quantum Dots 17
1.5. Core-Shell Quantum Dots Synthesis 21

Chapter 2. Overview of Hydrophilization Techniques *23*
2.1. General Approaches 23
2.2. Nanostructures Multiloaded with Quantum Dots 28

Chapter 3. Quantum Dots for Mycotoxin Detection *35*

Part 2. Development Of Sensitive Luminescent Labels Based On Quantum Dots **40**

Chapter 4. Synthesis, Modification, Bioconjugation of Silica Coated Quantum Dots *43*
Abstract 43
4.1. Introduction 44
4.2. Experiments 45
4.3. Results and discussion 50
4.4. Conclusions 56

Chapter 5. Multicolored Silica Coated Cdse Core/Shell Quantum Dots *57*
Abstract 57
5.1. Introduction 57
5.2. Experimental section 58
5.3. Results and Discussion 60
5.4. Conclusions 64

Chapter 6. Stability of Polymer-Coated Quantum Dots After Lyophilization *65*
Abstract 65
6.1. Introduction 65
6.2. Experimental Section 66
6.3. Results and Discussions 68
6.4. Conclusions 71

Chapter 7. Hydrophilic Quantum Dots Stability Against an External Low-Strength Electric Field *73*
Abstract 73
7.1. Introduction 74
7.2. Experiments 75
7.3. Results and Discussion 77
7.4. Conclusion 80

Chapter 8. Application of Synthesized Luminescent Biolabels For mycotoxin detection *81*
8.1. introduction 81
8.2. Experiments 83
8.3. Results and discussion 86
8.4. Conclusions 91

Part 3. Conclusions and Future Research **72**

Chapter 9. Final Discussion and General Conclusions *95*

Chapter 10. Broader International Context and Future Research *99*

REFERENCES **94**

SUMMARY **104**

SAMENVATTING **124**

ABOUT THE AUTHOR **132**

List of figures **142**

List of tables **146**

LIST OF ABBREVIATIONS

LIST OF ABBREVIATION

APTES	3-Aminopropyl-triethoxysilane
BSA	Bovine Serum Albumin
CEST	Carboxyethylsilanetriol, sodium salt (25%)
CNT	Carbon Nano Tubes
DHLA	Dihydrolopioc Acid
DMF	Dimethylformamide
DON	Deoxynivalenol
EDC	1-Ethyl-3-(3-dimethylaminopropyl)carbodiimide
EF	Electric Field
E_g	Band Gap energy
ELISA	Enzyme-Linked Immunosorbent Assay
FLISA	Fluorescence-Linked Immunosorbent Assay
FRET	Fluorescence Resonance Energy Transfer
FWHM	Full Width At Half-Maximum
GOPTES	(3-Glycidyloxypropyl)trimethoxysilane
IC_{50}	Half Maximal Inhibitory Concentration
IgG	Immunoglobulins G
LBL	Layer by Layer technology
LC	Liquid Chromatography
LC-MS/MS	Liquid chromatography-tandem mass spectrometry
LOD	Limit of Detection
MES	Morpholinoethanesulfonic acid
MPA	Mercaptopropionic Acid
MPEGTMS	[Methoxy(polyethyleneoxy)$_{6\text{-}9}$propyl]trimethoxysilane
NHS	N-hydroxysuccinimide
NP	Nanoparticles
OA	Oleic Acid
ODE	Octadecene
OLA	Oleylamine
OVA	Albumin From Chicken Egg White

PAMAM	Polyamidoamine
PBS	Phosphate Buffer Saline
PEG	Polyethylene Glycol
PL	Photoluminescence
PMAO	Poly(maleic anhydride-alt-1-octadecene)
QD	Quantum Dots
QY	Quantum Yield
SILAR	Successive Ion Layer Adsorption and Reaction
SLN	Sentinel Lymph Node
sNHS	N-hydroxysulfosuccinimide sodium salt
SPDP	N-hydroxysuccinimide ester
Sulfo-SMCC	3-SulfoN-hydroxysuccinimide ester sodium salt
TEM	Transmission Electron Microscopy
TEOS	Tetraethoxysilane
TOP	Trioctylphosphine
ZB	Zincblende
ZP	Zeta-potential

INTRODUCTION AND OBJECTIVES OF THE DISSERTATION

INTRODUCTION AND OBJECTIVES OF THE DISSERTATION

Today, a highly contaminated environment demands analytical methods with low limits of detection of different target molecules for multiplexed environmental monitoring and food quality control. In this regard, photoluminescence (PL) sensing offers possible sensitivity down to the single-molecule level.

Reliability, reproducibility and sensitivity of these methods are strongly dependent on the quality of the label used in the analysis. A suitable PL label (i) is conveniently excitable, (ii) is bright and photostable, (iii) is soluble and stable in physiological conditions, (iv) contains functional groups for conjugation, (v) has a low toxic effect on living cells and tissues, (vi) possesses appropriate steric and size-related properties and (vii) is available in a reproducible quality (Resch-Genger et al., 2008). Photoluminescent (PL) quantum dots (QDs) meet most of these mentioned requirements.

QDs have been found as exceptionally sensitive PL labels for human's life quality control, including food analysis. Nutrition plays a key role in human health and well-being, starting from embryonic development and continuing the whole life. It is not only important to balance the diet, but also to control bacterial and toxicant contamination of food and feed. For example, mycotoxins – i.e. secondary metabolites, produced by fungi – form a global problem as they are present in more than 25% of the worldwide crop (CAST, 2003) and they cause highly toxic effects on humans (Peraica et al., 1999). This necessitates strict regulations of mycotoxins in different matrices. A conventional analytical method of mycotoxin determination is chromatography, in particular high-performance liquid chromatography (LC) and gas chromatography with different detectors. Nonetheless, screening immunochemical methods, which are cost-effective, straightforward to perform and not laboratory-based, have also become very popular.

The most relevant screening immunochemical methods for mycotoxin analysis are enzyme linked immunosorbent assay (ELISA), immunochromatographic tests, also called lateral flow

test or strip test, dipstick tests, flow-through tests, tandem column tests. The non-instrumental estimation of results is based on visual evaluation. Therefore, different structures are used as visual labels, such as enzymes for catalytic enzymatic reactions of colored substrates, colloidal gold and luminescent labels. Enzymes are traditional labels for such methods. In this regards, fast immunochemical on-site test for T2 and HT2 toxins screening was developed in our group, using horseradish peroxidase enzyme and tetramethylbenzidine-based substrate (Goftman et al., 2012). Disadvantageous feature of enzymatic label is its high sensitivity towards environmental conditions, as well as necessity of using chromogenic substrate, and, consequently, impeded possibility of multiplex analysis, since each enzyme requires a separate substrate.

PL labels for immunoassay are now widely used because they provide high sensitivity and are capable of multiplexing. In some cases, the sensitivity of PL labels is comparable with that of enzymatic labels, but the assay procedure is considerably simpler, as they do not require addition of chromogenic substrate and luminescent signal can be read immediately.

There is a variety of PL chromophores from which to choose: small organic dyes, metal-ligand complexes and lanthanide chelates, fluorescent proteins, nanocrystal chromophores with size-dependent optical and physicochemical properties, which includes QDs, carbon and silicon nanoparticles.

Using organic fluorophores is the most obvious choice, as they are commercially available and emit light in wide range of spectra. However, low photostability appears to be their main limitation for using in immunoassay, since quenching of label during storage or analysis can directly affect sensitivity and reproducibility of the developed method. Moreover, spectral characteristics of organic fluorophores do not allow using them for development of multiplex analytical systems, because narrow absorption spectra require separate excitation source for each dye. These two main disadvantages play crucial role especially in case of on-site test formats of immunoassay.

In this regard, QDs-based labels are considered to be a better alternative compared to the conventionally used organic fluorophores. QDs are PL semiconductor nanocrystals (diameter usually 1-10 nm) with unique optical properties that are determined by the

constituent material, the particle's size and their surface chemistry. Thus, by varying the material of the QDs and their size, it is possible to obtain PL in the ultraviolet (UV), the visible or the infrared (IR) emission ranges. Unlike conventional fluorophores, QDs have a broad absorption spectrum and a narrow symmetric emission peak. These optical characteristics allow exciting QDs with different emission colors using only one energy source, which make them ideal labels for multiplexing. The photostability of QDs is high enough to perform long-term experiments; in the meantime, the high extinction coefficient and PL quantum yield (QY) enable single-molecule tracking.

The quality of the QDs-based label does not only strongly depend on the characteristics of the semiconductor core and shell(s), but also on the surface chemistry of the nanocrystals. First, the better the PL core is isolated and protected from oxidation, the higher the QY. Therefore, it is very important to find a synthesis route that provides not only a narrow particle size distribution and non-defect structure, but also allows covering up the core of the QDs with protective shells of wider band gap semiconductors. Second, water solubility of the QDs, as well as the availability of functional groups, is required. This may be achieved by hydrophilic stabilizing ligands, which appear on the QDs' surface after a hydrophilization step. Thus, not only the semiconductor core-shell structure synthesis approach, but also the way of surface modification plays a crucial role in the QDs' bioapplicability.

The overall aim of this doctoral research is to create bright, stable and sensitive PL labels for immunoassay, based on QDs. Thereto, CdSe based QDs with several CdS/ZnS shells and different emission colors are synthesized. To impart biocompatible properties to the QDs, two different approaches are used: encapsulation with amphiphilic polymers and covering with a silica shell. Both types of obtained labels are carefully characterized and their stability is compared. Further, the modified QDs are efficiently conjugated with antibodies and applied as novel labels in highly sensitive immunoassays for mycotoxin detection.

This thesis comprises of 10 chapters.

Chapters 1, 2 and 3 provide the necessary theoretical background on QDs. In Chapter 1, basic introductory information on QDs synthesis and optical properties is given. A survey of hydrophilization techniques is outlined in Chapter 2, including synthesis of biocompatible

enhanced labels. A review on the application of QDs in immunoassay for mycotoxin detection is presented in Chapter 3.

Chapter 4 details the development of a novel label for immunoassay based on silanized QDs, together with its modification and bioconjugation with antibodies.

Chapter 5 investigates the impact of the QDs' structure (namely, the amount and material of the wider band gap semiconductor shells) on the optical properties of silica coated QDs.

Chapter 6 depicts lyophilization as a convenient technique to improve the long-term stability of polymer-coated QDs.

Chapter 7 describes the stability of hydrophilic QDs, synthesized by two different approaches (encapsulation into amphiphilic polymers and covering with a silica shell), against an external low-strength electric field.

Chapter 8 discusses the application of the synthesized PL biolabels in immunoassay for the determination of mycotoxin deoxynivalenol in cereal samples.

Chapter 9 summarizes the work by providing a general discussion and conclusions, and Chapter 10 extends the possibilities for future research and describes international context of this research.

PART 1. SCIENTIFIC BACKGROUND

CHAPTER 1. BACKGROUND ON QUANTUM DOTS

1.1. QUANTUM CONFINEMENT

It is well–known that all crystalline inorganic solids can be divided into three classes: metals, insulators and semiconductors (Figure 1.1). The presence of a band gap with a certain energy (E_g) between valence and conduction bands determines their resistance. In bulk semiconductor materials, only a small percentage of electrons occupy the conduction band and the most of them are in the valence band. A sufficient amount of energy is needed for an electron to jump from the valence band to the conduction band.

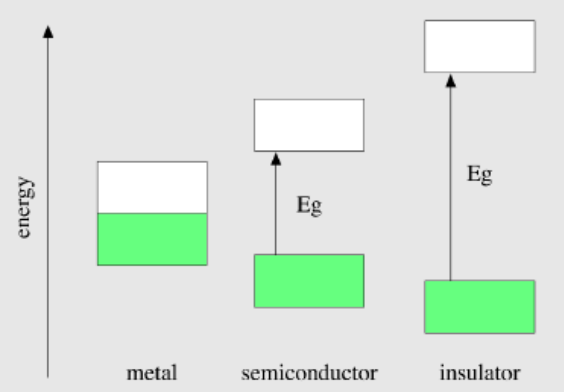

Figure 1.1. A simplified energy level diagram for metals, semiconductors and insulators. The green boxes represent the filled valence bands; the white boxes represent the empty (at 0 K) conduction bands. The arrows represent the band gap energy (Eg). Reprinted from (Murphy and Coffer, 2002)

Consider what happens when a bulk semiconductor is excited with an energy exceeded its band gap. Then, an electron will be promoted from the valence band to the conduction band, leaving a positively charged ‘‘hole’’ behind. The pair of an electron and a hole is called an exciton and the distance between them is termed as exciton Bohr radius. The exciton Bohr radius is a unique qualitative characteristic of each semiconductor. Mostly its value lies between 1 and 10 nm. But let us consider what happens when we are not dealing with bulk semiconductors, but when the size of the semiconductor fragment (particle), that is excited, is smaller than the exciton Bohr radius.

In this size range, when the exciton is created, the physical dimensions of the particle confine the exciton in a manner that is similar to the particle-in-a-box model of physical chemistry. Therefore, quantum effects, such as quantization of energy levels, are observed. These atomic-like energy levels of a QD can be visualized by means of the absorption spectrum (Figure 1.2). The first absorption peak – exciton peak - corresponds to the transition between the ground state and the lowest excited electron state. Upon irradiation, the electron is excited, leaving a hole in the valence band. Then, the electron relaxes back down to the valence band, recombines with the hole and emits a photon. Depending on the excitation energy, the electron can be excited to the lowest or to a higher state. Thus, a QD can be excited with energies higher than its first absorption peak.

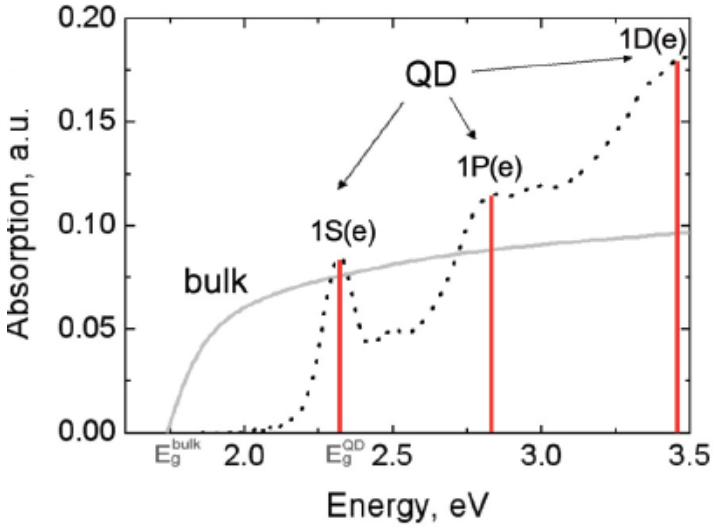

*Figure 1.2. Absorption spectrum of CdSe QDs: a schematic representation of discrete atomic-like energy levels of a QD (in red) and ensemble spectrum measured with a UV-Vis spectrometer (dotted line) in comparison with the continuous spectrum of bulk CdSe (E^{bulk}_g = 1.74 eV). Reprinted from (*Breus 2008)

Conversion between different excited electron states occurs extremely fast, i.e. within hundreds of femtoseconds. Therefore, although several peaks in the absorption spectrum exist, QD's emission peak is extremely narrow and its maximum wavelength is independent of the excitation wavelength (Breus 2008).

Another important consequence of the above described quantum confinement is that the band gap energy value is correlated with the particle size. In a smaller QD, the exciton is

confined to a smaller size, which increases the energy needed for the first excitonic transition and, hence, it results in higher absorption and emission energies. Thus, the smaller the size of the nanocrystal, the smaller the wavelength it emits. To describe this correlation, Brus has developed a popular effective mass model that relates particle size to the bandgap energy of a semiconductor QD (Brus 1986):

$$\boldsymbol{E_g}\,(\mathrm{QD}) = \boldsymbol{E_g}(\mathrm{bulk}) + (h^2/8R^2)(1/m_e + 1/m_h) - 1.8e^2/4\pi\varepsilon_0\varepsilon R,$$

where E_g is the bandgap energy of the QD or bulk solid, h is Plank's constant, R is the QD radius, m_e and m_h are the effective mass of the electron and the hole in the solid, and ε is the dielectric constant of the solid. For example, bulk CdSe has a band gap energy of 1.76 eV and a Bohr exciton diameter of 9.6 nm, whereas the band gap energy of 2–7 nm CdSe nanocrystals varies from 2.8 eV to 1.9 eV, with emission shifting between 450 and 650 nm (Petryayeva et al., 2013).

Consequently, the emission color of QDs PL does not merely depend on semiconductor material (Figure 1.3), but also on the size of the nanocrystals. This fact allows covering a large range of wavelengths (including visual and IR) by using QDs made from different semiconductors and by varying their size.

Although often depicted as spheres in most illustrations, QDs are crystalline materials with facets and a lattice structure analogous to the bulk semiconductor material. Depending on its size, each nanocrystal comprises hundreds to thousands of atoms, a large fraction (>10%) of which are located at the nanocrystal surface, as such exhibiting a high surface area-to-volume ratio.

1.2. OPTICAL PROPERTIES OF QUANTUM DOTS

Owing to the quantum confinement effect, QDs possess a number of very specific optical properties. Surely, the size-depending PL appears to be one of the most distinctive features. Further, the emission spectra of QDs are slightly shifted to longer wavelengths than the

exciton absorption peak, such that an effective Stokes shift is achieved. The broad absorption spectra and the very narrow (full width at half-maximum (FWHM) of ~ 30 nm) symmetric (Gaussian profile) emission peaks make QDs a very attractive instrument for multicolor imaging, using one excitation source. Also, owing to the exciton confinement and the inorganic crystalline structure, a superior resistance to photobleaching and chemical degradation is typical for QDs and their conjugates as illustrated in Figure 1.4.

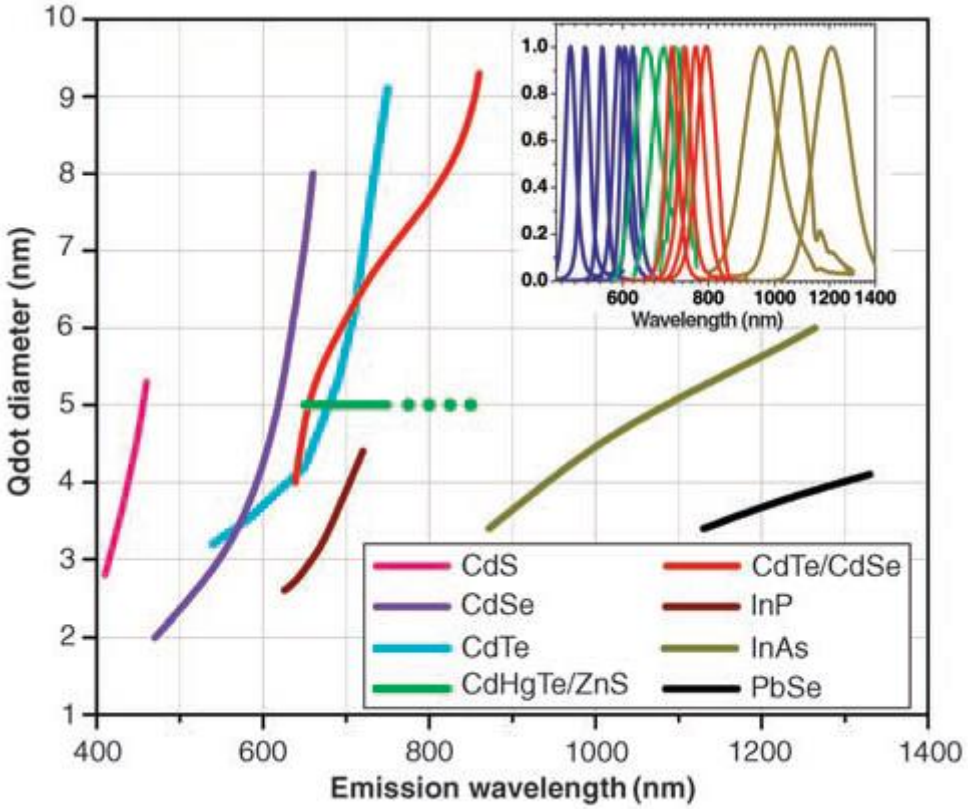

Figure 1.3. Dependence of emission maxima on the material and size of QDs. Reprinted from (Michalet et al., 2005)

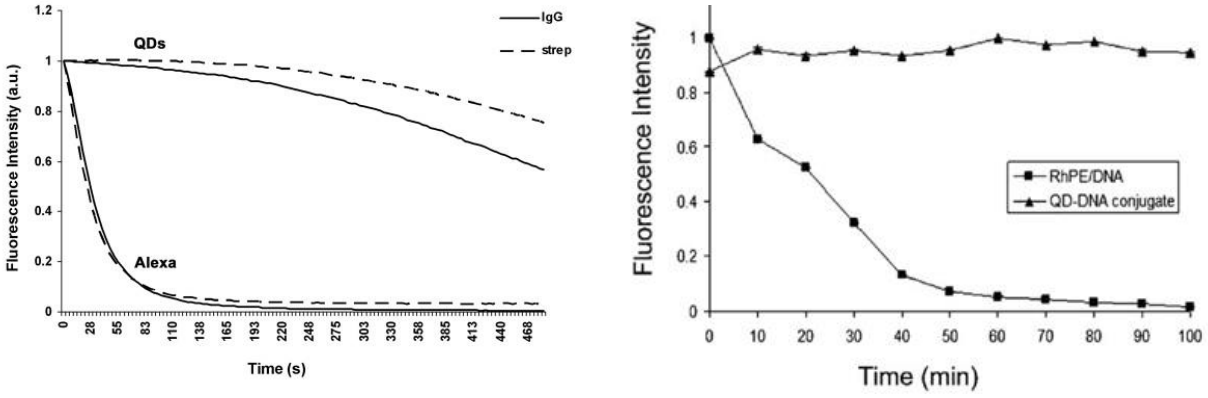

Figure 1.4. *Photostability profile of PL intensity changes of (A): QDs conjugates with immunoglobulins G (IgG) and streptavidin versus organic Alexa Fluor 594 conjugates (Monton et al., 2009), (B): QDs, conjugated with DNA, versus organic Rhodamine-DNA conjugates (Srinivasan et al., 2006) under laser radiation*

Although, conventionally used organic dyes in average possess a higher QY (~ 90%), whereas QDs' QY normally ranges between 30 and 60%, QY up to 90% has been reported for CdSe/CdS QDs (Chen et al., 2013). Moreoever, the extinction coefficient of QDs (10^6 M^{-1}/cm^{-1}) and their two-photon absorption cross-section (10^3 – 10^4 GM) are an order of magnitude higher, which makes QDs up to 20 times brighter than organic fluorophores. Together with their high photostability, it allows performing long-term (up to a few hours) imaging and tracking of single molecules in living organisms and tissues with confocal microscopy, total internal reflection microscopy, or basic wide-field epifluorescence microscopy (Friedrich et al., 2009; Michalet et al., 2005).

QDs exhibit longer radiative lifetimes ($\tau_R \sim 10$ ns), relative to the bulk exciton recombination time (τ_R of 1 ns) (Nirmal et al., 1995). Compared to organic dyes, it is significantly higher (Resch-Genger et al., 2008). This fact allows time-gated detection, where their signal can be distinguished from the background, owing to the fact that auto fluorescence usually has much shorter lifetime (Zhang 2011).

The surface of QDs is receptive to the further modification, as such tailoring the QD's composition and imparting it with desirable properties, i.e. water-solubility. This, together with the QD's size which is comparable to the protein size, significantly simplifies a bioconjugation process and opens an avenue for future perspectives.

1.3. STRUCTURE OF QUANTUM DOTS

Despite the great diversity of semiconductor materials that may be used for production of QDs, CdSe is the undeniable "flagship". Partly, this is due to its bandgap energies. In bulk and at room temperature, the E_g for CdSe is 1.7 eV (corresponds to ~ 720 nm). Thus, QDs made of this material have an E_g in the visible range and the corresponding onset of PL is readily visualized and monitored with standard equipment and naked eye. Another explanation of the popularity of CdSe is the availability of precursors and ease of the semiconductor's crystallization (Murphy and Coffer, 2002). Nowadays, efficient synthesis protocols are accessible to the general scientific public, together with commercially available high-quality CdSe-based QDs.

Although CdSe QDs are highly ordered crystalline systems, the lattice structure of the nanocrystal abruptly terminates at its surface, yielding localized ''trap'' states within the quantum confined band gap (Petryayeva et al., 2013). These states encourage non-radiative pathways for recombination of the exciton. Therefore, to improve emission efficiency, the core nanocrystal should be coated with a few layers of a structurally similar semiconductor with a higher band gap energy. The most popular shells for CdSe QDs are ZnS and CdS, as presented in Figure 1.5.

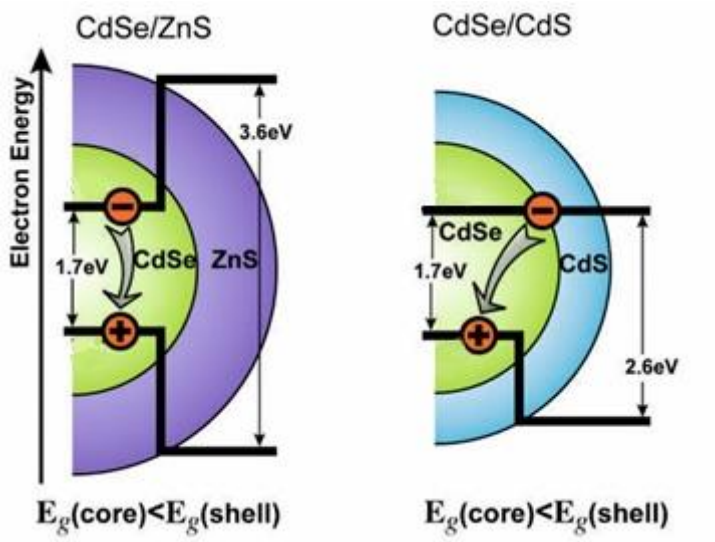

*Figure 1.5. Two possible core-shell structures of CdSe-based QDs.E_g isbandgap energy. Reprinted from (*Petryayeva et al., 2013)

Basically, the purpose of adding a wider band gap semiconductor shell is to offer the best confinement of the exciton inside the core. Using a ZnS shell (E_g = 3.6 eV) yields a complete

confinement, although the shell growing is typically accompanied by a 5-10 nm red-shift of the emission maximum. Nevertheless, the ZnS shell increases the QY of CdSe QDs about 10 times (Hines and Guyot-Sionnest, 1996).

Using semiconductors with intermediate values of band gaps, like CdS (E_g = 2.4 eV) allows the electron to be delocalized over the whole nanocrystal but the hole is confined to the core. Since this process shifts the energy bands, it is not only easy to improve the PL properties, but also to vary the emission maximum.

It is important to remember that a 12% lattice mismatch between CdSe and ZnS exists. This limits the growth of ZnS to a few atomic layers as otherwise lattice strain will detrimentally degrade the PL properties (Rosenthal et al., 2011). Effective approaches for growing thicker shells and relaxing lattice mismatch have been reported, including incorporating a small amount of Cd into the shell material and synthesizing gradient or multi-shell structures (e.g., CdSe/ CdS/ZnS) (Xie et al., 2005). To improve the PL and as an alternative to size-tuning, QD core materials can also be alloyed (Jing et al., 2009).

1.4. SYNTHESIS OF CdSe QUANTUM DOTS

Several routes have been used to synthesize QDs, including top-down processing methods, based on grinding of a bulk semiconductor, and bottom-up approaches, where QDs self-assemble in the solution following a chemical reduction (Valizadeh et al., 2012).

Among all physical and chemical pathways of QD preparation, the colloidal chemistry methods are the best routes to synthesize monodisperse nanocrystals with a proper surface functionality providing high PL efficiency and narrow size distribution (Frigerio et al., 2012). It is important to note that only samples with a standard deviations ≤ 5% in diameter are referred to as monodisperse. This corresponds to ± one lattice constant throughout the 1–15 nm size range. Also, QDs must be uniform not only in size and shape, but they must also have well-formed crystalline cores and a controllable surface chemistry (Murray et al., 2000).

The first colloidal synthesis of QDs was reported by Bawendi and coworkers in 1993 (Murray et al., 1993). The production of QDs was carried out by quick injection of Cd and Se precursors into an organic coordination solvent (usually alkylphosphines, alkylphosphine oxides,

alkylamines) at a high temperature (150°C – 350°C). To this day, this very reproducible method is the most popular technique for the synthesis of CdSe nanocrystals. Later on, it has been considerably improved (Talapin et al., 2001; Qu et al., 2001), allowing to use less toxic materials and to reach high QY and a size dispersion of about 5 –10% (Subila et al., 2013).

In the hot injection synthesis, burst nucleation leads to a high degree of supersaturation. This should result in a short nucleation event, which is stopped by the resulting drop of the supersaturation and the temperature. Next, it is assumed that nucleation is followed by a continuous growth at a lower temperature, thereby maintaining the initial sharp size distribution during the growth phase (Figure 1.6). In addition, improvement of initial size distribution is based on the fact that when growth is limited by the diffusion of reagents to the QDs, the increase of the QD radius, r_{QD}, with time drops as $1/r_{QD}$. Since smaller particles grow faster than bigger particles under this condition, the initial particle size distribution narrows during growth (Abe et al., 2012).

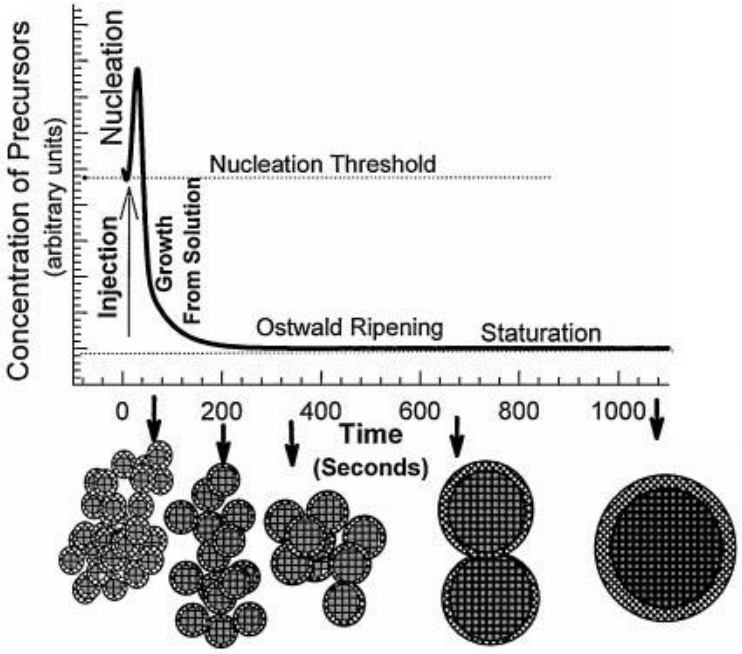

*Figure 1.6. The stages of nucleation and growth for the preparation of monodisperse QDs in the framework of the La Mer model. Reprinted from (*Murray et al., 2000)

As the crystallite grows, the crystalline structure continuously changes to yield the most stable polymorph for a given size, until the lattice energy exceeds the energy difference between the metastable and thermodynamic phases. In case of CdSe, first the zincblende (ZB)

structure appears, and with further growth of the nanocrystals, it converts to wurtzite through a pseudo ZB phase (Figure 1.7) (Washington et al., 2012). These growth phases are dependent on the monomer concentration in the solution, and many parameters, such as temperature, each precursor's initial concentration, solvent composition, etc., can be tuned to achieve the desired structure and size of QDs.

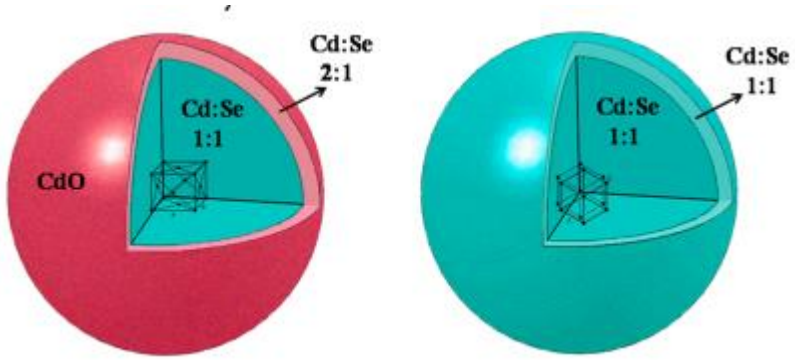

*Figure 1.7. Schematic representation of the elemental distribution in zincblende (A) and wurtzite (B) CdSe QDs based on the X-ray photoelectron spectroscopy analysis. Reprinted from (*Subila et al., 2013)

As all nanoparticles (NPs), QDs have a strong tendency to agglomeration. Stabilizing ligands are not only dealing with this liability during storage, but also playing an important role in QD's synthesis. The labile nature of these ligands is a key requirement, desorbing from the particle surface to allow growth, yet coordinating strongly enough to allow particle isolation and to provide the required protection for the NP. The delicate balance between forming too many nuclei, which results in the defocusing of the size distribution by Ostwald ripening, or too few nuclei, which results in growth that is too fast to reach the required size and distribution, is achieved by simply altering the concentration of the capping agent and thus the amount of metal complex available for the reaction (the monomer concentration) (Green 2014, Huang et al., 2010)

Nowadays, colloidal synthesis of CdSe cores mainly occurs at 150-350^{o}C in octadecene (ODE) under an inert atmosphere, and various coordinating ligands (Figure 1.8) are leverage to enhance the monodispersity of nanocrystals and their QY (De Nolf et al., 2015).

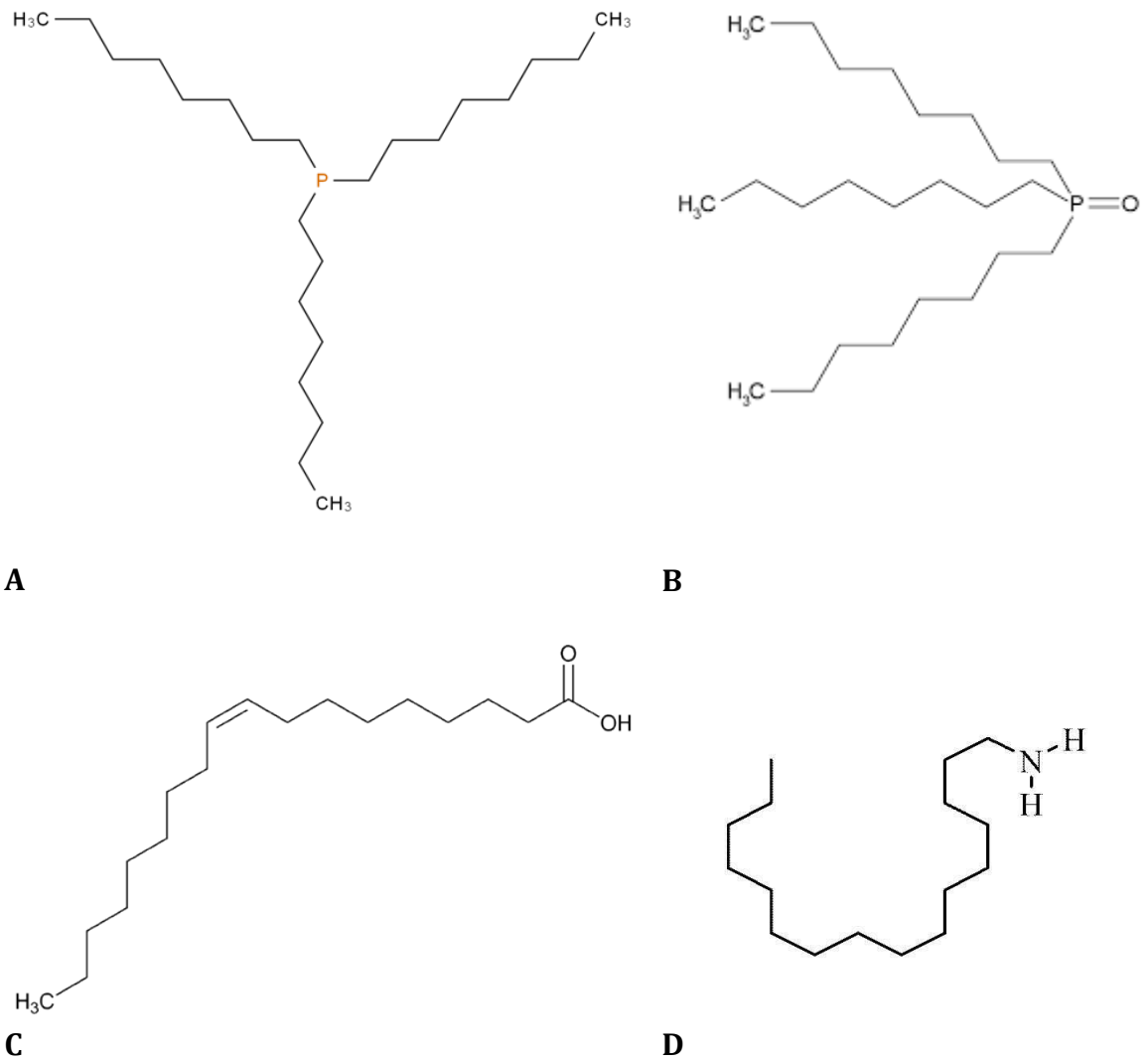

Figure 1.8. The most frequently used coordinating ligands for CdSe core synthesis: A – trioctylphosphine, B – trioctylphosphine oxide, C – oleic acid, D – hexadecylamine

CdSe core synthesis is well-studied and various empirical equations are available, that describe dependence of the size of CdSe nanocrystals for different structural modification on the position of their exciton absorption peak (Capek et al., 2010, Gong et al., 2013). Quite a few techniques exist, that are employed to reveal the size, shape, and internal structures of these nanocrystals. They comprise of transmission electron microscopy (TEM), wavelength dispersive x-ray spectroscopy, x-ray photoelectron spectroscopy, small-angle x-ray scattering, and wide-angle x-ray scattering (Dabbousi et al., 1997).

1.5. CORE-SHELL QUANTUM DOTS SYNTHESIS

As already stated in Section 1.3, to improve emission efficiency it is beneficial to coat the core of QDs with few shells, being semiconductors with a higher E_g. A similar crystalline structure of the shell and the core is a necessary condition, otherwise the shell will not grow uniformly, and the difference in structures could result in defects on the interface. ZnS is considered the best shell for CdSe, because neither the electrons nor the holes leave the CdSe core to the ZnS shell due to the band gap energy (table 1.1). Moreover, ZnS are not prone to form solid solution with CdSe core (Hines and Guyot-Sionnest, 1996), which is also important for keeping the exciton trapped inside the fluorescent core.

Table 1.1. Crystalline structure constants of a number of semiconductors

Semiconductor	**Crystalline lattice type**	**Band gap (E_g), eV**	**Crystalline lattice parameters, nm**
CdSe	wurtzite	1.74	0.43/0.7
CdSe	sphalerite	1.74	0.61
CdS	wurtzite	2.49	0.41/0.67
ZnS	sphalerite	3.61	0.54
ZnS	wurtzite	3.61	0.38

The number of shell monolayers is controlled by the amount of precursors that are added. Although more layers seem to protect the core better, they increase the strain in the nanocrystals due to lattice mismatch. To reduce this strain, a middle shell of CdS can be grown in between the CdSe core and the outer ZnS shell, since the lattice parameters of CdS are closer to that of CdSe than ZnS (table 1.1); such that the ZnS shell grows in a nearly defect free. But in this case, the Successive Ion Layer Adsorption and Reaction (SILAR) method is used to produce such core–shell structures. The method is based on alternating the addition of metal and chalcogenide precursors to the QD solution at high temperatures, as such avoiding nucleation of nanocrystals of the shell material and controlling the number of layers with high accuracy (Li et al., 2003; Jing et al., 2009; Talapin et al., 2004). The shelling process always yields a red shift of the emission maxima and an increase of the PL.

CHAPTER 2. OVERVIEW OF HYDROPHILIZATION TECHNIQUES

2.1. GENERAL APPROACHES

Applications of QDs have evolved tremendously over the last decade, particularly in the areas of bioimaging and bioanalysis. Since the first seminal demonstration of QDs for biological imaging in 1998 (Bruchez et al., 1998), thousands of research articles on QDs synthesis and modification have been published. Researchers have exploited the brightness, photostability, size-dependent optoelectronic properties, and superior multiplexing capability of QDs for a myriad of applications. Some of the more prominent applications include energy transfer–based sensing, cellular and *in vivo* imaging, drug delivery and theranostics (Petryayeva et al., 2013).

The most important requirements for biochemical applicability of QDs are: 1) the surface cap should preserve or even improve the optical properties; 2) the availability as monodisperse and stable aqueous suspensions over a wide range of pH and ionic strength; 3) the presence of functional groups for bioconjugation; 4) protection against chemical/biochemical/physical influences; and 5) a minimal impact from the environment on the QDs' properties and, *vice versa*, a minimal influence of the QDs' components on the environment (Biju et al., 2010). The latter is especially important for *in vivo* applications. In this regard, a lot of attention is paid to the optimization of the capping layer, which can provide all of the above listed properties.

There are two well-known common approaches for making QDs water soluble: ligand exchange, i.e. the substitution of native hydrophobic ligands with hydrophilic ones, and covering with amphiphilic molecules, a technique also known as encapsulation (Figure 2.1). Silica covering is a method that combines the main advantages of the two approaches as it allows maintaining the PL properties of the initial QDs and controlling the size of the NPs.

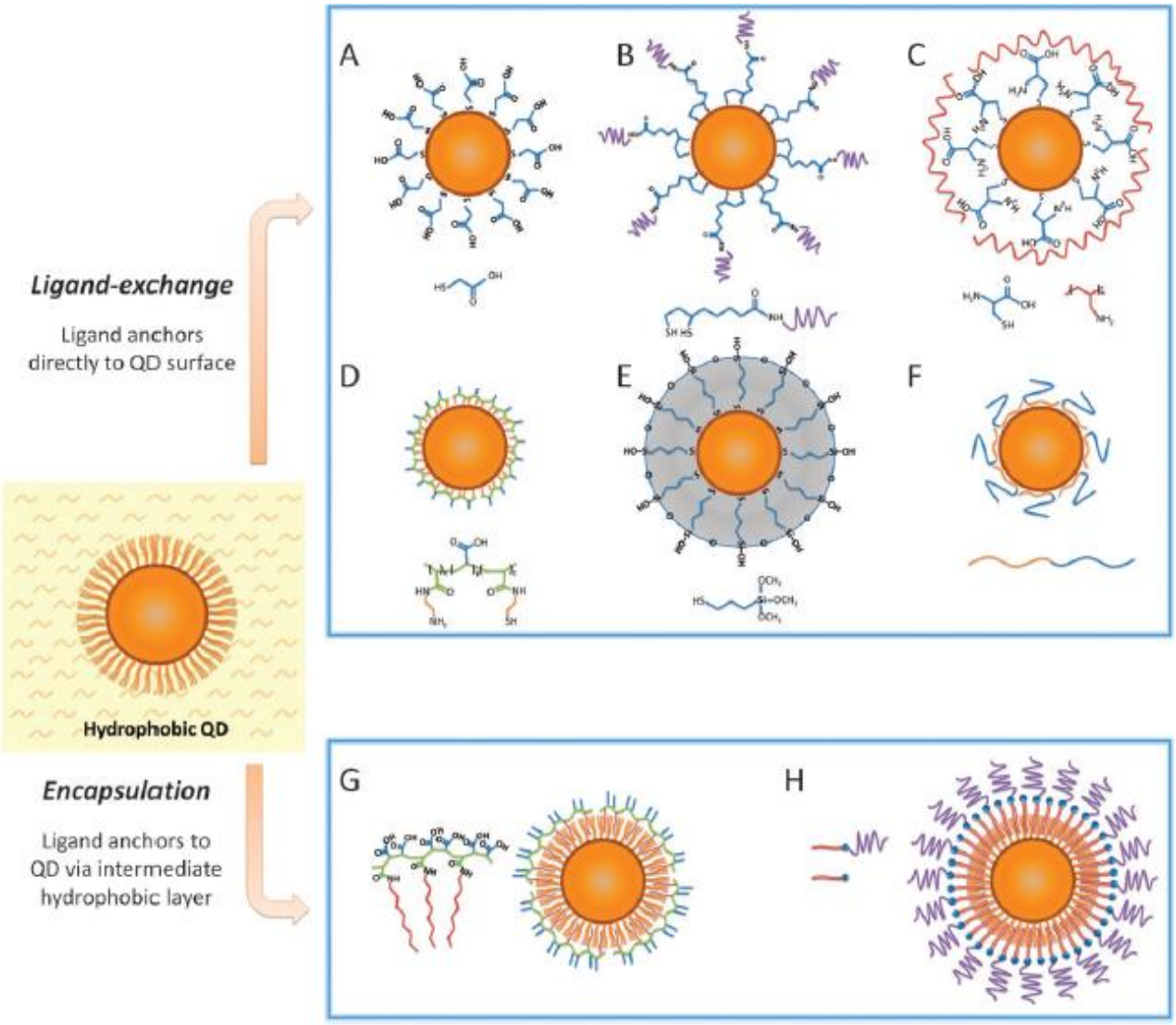

Figure 2.1. Routes for water-solubilization of hydrophobic QDs. Ligand-exchange procedures (A–F) involve replacing the native hydrophobic surface ligands with hydrophilic ones by anchoring ligand directly to the QD surface. (G–H) Encapsulation procedures preserve the native QD surface structure and over-coat QDs with amphiphilic molecules (such as polymers or lipids) via hydrophobic interactions. Reprinted from (Zrazhevskiy et al., 2010)

2.1.1. LIGAND EXCHANGE METHOD

Often, the hydrophobic stabilizing ligands, which appear on the QD's surface during its synthesis, are linked to the surface metal atoms through carboxyl, oxophosphonic, and amino groups. To substitute them, hydrophilic ligands should have a higher affinity to the QD's surface. For example, mercapto-groups exhibit a high affinity to surface zinc ions.

In 1998, Nie's group (Chan and Nie, 1998) developed the first hydrophilic CdSe/ZnS core-shell QDs coated with mercaptoacetic acid. Since then, other monothiol ligands such as mercaptopropionic acid (Mitchell et al., 1999; Kirchner et al., 2005), cystamine (Resch-

Genger et al., 2008), cysteine (Liu et al., 2007) and cysteine residues (Sukhanova et al., 2002) have been used to render QDs water-soluble. However, the long-term colloidal stability of QDs coated with single thiol ligands is still questionable, due to their dynamic off-rate. Therefore, in 2001 Mattoussi et al. developed bidentate thiol ligands, e.g. dihydrolipoic acid (DHLA) which elongated the shelf life to 1-2 years (Jaiswal et al., 2003). Nonetheless, DHLA is not able to preserve the high PL of QDs due to its lower density on the nanocrystal surface. Moreover, the aqueous solubility of DHLA-coated QDs again counts on the deprotonation of the carboxyl group and, hence, the pH stability is still limited to basic media. These problems were partially solved by using polyethylene glycol (PEG) contained DHLA derivatives (Delehanty et al., 2012). Besides DHLA and the modified DHLA, other bidentate thiols such as dithiothreitol (Pathak et al., 2001), carbodithioic acids (Querner et al., 2004), dithiocarbamates (Dubois et al., 2007; Wang et al., 2008) and thiol-modified–cyclodextrin (Palaniappan et al., 2004) have been successfully used as QDs' ligands (Zhang 2011).

On the one hand, one of the major advantages of the ligand exchange method is that water-soluble QDs with small hydrodynamic sizes can be prepared. On the other hand, surface defects caused by ligand exchange often leads to quenching of the PL and to a shift of the emission maxima (Baker and Kamat, 2010), due to oxidative destruction of the crystalline structure (Figure 2.2).

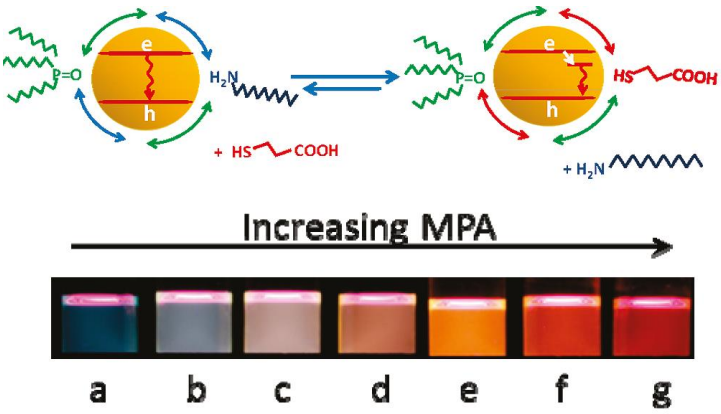

Figure 2.2. Ligand exchange between dodecylamine and 3-mercaptopropionic acid (MPA) leading to detuning of emission (red shift) due to the appearance of trap emission maximum. Reprinted from (Baker and Kamat, 2010)

2.1.2. ENCAPSULATION TECHNIQUE

The encapsulation method uses amphiphilic molecules and allows retaining the original hydrophobic ligands on the QD's surface. The hydrophobic chains of amphiphilic ligands are oriented to the original hydrophobic ligands on the QDs due to hydrophobic interactions, whereas the amphiphilic molecules' hydrophilic fragments remain exposed, as such providing aqueous solubility.

Commonly used amphiphilic ligands include surfactants such as phospholipids and amphiphilic polymers (Wu et al., 2002). The use of amphiphilic polymers is preferred, because a single polymer chain contains multiple hydrophobic units, which lead to strong interaction with the initial organic coating (Yu et al., 2007). It was proven that introduction of PEG chains into amphiphilic molecules results in an improved colloidal stability of QDs over a wide pH range and reduces non-specific binding to biomolecules and carriers (Gao et al., 2004). The first amphiphilic polymers used for QD encapsulation were not commercially available and their modification with PEG chains was time-consuming and laborious. Later on, it was demonstrated that application of available low-cost polyether amine Jeffamine M1000 for modification of maleic anhydride-based polymers allowed obtaining high-quality polymer coatings (Lees et al., 2009; Pichaandi et al., 2014; Speranskaya et al., 2014).

Since encapsulation preserves the hydrophobic ligands on the QD surfaces, the water-soluble QDs maintain the high QYs of the original QDs relatively well after encapsulation. However, overcoating the initial hydrophobic ligands with polymeric material results in large hydrodynamic diameters (Delehanty et al., 2012). Also, the size and shape of the polymer shell are very sensitive to the changes in environment, e.g. pH or ionic strength. In terms of *in vivo* application, for example, this complicates their molecular binding and might inhibit efficient biodistribution and renal clearance.

Another way to encapsulate QDs is to introduce them into large vehicles, such as liposomes. Liposomes (lipid vesicles), first described by Bangham in 1965, are spherical vesicles, whose membranes contain one or more phospholipid bilayers (uni-, oligo-, and multilamellar vesicles). The lipid molecules consist of hydrophilic head groups and hydrophobic tails. In aqueous solutions they self-organize in order to increase their solubility in the surrounding medium and to minimize the surface-to-volume ratio. Liposomes are promising carrier for QDs, because they can be loaded with a large number of NPs, both hydrophobic and

hydrophilic (Beloglazova et al., 2013). Additionally, the biomimetic lipid bilayers of liposomes provide a high biocompatibility, thereby enhancing the effectiveness of PL NPs for biological application *in vitro* and *in vivo* (Chen et al., 2006).

The main disadvantage of using liposomes is their size (around 200 nm and more). Also, liposomal dispersions are not thermodynamically stable. When vesicles encounter each other in a suspension, they may fuse to form larger particles. Therefore, the liposomes' size could become polydisperse in time. During this fusion process, liposomes are prone to leak away their content and to lose their attractive properties that complicate their application for biolabeling and biomarking (Beloglazova et al., 2015).

2.1.3. SILICA COATING

Silica covering is a method that combines the main advantages of the two approaches, described above, as it allows maintaining the PL properties of the initial QDs and controlling the size of NPs. Also, for biological and analytical applications, silica coating offers benefits on several counts. First, it is inert in aqueous and non-aqueous solvents, thus the silica shell dramatically reduces the release of harmful ions (Vibin et al., 2011). As the silica shell is a rather rigid structure, it protects the PL core from destruction.

Second, silica coating is optically transparent and different functional groups (amines, carboxyls or PEG) can easily be introduced onto the silica shell due to the similar structure of all silica precursors and their ability to condensate with each other.

Third, several QDs can be loaded into the silica bead. In a molecular recognition event, the numerous QDs, instead of one single QD, amplify the analytical signal output. Moreover, several QD-based techniques, such as luminescent, electrogenerated chemiluminescent and electrochemical detection, offer a high sensitivity. The combination of numerous QDs in one label with a highly sensitive detection of each QD, enables the detection of analytes at low concentrations.

Fourth, multimodal NPs can be located in one silica bead. For example, silica nanohybrids integrated with QDs and magnetite nanocrystals or gold NPs can be used as multifunctional agents in diagnostics for dual-modality imaging, including computed tomography and

magnetic resonance imaging, for controllable drug delivery and photothermal treatment (Hsu et al., 2011; Xia et al., 2014; Ma et al., 2012; Jiang et al., 2014).

Silica coating of QDs usually involves initial ligand exchange with silane molecules, such as tetraethoxysilane (TEOS), to form nucleation sites on the QD surface. This is followed by further shell growth through hydrolysis and condensation (Gerion et al., 2001; Wu et al., 2013), or via a reverse microemulsion method (Koole et al., 2008; Wang et al., 2012). In case of the latter, the hydrolysis is confined inside the aqueous micelle core where precursors condense to form the NPs. Optimized synthetic protocols and experimental conditions allow obtaining NPs with a diameter in the range of about 15–200 nm (Darbandi et al., 2010). The preparation of loaded silica NPs within a microemulsion is a convenient route toward monodisperse particles of controllable size. Moreover, the reverse microemulsion method makes it possible to vary the number of NPs loaded inside one silica bead by changing the components' concentration ratio (Isnaeni et al., 2013; Wang et al., 2012; Goryacheva et al., 2015; Goftman et al., 2016).

2.2. NANOSTRUCTURES MULTILOADED WITH QUANTUM DOTS

Based on

Irina Yu. Goryacheva, Elena S. Speranskaya, Valentina V. Goftman, Dianping Tang, Sarah De Saeger. **Synthesis and bioanalytical applications of nanostructures multiloaded with quantum dots.** *Trends in Analytical Chemistry 66 (2015), 53–62.*

As stated before, numerous QDs, involved in a molecular recognition event, amplify the analytical signal output. Thus, detection with a multiloaded label offers higher sensitivity. Moreover, QD-containing nanocomposites combine the properties of both materials: PL from QDs and, for example, electrochemical characteristics of the carrier, its permeability, solubility, reactivity or biocompatibility. An important advantage of enhanced labels is the

possibility of using the same signal-generation and transduction methods as in the case for labels based on single QDs.

To be a suitable label for bioimaging and immunoassay, the nanostructures should be stably dispersed in water solutions. So, if the support material is not water soluble, the label production process should not only include decoration of the carrier with QDs, but also a hydrophilization step. Assembling of several QDs on one carrier was partially discussed for silica coated QDs and liposomes loaded with QDs. In the following sections, two carriers with a different organic structure are considered: dendrimers and layer-by-layer hollow microcapsules, which allow collecting QDs of both hydrophobic and hydrophilic nature.

2.2.1. MICROCAPSULES CONSTRUCTED BY LAYER-BY-LAYER TECHNIQUE

The layer-by-layer (LBL) technique is based on the sequential absorption of substances with different electrostatic properties. It is simple and cheap, and it is extensively used for a wide variety of materials (e.g., polyions, metals, ceramics, NPs, and biological molecules). Most often, these substances are synthetic or natural polycations and polyanions (Decher 1997), but other compatible systems, e.g., streptavidin-biotin (Chen et al., 2011), could be used too. By varying the number of layers, the LBL technique allows regulating the size of the structure. Also, other properties, such as the external charge and the density of labels, may be varied. Commonly, electrostatic attraction between consecutively deposited, oppositely charged molecules, leads to the formation of a stable film assembly. Strong electrostatic interactions between polycations and polyanions, which is the driving force for the deposition of subsequent shell layers, cause an over-charge of the external layer. First, this strategy was used for the formation of multilayer films on flat macroscopic surfaces. Later, this technique was applied to obtain multilayers around charged colloidal particles (Sukhorukov et al., 1998). The LBL technique for multilayer formation may use templates, such as latex colloids, calcium carbonate and silica, which can later on be removed (dissolved) from the final nanocomposite.

In case of association of several QDs, the LBL method is a convenient route, because, it is a facile self-assembly method, that avoids complicated chemical reactions and equipment. Furthermore, the loading, composition, density and distribution of QDs in the LBL structure can easily be controlled by the number of subsequent absorption cycles and the kind of layer-

formative material (e.g., the nature of the polymer). Additionally, QDs may be incorporated in the template and in the structures formed by the LBL technique. An example of creation of QD loaded LBL structures for drug delivery is presented in Figure 2.3.

The size of the LBL assembly is determined by the size of the template and it is found to be in the range 0.2–3 μm (Generalova et al., 2011; Xiang et al., 2011). When preparing without a template, the size of the particle mostly depends on the number of layers and the nature of the polyelectrolyte. The size and topology of the microspheres and also external coating can be selected to meet the requirements for their further application. Antibodies attached to the outer wall of the capsules can specifically bind to the targeted analyte or attach to the targeted place (Adamczak et al., 2012).

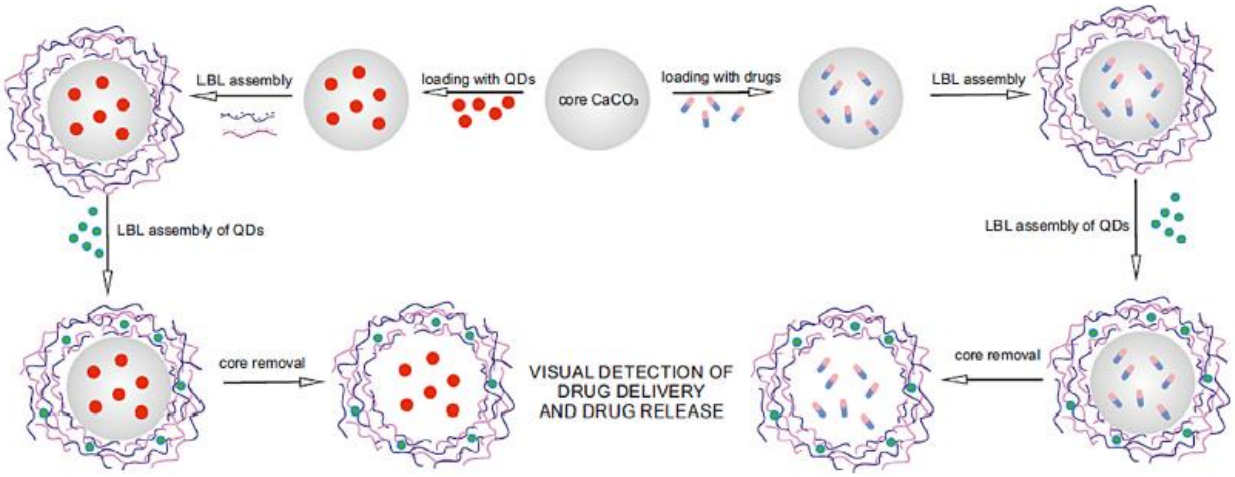

Figure 2.3. QDs in LBL technology for drug delivery

To obtain a high QD loading, $CaCO_3$-NPs are used as templates for LBL association of QDs by the electrostatic adsorption technique. The templates can be dissolved in ethylene diaminetetraacetic acid or hydrochloric acid. QDs may be present in both the shell and the hollow core of the LBL structure. The color of the synthesized structures is more intense after removal of the $CaCO_3$ template, possibly because most of the QDs then show their native color (Zhang et al., 2013). Comparison of the PL properties of QDs incorporated into LBL structures formed by synthetic polyelectrolytes on the one hand and natural polyelectrolytes on the other does not show any significant difference. At the same time, it was found that encapsulation of QDs in layers of biocompatible electrolytes reduced their cytotoxicity. In contrast, capsules prepared with synthetic polyelectrolytes did not show such an effect (Adamczak et al., 2012).

The LBL technique provides good perspectives for analytical applications because of the possibility to vary size, charge, permeability and stability of the obtained structures. Also the distance between the QDs and the external surface may be altered.

2.2.2. DENDRIMERS

Dendrimers are repetitively branched tree-like molecules, which are receiving considerable attention for application in chemical and biological areas, due to their numerous terminal groups that can be functionalized and conjugated with NPs and molecules of interest. They are highly ordered, regularly branched and essentially monodisperse single compounds, which exhibit a more globular conformation as their generation number increases (Figure 2.4) (Grayson et al., 2001; Higuchi et al., 2011).

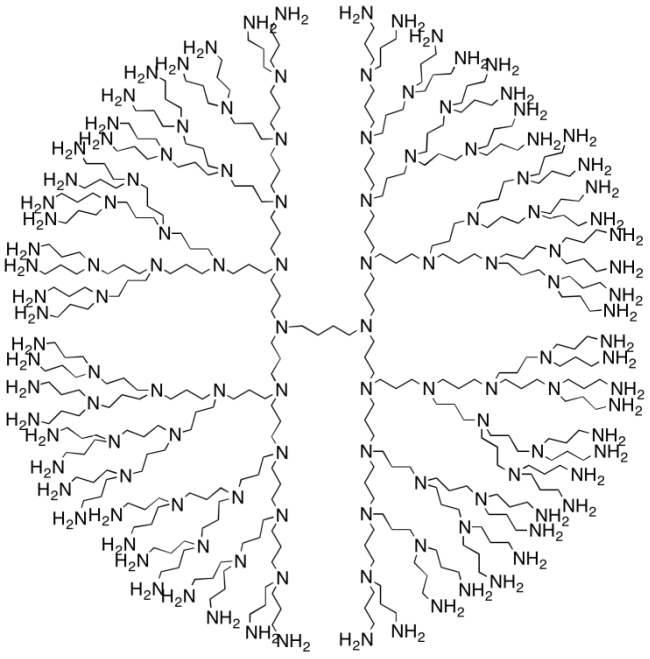

Figure 2.4. Basic structure of dendrimers

The most popular material for dendrimers is poly(amidoamine) or PAMAM. PAMAM dendrimers are water-soluble polycations, which can be protonated in aqueous solution at termini (primary amines) and at branch points (tertiary amines). The extent of protonation depends on the solution's pH (Geraldo et al., 2011). The amino groups on non-modified

PAMAM can be easily activated or modified and bioconjugated. PAMAM dendrimers of different generations are commercially available in both non-modified (only amino- groups) and modified (with hydroxy-, carboxy-, and trimethoxysilyl- groups) form. For conjugation with QDs, dendrimers of the third, fourth or fifth generation (G3, G4 and G5, respectively) are usually employed.

The ratio QD/dendrimer is important. Some approaches only cover a single QD with dendrimers to improve signal stability, to allow cell penetration, to optimize charge, or to introduce groups for conjugation. Other applications need more complex nanocomposites, consisting of multiple QDs. For this purpose, dendrimer nanoclusters are prepared by crosslinking PAMAM dendrimers with homobifunctional amine reactive agents, such as N-hydroxysuccinimide (NHS) functionalized polyethylene glycol (NHS-PEG-NHS) (Figure 2.5). The presence of a PEG spacer arm helps to maintain the high water solubility of the dendrimer clusters. The nanocluster size is regulated by changing the molar ratio between the PAMAM dendrimer and the crosslinker (Cheng et al., 2010). The average diameter of the obtained nanoclusters is about 150 nm.

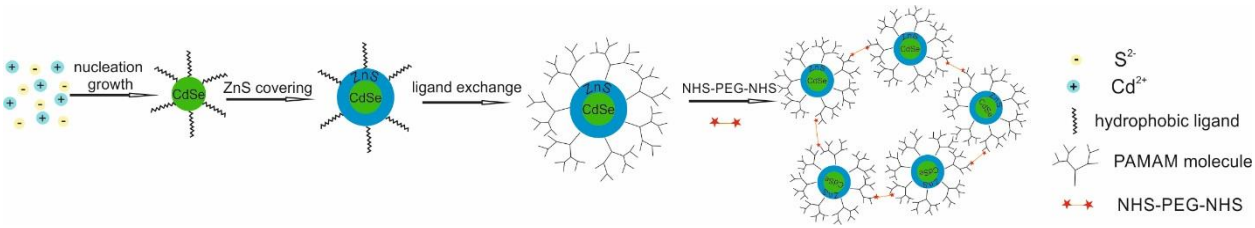

Figure 2.5. Preparation scheme of multi-label dendrimer-covered QDs

As “hosts”, dendrimers can also be a carrier for multifunctional hybrid structures. For example, by incorporating magnetic NPs, superstructures with a highly intense electrochemiluminescence, fluorescence and magnetic properties can be obtained. Furthermore, nanocomposites with excellent magnetic properties can be easily labeled, separated and immobilized (Jie et al., 2012). As there are a lot of terminal amino groups on the surface of the dendrimer (64 for PAMAM G4), they also increase the capacity for loading QDs on “inert” carriers, such as carbon nanotubes (CNTs), from which high-density

composites can be synthesized. Furthermore, the density of QDs on the synthesized composites is easily controlled by varying the ratio of NP/CNT (Zeng et al., 2008).

2.2.3. CONCLUSIONS

Nanostructures multiloaded with QDs offer very elegant ways of interfacing biomolecular recognition events with inherent signal amplification. Note, that association of several QDs in one structure does not appreciably change the properties of the QDs, which means that the same readers as for single QDs can be used. The variability of the amount of QDs, their distribution inside the nanostructures, the density and the composition of functional groups on the surface (with the exception of dendrimer-based structures), the size and the stability, the availability of QDs for external substances (e.g., energy acceptors), and the possibility of controlling and tailoring their properties in a very predictable, precise manner are attractive characteristics, ensuring that the nanostucture meet the needs of analytical applications.

CHAPTER 3. QUANTUM DOTS FOR MYCOTOXIN DETECTION

Mycotoxins are secondary metabolites produced by fungi. They form a worldwide problem as they are present in 25% of the global crop. Several core food commodities, such as cereals, nuts, dried fruit, coffee, cocoa, spices, pulses and some fruits are amenable to mycotoxin contamination. Fungi can poison crops with mycotoxins on the field (pre-harvest) or during transportation, storage or processing (post-harvest). However, they can also enter the food chain via bioaccumulation in eggs, milk and meat from animals eating contaminated feeds (Turner et al., 2015). Mycotoxins are mainly produced by *Aspergillus, Fusarium, Alternaria and Penicillium* species. One species is capable to produce several toxins simultaneously, as such possibly causing additive or synergetic effects. Thus, the mycotoxin problem requires robust analytical methods for multianalyte detection.

Mycotoxins are reasonably small molecules of approximately 300 - 700 Da (Figure 3.1). They possess carcinogenic and mutagenic properties as well as highly toxic effects on liver, kidneys and immune and reproductive systems. Mycotoxins are physically and chemically very stable and tend to survive storage and food processing even at extreme temperatures. Therefore, very strict legislations of maximum levels for mycotoxins are maintained all over the world (Marroquín-Cardona et al., 2014).

Conventional methods for mycotoxin detection leverage chromatographic techniques, including LC coupled to ultraviolet, fluorescence or mass spectrometric detection or gas chromatography. Sophisticated instrumental configurations combined with extensive sample preparation, lead to high sensitivity and flexibility, as well as ability to detect multiple analytes (sometimes over 50) at ppb levels in complex samples (Anfossi et al., 2016).

Chromatographic techniques are the gold standard for mycotoxin detection against which all other techniques are compared (Turner et al., 2015). However, the timing of the mycotoxin analysis is vitally important. Since contamination can occur pre-harvest (in the field) and post-harvest (during harvest, transport and subsequent storage), the need for fast screening

methods of analysis, which can be applied in-field, emerges. Still, in-field analysis cannot rely on the use of complex, expensive equipment as chromatographs (Figure 3.2).

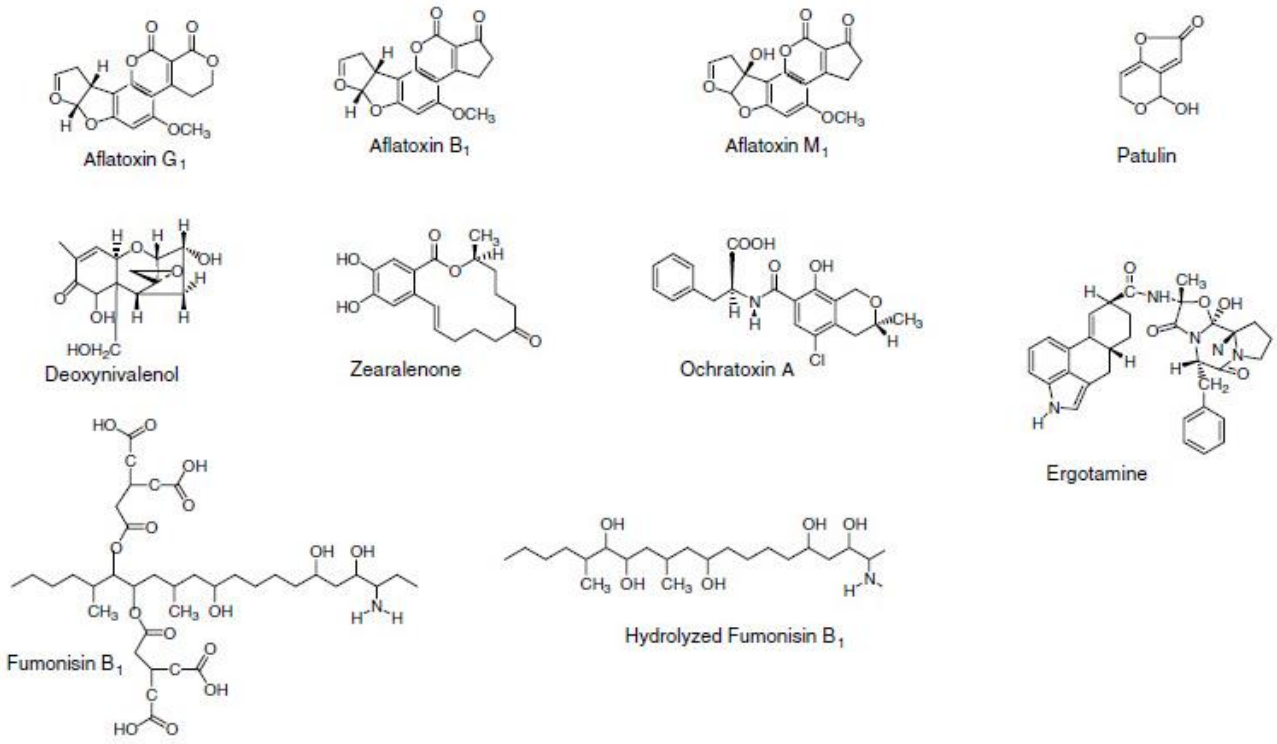

Figure 3.1. Structures of common mycotoxins

In this regard, immunoassay, based on a specific interaction between an antibody and an antigen, provides a valuable alternative to chromatographic methods. It is a rapid, sensitive approach with several easily visualized detection mechanisms, including color, luminescence (chemiluminescence) and magnetic recognition systems.

Immunoassay with luminescent detection is very sensitive and it enables the simultaneous use of multiple labels with different spectral characteristics (multiplexing). The sensitivity of PL labels is comparable or even higher then conventionally used enzymatic labels, but the assay procedure is essentially easier (Goryacheva et al., 2013). Given the high PL brightness, the emitted light may be used as the analytical signal, which can be recorded immediately

after the removal of the unbound conjugate molecules without the need to add a chromogenic substrate. Additionally, in contrast to enzymes, PL labels are less sensitive to environmental conditions, which make the analysis more representative.

Chromatographic-based methods		Immunochemical-based methods
• Validation (in compliance to regulations) • Allows compound identification and structural elucidation of unknown • Multi-target	Strength	• Limited sample treatment • Simple, cheap, portable • Managing of large number of samples
• Expensive • Sophisticated (skilled personnel is required for operating and interpreting results) • Operated in laboratory	Weakness	• Excessively selective • Long time needed for the development (to obtain bioreagents, mainly antibodies)
• Simplified (QuEChERS) sample preparation for high-throughput and multiresidue analysis • Biomarkers in biological fluids	Opportunities	• Provide up-to date information on occurrence • Provide epidemiologic data
• Emerging mycotoxins • Masked mycotoxins	Threats	• New matrices • Multiplex analysis

Figure 3.2. Comparing chromatographic-based and immunochemical-based methods for mycotoxin detection. Reprinted from (Anfossi et al., 2016)

PL sensors for mycotoxin determination can be performed in three different formats: a direct competitive format, based on the PL of a special label; an indirect competitive format with PL labelled antibodies; and a non-competitive format, based on the native fluorescence of the mycotoxin molecules.

According to scientific databases, such as Web of Science and SciFinder, about 100 papers describing luminescent immunoassays for mycotoxin detection have been published over the past 20 years. Mostly, the presented techniques leverage organic fluorophore molecules for labeling immunoreagents.

More often, the following formats of immunoassay are used to determine mycotoxins in food and feed with luminescent detection.

1) Fluorescence labeled immunosorbent assay (FLISA): classic microplate immunoassay coupled to luminescent reader (Vellapan et al., 2008).

2) Fluorescence polarization immunoassay, based on the competition between mycotoxin and a mycotoxin-fluorescein tracer for a mycotoxin in specific antibody (Maragos 2009).

3) The immunochromatographic strip tests, also known as lateral flow immunoassay, in which the sample flows by capillary forces along an analytical membrane that contains immobilized immunoreagents (Di Nardeo et al., 2016).

A number of QDs' distinctive characteristics, already discussed in previous chapters, make them a valuable multifunctional label for those described immunoassays (Geszke-Moritz and Moritz, 2013). Recently, a few articles were devoted to the development of rapid QD-labeled immunoassays for determination of several mycotoxins in different matrices (table 3.1). In these studies, it was shown that the high QY of QDs allows reaching considerable sensitivity (Speranskaya et al., 2014). Moreover, multi-mycotoxin detection is feasible by labeling conjugates with QDs that emit light in different parts of the spectrum (Beloglazova et al., 2014).

Given their nanoscale size and large surface areas, together with unique optical properties, QDs have become the ideal transfer mediation for the development of fluorescence resonance energy transfer (FRET) immunosensors for mycotoxin detection (Xu et al., 2014; Zekavati et al., 2013). It is important to note that QDs can act both as donor and acceptor of energy. Thus, it is possible to use two types of QDs, with appropriate emission and absorption wavelengths, or QDs in combination with organic fluorophores and fluorescent proteins.

Diverse formats of immunoassay are available for mycotoxin analysis with QD labels. The most common one is FLISA (Zhang et al., 2014; Beloglazova et al., 2015). This screening method is widely spread, not only owing to its sensitivity and reproducibility, but also because of the availability of equipment. Other formats, like immunochromatographic (Di Nardo et al., 2016; Wang et al., 2011) or column-designed tests (Beloglazova et al., 2014; Beloglazova et al., 2012; Wang et al., 2013; S Speranskaya et al., 2014), do not require any

equipment, not to perform the analysis, nor for interpretation of results. This extends the applicability of these tests to *in-field* usage, offering the chance to rapidly and conveniently check the quality of food and feed.

Taking into account this successful apposition of immunofluorescent methods for mycotoxin detection, the fabrication of novel PL QD-based immunolabels has become of high importance.

Table 3.1. Existing QD-based methods for mycotoxin detection and their sensitivity parameter

Mycotoxin	Matrix	QD structure	Method	Sensitivity	Reference
Aflatoxin B_1	peanuts	CdTe stabilized with glutathione	FLISA*	LOD* 0.016 ng/mL	Zhang et al., 2014
Zearalenone Aflatoxin B_1	maize wheat	CdSe/CdS/ZnS loaded in silanized liposomes		IC_{50}* 2.2 and 2.6 mg/kg	Beloglazova et al., 2015
Aflatoxin B_1	wheat and maize	CuInS/ZnS coated with polymer		LOD 0.03 ng/mL	Speranskaya et al., 2014
Deoxynivalenol	model solutions	CdSe/CdS/ZnS covered with silica		LOD 473 ng/mL	Goftman et al., 2016
Fumonisin B_1	maize flour	CdSe/CdS/ZnS coated with polymer	immunochromatographic test	LOD 28 mg/kg	Di Nardo et al., 2016
Ochratoxin A	red wine	aptamer-modified QDs		LOD 1.9 ng/mL	Wang et al., 2011
Aflatoxin B_1	rice grain	Commercial NanoTech.,LLC	FRET*	LOD 0.04 ng/mL	Xu et al., 2014
Aflatoxin B_1	model samples	TGA* capped CdTe		LOD $2*10^{-11}$ M	Zekavati et al., 2013
Zearalenone	wheat and maize	CdSe/CdS/ZnS loaded in liposomes	Column test immunoassay	LOD 20 μg/kg	Beloglazova et al., 2013
Deoxynivalenol Zearalenone Aflatoxin B_1 T_2 toxin	wheat and maize	CdSe-based coated with polymer		Cut off levels: 500 μg/kg 100 μg/kg 2 μg/kg 100 μg/kg	Beloglazova et al., 2014
Zearalenone	wheat	CdSe/ZnS stabilized with MPA*		5 ng/ml	Beloglazova et al., 2012
Aflatoxin M_1	milk	CdSe/CdS/ZnS loaded in liposomes		Cut off 0.05 μg kg	Wang et al., 2013
Deoxynivalenol	maize	CdSe-based coated with polymer		LOD 25 ng/mL	Speranskaya et al., 2014.
Aflatoxin B_1	peanuts	PbS stabilized with TGA	electrochemical immunoassay	0.018 ng/mL	Zeng et al., 2015

** FLISA is a fluorescent linked immunosorbent assay*
FRET is a Förster resonance energy transfer
LOD is a limit of detection
IC_{50} is a half maximal inhibitory concentration
TGA is a thioglycolic acid
MPA is a mercaptopropionic acid

PART 2. DEVELOPMENT OF SENSITIVE LUMINESCENT LABELS BASED ON QUANTUM DOTS

CHAPTER 4. SYNTHESIS, MODIFICATION, BIOCONJUGATION OF SILICA COATED QUANTUM DOTS

Based on

Valentina V. Goftman, Tangi Aubert, Dries Vande Ginste, Rik Van Deun, Natalia V. Beloglazova, Zeger Hens, Sarah De Saeger, Irina Yu. Goryacheva, **«Synthesis, modification, bioconjugation of silica coated fluorescent quantum dots and their application for mycotoxin detection»**, Biosensors and Bioelectronics, 2016, 79, 476–481.

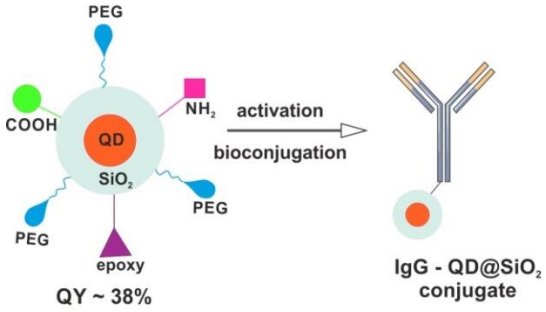

ABSTRACT

To create bright and stable PL biolabels for immunoassay detection of mycotoxin deoxynivalenol in food and feed, CdSe/CdS/ZnS core-shell QDs were encapsulated in silica capping layer through a water-in-oil reverse microemulsion process. The optical properties and stability of the obtained silica coated QDs (QD@SiO_2), modified with amino, carboxyl and epoxy groups and stabilized with polyethylene glycol fragments, were characterized in order to assess their bioapplicability. The developed co-condensation techniques allowed maintaining 80% of the initial PL properties and yielded stable PL labels that could be easily activated and bioconjugated.

4.1. INTRODUCTION

In the beginning of the QDs era, these NPs were mostly considered as relevant materials in the photonics and electronics domain, given their potential use in displays and related optoelectronic applications. Since 1998, however, the QDs' unique optical properties, such as high photostability, size-tunable emission with narrow symmetrical peaks and broad absorption spectra, have found great perspectives in biomedical research (Bruchez et al., 1998). As it was discussed in Chapter 2, to apply QDs for biomedical purposes, a lot of attention is paid to the capping layer. So far, silanization is one of the widely used methods for QDs hydrophilization (see Section 2.1.3).

Silica covered QDs have a highly hydrophilic surface, which makes them one of the most friendly nanohybrids for biomedical applications such as drug and gene delivery, bioimaging and therapy (Knopp et al., 2009). However, for bioanalysis and biotechnological applications, QDs should be linked to biomolecules, such as antibodies or antigens. Prevalence of the amino-modified silica NPs with 3-aminopropyl-triethoxysilane (APTES) can be explained because of the commonly used technique for amino-activation and the subsequent conjugation with carboxyl-containing biomolecules (Hermanson, 2008). Another common way is to attach carboxyl groups on the surface of silica NPs (using, e.g., sodium carboxyethylsilanetriol), followed by their activation and conjugation with amino-contained biomolecules (Bagwe et al., 2006; Qhobosheane et al., 2001; Hlavacek et al., 2014). Both methods require activation of either an amino or a carboxyl group for the peptide bond formation. In contrast, epoxy groups are very active and allow conjugation of thiol, amino, carboxyl or hydroxyl containing ligands, depending on pH and without any activation step (Hermanson, 2008). Moreover, high immobilization efficiency (more than 90%) can be reached by using silica NPs containing epoxy groups (Hurley et al., 2013). An additional advantage of epoxy groups is their stability. More specifically, they are stable enough to perform long-term incubations in alkaline or neutral conditions (Zhang et al., 2011).

Bioapplication of silanized NPs is often burdened with non-specific adsorption of NPs on different surfaces, as well as biomolecules on the NP surface. A PEG layer is helpful to minimize non-specific interactions of the QDs with biological material (Jokerst et al., 2011) and to increase biocompatibility of the NPs. Non-specific binding is hostile for all types of labeling and analysis (Suzuki 2012). In the case of silica NPs, PEG plays another important

role at the same time, i.e. the PEG layer increases the buffer stability of silanized NPs, which is important for conjugation with biomolecules and further application.

Because of the great diversity of silica precursors, all with a similar structure, it is very convenient to combine functional modification with PEG addition. Combination of PEG-silanes and APTES yields a good colloidal stability of the obtained NPs, even when the salt concentration of media is changed up to 1 M and for pH values within the range of 1 to 13, as shown for dye-containing NPs in (Li et al., 2014). Combination of PEG-silanes and epoxy-silanes on the surface of NPs provides an easy way for covalent binding with antibodies without activation on the one hand and good buffer stability on the other hand (Hurley et al., 2013). In (Kobayashi et al., 2013), initially water-soluble QDs were covered with a silica shell, followed by a modification with functional silica precursors and PEG-containing polymers, as well as in (Wang et al., 2012), where after silica covering a PEG-containing polymer was used to increase stability and biocompatibility. Still only few articles describe modification using a PEG-containing silica precursor (Wolcott et al., 2006; Hsu et al., 2011).

In this chapter, in order to obtain stable bright and sensitive PL labels, we investigate the impact of several functional groups in combination with PEG fragments on the quality of the QD@SiO_2 NPs. In particular, the PL properties of silica covered QDs, being amino-, carboxyl- and epoxy-modified NPs, are thoroughly described and carefully compared with their PEG-terminated modifications. Also, stability characteristics, performed via ζ-potential measurements, are presented and the impact of pH of the surrounding media is investigated. Furthermore, silica coated QDs modified with diverse functional groups with increased buffer stability and biocompatibility may be used as novel PL labels, opening up a wide range of promising applications.

4.2. EXPERIMENTS

4.2.1. Chemicals

Cadmium oxide (CdO, 99,99%), selenium powder (Se, 99,99%), sulfur powder (S, 99%), zinc acetate ($Zn(OAc)_2$, 99,99%), oleic acid (OA, 90%), 1-octadecene (ODE, 90%), oleylamine (OLA, 70%), octadecylamine (ODA, 90%), trioctylphosphine (TOP), rhodamine 6G, 1-ethyl-3-(3-dimethylaminopropyl)carbodiimide (EDC), N-hydroxysulfosuccinimide sodium salt (sNHS), TEOS, APTES, (3-Glycidyloxypropyl)trimethoxysilane (GOPTES), morpholinoethanesulfonic acid (MES), phosphate buffered saline tablets, bovine serum

albumin (BSA), surfactant Brij L4 (M_n~362 g/mol), were purchased from Sigma-Aldrich (Bornem, Belgium). 2-[methoxy(polyethyleneoxy)$_{6-9}$propyl]trimethoxysilane (MPEGTMS) was purchased from Gelest Inc. (USA). Carboxyethylsilanetriol, sodium salt (25%) (CEST) in water was kindly provided by ABCR company (Germany). Polyclonal rabbit anti-mouse immunoglobulins (IgG) 2 g/L were purchased from Dako Denmark A/S (Glostrup, Denmark). Agarose was purchased from GE Healthcare Bio-Sciences AB (Uppsala, Sweden). All organic solvents (ethanol, butanol, toluene, chloroform, dimethylformamide (DMF)) and ammonium solution (25%) were purchased from Sigma-Aldrich (Bornem, Belgium) and were used without further purification. All other chemicals and solvents were of analytical grade. Ultrapure MilliQ water was used throughout.

4.2.2. Synthesis of CdSe core nanocrystals

CdSe QDs were prepared via the well-known rapid hot-injection method (Hines and Guyot-Sionnest, 1996) as described in (Speranskaya et al., 2014). CdSe cores were synthesized as follows: 1 mmol of a Se-precursor solution (0.1 M Se in TOP and ODE) was injected into a three-neck flask containing 1 mmol of Cd-precursor solution (0.1 M CdO in OA and ODE, molar ratio of solvents 1:8 correspondingly) at 260 °C. The reaction was stopped after 20 s. Next, to isolate the CdSe QDs, a butanol-ethanol mixture was added and a centrifugation was performed. Finally, the precipitate was dissolved in toluene and stored at 4 °C. The size (2.5 nm) and concentration (8 μM) of the obtained CdSe nanocrystals were estimated according to the formula presented in (Capek et al., 2010).

4.2.3. Synthesis of core/multishell QDs

Core/shell QDs were produced by means of the SILAR technique described in (Li et al., 2003; Reiss et al., 2009) with slight modifications (Speranskaya et al., 2014). First, ODE, ODA and 0.3 μmol of CdSe cores were loaded into a 100 mL three-neck flask and heated at 100 °C under Ar for 1 hour. Next, S-precursor (0.1 M S in ODE), Cd-precursor (0.1 M CdO in OA and ODE) and Zn-precursor (0.1M $Zn(Ac)_2$ in OLA and ODE (molar ratio of solvents 1:3 correspondingly) were successively added, waiting 10 min between each injection at 220 ^{o}C. The amount of the injection solution was calculated by the method presented in (Reiss et al., 2009), based on the calculation of the number of surface atoms. Upon completion of the

synthesis, the reaction mixture was purified by acetone addition and centrifugation. Finally, the precipitate was dissolved in toluene and stored at 4 °C. By means of this method, orange-emitting QDs with nominal structure CdSe/2CdS/2CdZnS/2ZnS (λ^{em}=600 nm) were synthesized.

4.2.4. Synthesis of silica coated QDs

The obtained QDs were encapsulated in silica NPs through the microemulsion process (Figure 4.1). First, 1 mL of hexane, 0.32 mL Brij L4 as surfactant and 50 µL H_2O were mixed and let to stir for 30 min to form the microemulsion. Then, 1 nmol of QDs in chloroform was slowly added. Thirty min later, 30 µL of TEOS was added, followed by the addition of 10 µL NH_3 solution, which acts as the catalyst of the hydrolysis process. Subsequently, the reaction mixture was let react for 24 h at room temperature and the NPs were precipitated from the microemulsion using ethanol, centrifuged and the resultant precipitate of QD@SiO_2 particles were washed 3 times with hexane and at least 5 times with deionized water. Finally, aqueous dispersions of the composite particles were obtained via sonication.

4.2.5. Modification of silica coated QDs

To functionalize the QD@SiO_2, a co-condensation of CEST, GOPTES or APTES with TEOS was performed. CEST, or GOPTES, or APTES (1.5 µL) was added to the microemulsion after 24 h of ageing and left for another 24 h of stirring, followed by the purification process described in previous section. PEG-terminated QD@SiO_2 were then prepared via additional coating procedures in the water-in-oil microemulsion. MPEGTMS (3 µL) was added to the microemulsion and after 24 h of stirring together with modification silica reagents, the NPs were separated from the solution and rinsed 3 times with hexane and 5 times with water using high-speed centrifugation (20 000 g). Finally, aqueous dispersions of the composite particles were obtained via sonication.

4.2.6. Conjugation of silica coated QDs with IgG

The same bioconjugation technique was applied in parallel to carboxyl-modified QDs (QD@SiO_2-COOH) and to PEG-terminated carboxyl-modified QDs (QD@SiO_2-PEG-COOH), in

order to compare their binding ability. Further, a similar comparison was performed for the amino- and epoxy-modified QD@SiO_2 NPs.

Conjugation of carboxyl-modified QD@SiO_2

QD@SiO_2-COOH and QD@SiO_2-PEG-COOH NPs were conjugated with IgG by means of the EDC/sNHS activation method described in (Hlavacek et al., 2014). An activating mixture was prepared by dissolving 0.4 mg EDC and 1.2 mg sNHS in 100 µL of 100 mM MES buffer, pH 6.0. A volume of 700 µL of QD@SiO_2 NPs dispersed in water was combined with 50 µL of the activating mixture and incubated for 5 min at room temperature to prepare succinimide-activated NPs. The surface-activated NPs were added to 300 µL of IgG (2 mg/mL) and incubated for 3 hours at room temperature.

Conjugation of amino-modified QD@SiO_2

QD@SiO_2-NH_2 and QD@SiO_2-PEG-NH_2 NPs were conjugated with IgG by means of the method described in (Liu et al., 2007). After washing with DMF twice, 700 µL of NPs was mixed with 10% succinic anhydride in DMF (0.32 g succinic anhydride, 3 mL DMF). The reaction continued for 18 h under N_2 gas at 4 ^oC. Through this process, carboxyl groups were formed onto the NPs' surface. Next, the NPs dispersed in Milli-Q water were added to 0.2 mL 100 mM MES buffer, containing 0.01 g EDC and 0.015 g sNHS and mixed for 5 min. Finally, 300 µL IgG (2 mg/mL) was introduced and mixed 2 h at 37 ^oC, followed by adding 1.4 mg BSA to reduce the effects of non-specific binding of the obtained conjugates.

Conjugation of epoxy-modified QD@SiO_2

QD@SiO_2-epoxy and QD@SiO_2-PEG-epoxy NPs were conjugated with IgG by means of the method described in (Wang et al., 2010). NPs (500 µL) incubated with 300 µL IgG (2 mg/mL) in phosphate-buffered saline (PBS) for 12 h under gentle stirring. The unreacted and non-specific sites were blocked in a 10 mg/mL BSA–PBS solution.

The prepared conjugates were kept at 4 °C.

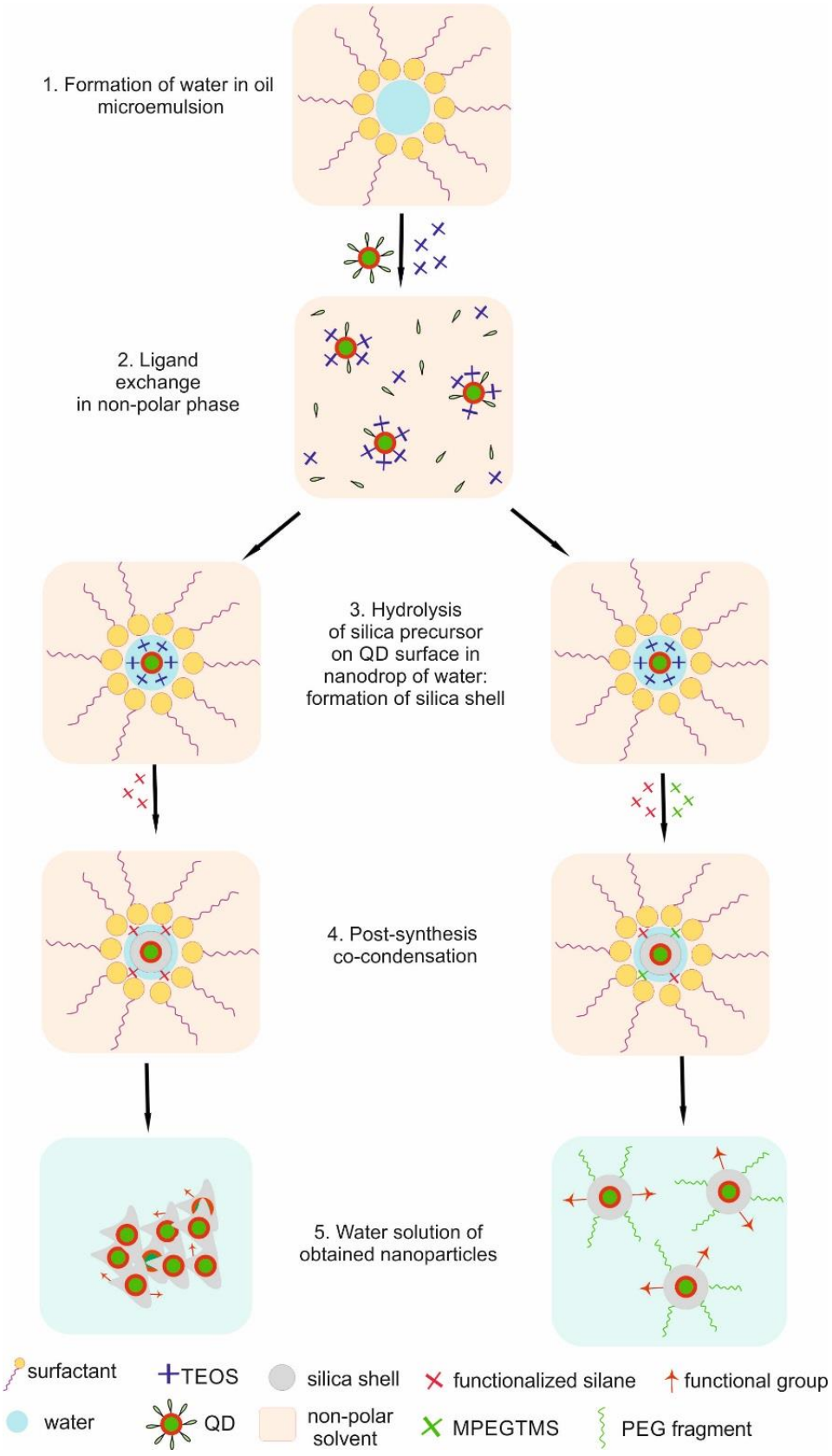

Figure 4.1. Reverse microemulsion synthesis of silica coated QDs (QD@SiO_2) and subsequent modification with reactive functional groups (on the left) and PEG-fragments together with reactive functional groups (on the right), where the reactive functional groups are amino, carboxyl or epoxy

4.3. RESULTS AND DISCUSSION

4.3.1. Synthesis and characterization of the QDs and the QD@SiO_2 NPs

CdSe cores were prepared via a rapid hot-injection method in ODE. To improve the PL intensity and stability, CdSe nanocrystals were covered with several shells of the wider band gap CdS and ZnS semiconductors (Xie et al., 2005). The PL QY of core-shell particles reached 53%, which is 10 times more than the QY of uncovered CdSe cores. An alloy layer of CdZnS was added between the CdS and ZnS layers due to the critical impact of the thickness and the composition of higher bandgap inorganic shells on the PL properties of QDs after their hydrophilization. It was shown before (Zhang et al., 2008) that addition of an alloy CdZnS layer between CdS and ZnS shells allows retaining the original QY after the reverse microemulsion silanization process. In this chapter, CdSe QDs with two intermediate CdZnS shells were synthesized according to the method described in the experimental section. They showed a uniform spherical shape of nanocrystals with an average diameter of 7 nm (Figure 4.2), and exhibited a relatively small QY drop from 53% to 43% after silica covering (table 4.1).

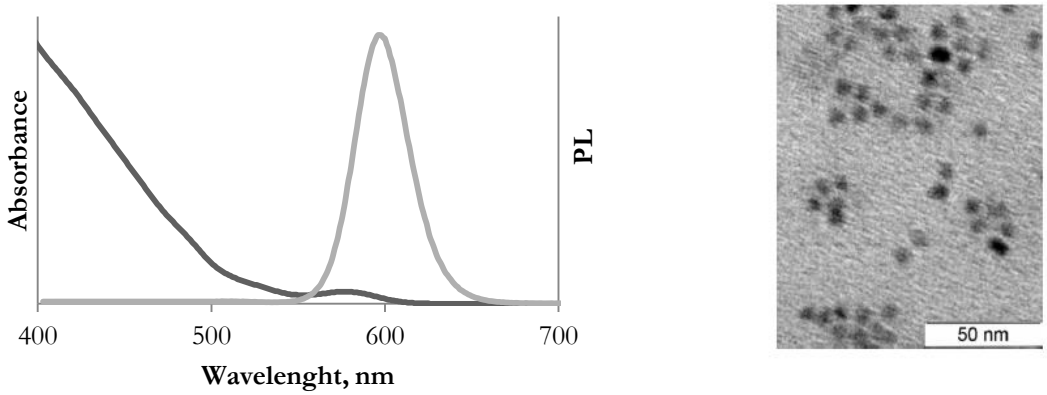

Figure 4.2. Characteristics of the synthesized CdSe/2CdS/2CdZnS/2ZnS QDs: absorption (left) and PL (right) spectra of the QDs (A); TEM micrograph (B), which shows a spherical form of the obtained nanocrystals and their average diameter of 7 nm

The microemulsion for performing silanization can be obtained by various compositions of non-polar phases and surfactants (Wang et al., 2014). More than often, Igepal and Brij are

used as non-ionic surfactants with cyclohexane and *n*-heptane (or *n*-hexane) as the corresponding non-polar phase. Several factors have an impact on the microemulsion's stability and, consequently, on the quality of the silica covering. First of all, the molar ratios in the triple surfactant - water - solvent system affect the micelles' size and their stability. Second, as QDs act as nucleation centers for the growth of the silica nanospheres, it is very important to determine the optimal ratio between the amount of QDs and amount of micelles.

Table 4.1.QYs (%) of synthesized QD@SiO_2 NPs modified with the indicated reagents in comparison to the QY of initially uncovered hydrophobic QDs

Initial uncovered	TEOS	APTES	CEST	GOPTES	MPEGTMS	MPEGTMS +APTES	MPEGTMS +GOPTES	MPEGTMS +CEST
53	43	40	40	40	38	38	36	36

The silica shell renders the QDs water soluble, meanwhile also playing the role of a protective layer preventing 1) core oxidation and 2) possible leaking of heavy metal ions to the surrounding media (Chu et al., 2008; Aubert et al., 2014). Owing to this, the thickness of the silica shell is crucial for the nanohybrids quality and their further application. Therefore, the direct linear relationship between the amount of TEOS added to the microemulsion system and the volume of the silica shell is a big advantage of the advocated approach. The QD@SiO_2 NPs, obtained by means of the method described in the experiments, show a good morphology with mostly one single QD perfectly in its center and surrounded by a homogeneous silica shell. They have an average diameter of 32.4 ± 2.8 nm, corresponding to a silica shell thickness of about 12 nm (Figure 4.3).

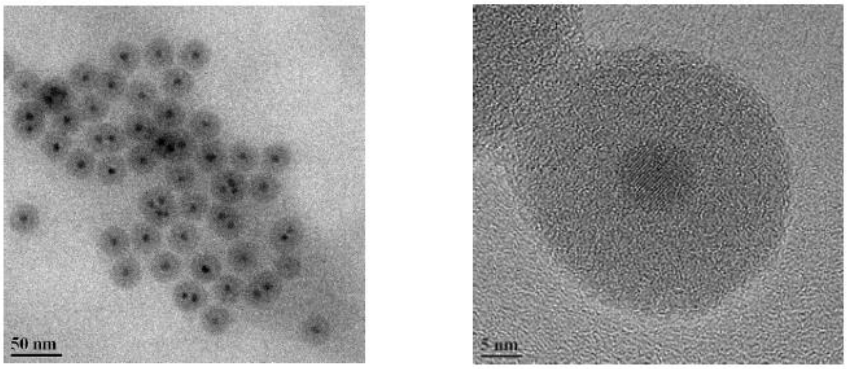

Figure 4.3. TEM images of the obtained QDs covered with silica shell

4.3.2. Modification of QD@SiO_2 with diverse silica reagents

Reactive functional groups can be introduced onto the surface of silica NPs by either the co-condensation process or by post-synthesis surface modification (Wang et al., 2014). Co-condensation implies the addition of a modification silica reagent in the microemulsion system after the first silica shell formation. This method provides a uniform distribution of the functional groups over the silica surface and it maintains the size distribution of the NPs. In this work, several modification reagents, namely APTES, GOPTES, CEST and MPEGTMS were introduced in the microemulsion system after the initial silica shell formation.

Table 4.2. ζ-potential measurements in water solutions of QD@SiO_2 and modified with the indicated precursors

Modification reagent	TEOS	APTES	CEST	GOPTES	MPEGTMS
ζ-potential, mV	-20 (±4)	+ 14 (±5)	- 34 (±5)	- 50 (±4)	- 22 (±10)

Unmodified QD@SiO_2 NPs have a negative ζ-potential due to the hydroxyl groups which appear after the TEOS hydrolysis. After modification with amino groups, the ζ-potential shifts into the positive region, while addition of carboxyl and epoxy groups leads to a further decrease of the initially negative ζ-potential (table 4.2). Amino-modified silica NPs are not stable because of the compensation of positive charge on the partially protonated amino group in the water solution (Bagwe et al. 2006). To find optimal stability, APTES was used in different percentages of the TEOS amount, up to 10%. But only particles obtained with small APTES/TEOS ratios (less than 0.2%) form stable water solutions. The amine modified

QD@SiO_2 NPs were here prepared with an APTES/TEOS volume ratio of 0.05%, resulting in NPs with a ζ-potential of +14 mV.

Addition of carboxyl groups using co-condensation with CEST increases the negative charge on the QD@SiO_2 surface, which makes them more stable in water solution because of supplementary repulsion (table 4.2). The same effect was observed for NPs modification with GOPTES.

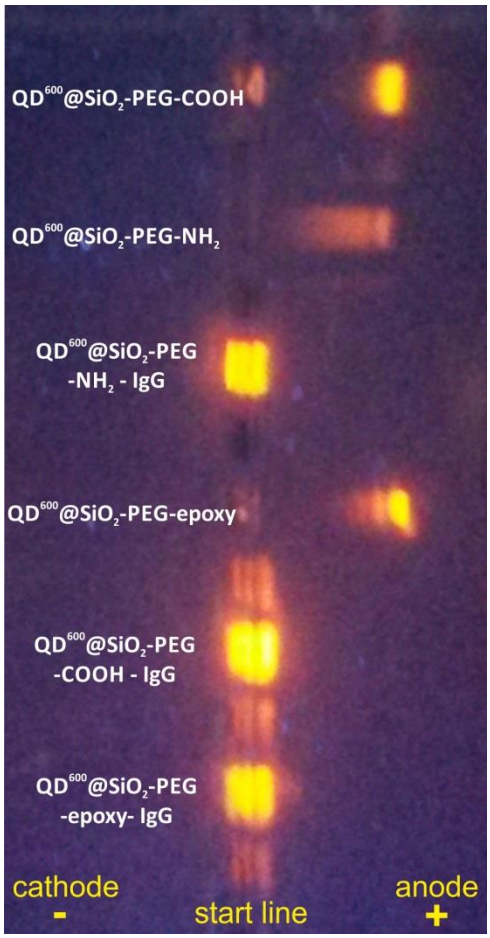

Figure 4.4. Gel electrophoresis of the obtained QD@SiO_2-PEG NPs, modified with amino, epoxy and carboxyl groups and their conjugates with IgG

PEG is a water-soluble amphiphilic polymer with excellent biocompatibility and it is frequently used in biomedical applications, such as drug delivery. PEGylation can reduce the reticuloendothelial system uptake and prolong blood circulation. With covalently bound PEG chains, NPs achieve longer blood circulation half-lives than their counterparts with only

surface-absorbed PEG (Hsu et al., 2011). PEG fragments were incorporated onto the silica surface to overcome instability of the modified QD@SiO_2 in water and especially in buffer solutions. For PEGylation of QD@SiO_2 NPs, MPEGTMS, containing 6-9 PEG fragments, was used. It is critical to use silica terminated with PEG chains of a low molecular weight to prevent steric blocking of the functional groups on the NPs surface. Also, according to results of our previous experiments, usage of longer PEG chains causes more significant drop of the QY of QD@SiO_2 after modification with PEG-contained substances. PEG-addition gives an extra negative charge (around -20 mV) to the NPs (table 4.2). As such, even positively charged amino-modified QD@SiO_2 acquire a small negative charge after PEGylation. This forces QD@SiO_2-PEG-NH_2 to migrate to the positive electrode during electrophoresis in the agarose gel (Figure 4.4). It is important to notice that all modified QD@SiO_2 NPs have a good brightness; the QY does not drop significantly after the modification step and remains in the range 36 to 40% (table 4.1).

4.3.3. Stability of the modified QD@SiO_2 NPs in buffer solutions

In general, the silica NPs are stable in an aqueous phase owing to the electrostatic repulsion between the negative charges of the deprotonated silanol groups on the particle surface. However, dispersion in buffer solution, including biological fluids, could cause silica NPs to aggregate and precipitate (Hsu et al., 2011). Thus, both QD@SiO_2-COOH and QD@SiO_2-epoxy, despite the sufficient ζ-potentials, possess a poor buffer stability, which significantly complicates conjugation with biomolecules.

To evaluate applicability of the synthesized QD@SiO_2 NPs for conjugation with biomolecules, their stability in buffer solutions was investigated. Four the most frequently used for bioconjugation buffers were prepared: MES solution (pH 6.5), PBS (pH 7.5), sodium tetraborate solution (pH 8.5), sodium carbonate buffer (pH 9.6). To set up a wide pH range acetic acid/sodium acetate solution (pH 3.5) and potassium chloride/sodium hydroxide solution (pH 14) was made. Colloid water solution of QD@SiO_2 NPs put into prepared buffer and left them for 72 h. With time, the QD@SiO_2-NH_2 NPs without PEG fragments lose their stability and start to precipitate. It is clearly seen that at pH 6.5 and 7.5 precipitations had occurred already after 24 h of storage for QD@SiO_2-NH_2 (Figure 4.5). Probably, it can be explained in terms of amino-group's instability at the neutral pH. Also, quenching of the PL properties occurs, especially in an alkaline environment. In contrast, PEG-terminated

QD@SiO_2-NH_2 NPs preserves initial stability and optical properties, even after 72 h of storage (Figure 4.5). The pairs of PEGylated/not PEGylated epoxy and carboxyl modified NPs showed similar behavior. In summary, PEGylated QD@SiO_2 is more stable independently of the buffer capacity of the surrounding solution, which gives an advantage for bioconjugation of these NPs.

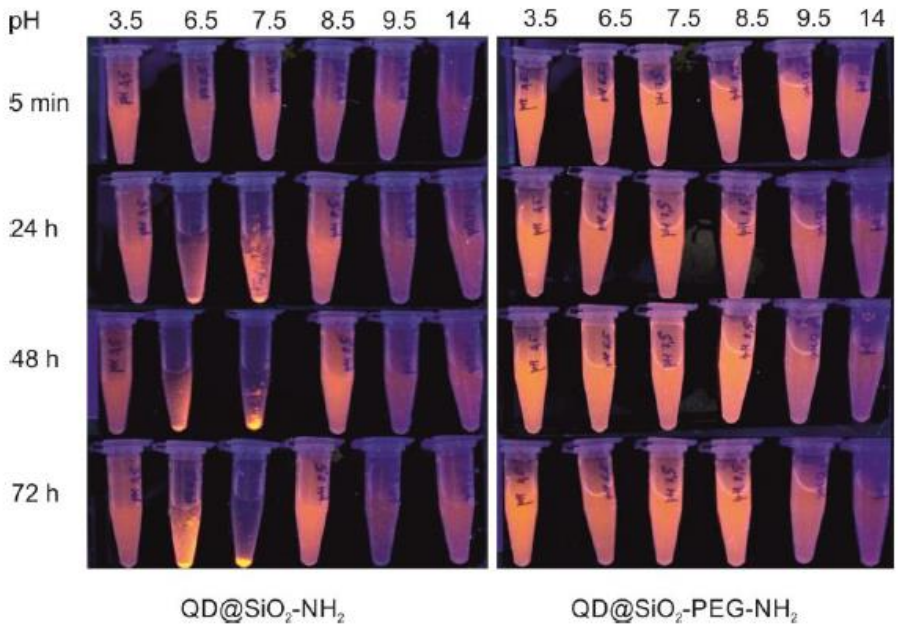

Figure 4.5. pH stability comparison of the synthesized QD@SiO_2-NH_2 and QD@SiO_2-PEG-NH_2

4.3.4. Conjugation of modified QD@SiO_2 NPs with IgG

QD@SiO_2-COOH and QD@SiO_2-PEG-COOH NPs were conjugated with IgG by means of the commonly used EDC/sNHS activation method (Hermanson, 2008). QD@SiO_2-COOH NPs lost their stability even after the activation process itself. In particular, after addition of EDC and sNHS, the NPs precipitated. In contrast, the QD@SiO_2-PEG-COOH NPs form a stable colloid solution during the activation and after the conjugation process. The same observation was made for both the amino-modified NPs, i.e. PEG-terminated QD@SiO_2-NH_2 are stable and precipitation does not happen during and after the bioconjugation process which involves the activation step using succinic anhydride and EDC-sNHS mixture.

The main advantage of using epoxy-modified NPs is high chemical activity, which eliminates the need of an activation step. But their buffer stability is poor, as such preventing efficient

binding with biomolecules. Thus, the presence of PEG-fragments on the NPs' surface plays a key role in successful bioconjugation. The length of the PEG chain (6 – 9 PEG fragments) in MPEGTMS is short enough not to block active groups that are available for bioconjugation, which is demonstrated via gel-electrophoresis (Figure 4.4). Gel electrophoresis is a commonly used technique to separate proteins, oligonucleotides, as well as NPs and their conjugates with biomolecules, based on their overall electrophoretic mobility, due to differences in molecular weight and/or overall charge. An efficient binding of QD@SiO_2 – PEG modified with carboxyl, amino and epoxy groups with IgG was proven with gel electrophoresis, i.e. the obtained QD@SiO_2-IgG conjugates and free QD@SiO_2 moved with different rates through the agarose gel (Figure 4.4). Negligible broadening of the conjugate line after electrophoresis can be explained by the fluctuation of the conjugates' masses.

4.4. CONCLUSIONS

In this chapter, the microemulsion synthesis of silica coated CdSe based QDs was clearly demonstrated. The advocated silanization method is a convenient way to obtain high quality water soluble QD@SiO_2 NPs with a controllable size whilst high PL properties are maintained. Both the size distribution and the PL properties were carefully investigated. Further, a co-condensation process allows the easy attachment of diverse functional groups to the silica surface, including PEG-fragments. This improves the buffer stability of the modified QD@SiO_2 NPs, rendering these novel PL biolabels very suitable for immunoassay detection of food contaminants. Moreover, owing to the increased buffer stability, PEG addition also makes conjugation with biomolecules (e.g. IgG) more efficient. This was investigated for QD@SiO_2 NPs modified with 3 different functional groups (amino-, carboxyl- or epoxy) and illustrated in this chapter with gel-electrophoresis.

CHAPTER 5. MULTICOLORED SILICA COATED CdSe CORE/SHELL QUANTUM DOTS

Based on

Valentina V. Goftman, Alexey V. Markin, Sarah De Saeger, Irina Yu. Goryacheva, ***"Multicolored silica coated CdSe core/shell quantum dots"*** SPIE Proceedings 2016, V. 9917, №16. Saratov Fall Meeting 2015: Third International Symposium on Optics and Biophotonics and Seventh Finnish-Russian Photonics and Laser Symposium – 2015, Saratov, Russia.

ABSTRACT

Silanization is a convenient route to obtain water-soluble QDs with different structures. Green, orange and red emitting CdSe-based QDs were synthesized by varying the number and the material of the wider-band gap shells and the PL properties of the QDs were characterized before and after silanization. It was shown that the structure of the QD influences the QY of the silanized QDs: the better the CdSe core is protected with wider-band gap semiconductor shells, the more the PL properties remain present after water solubilization. The proposed silanization method allows imparting highly hydrophilic properties to QDs with different emission colors. Hence, silica coated QDs have a great perspective for multiplex analysis.

5.1. INTRODUCTION

Nowadays, the quality of human life is determined by the accuracy of diagnostics, treatment, food control and environmental monitoring. This requires availability of sensitive multiplex assays, which simultaneously measure multiple analytes in a single cycle of the analysis. Fluorescence-based assays, especially combined with immunological techniques, can meet these requirements. QDs have been widely applied for the multiplexed simultaneous detection of different targets (Ruedas-Rama et al., 2012; Brazhnik et al., 2015; Zeng et al., 2015; Costas-Mora et al., 2014; Vu et al., 2015; Beloglazova et al., 2014).

Encapsulation of hydrophobic QDs into a SiO_2 shell is a well-known approach to make QDs soluble in water. Silica coated NPs have several advantages. In the first place, silica may

provide both chemical and physical shielding from the direct environment, thereby improving the stability. For example, it can reduce the release of heavy metal ions; prevent photooxidation processes and aggregation of the nanocrystals. Furthermore, the silica shell is highly hydrophilic and the surface chemistry of colloidal silica is well investigated. Therefore, this approach facilitates not only solubilization in different solvents, but it also enhances the bioapplicability and allows modifications of the composite particles for further use. In addition, silica spheres can contain multiple NPs per particle (e.g., gold, silver, magnetite), and can as such serve as the starting point for the development of multimodal contrast agents (Koole et al., 2008).

We are aiming to investigate how the structure (and consequently, the emission color) of the QDs impacts QY of the silica coated QDs (QD@SiO_2), obtained by means of the reverse microemulsion method, in order to obtain stable and bright multicolor labels.

5.2. EXPERIMENTAL SECTION

5.2.1. Chemicals

Cadmium oxide (CdO, 99,99%), selenium powder (Se, 99,99%), sulfur powder (S, 99%), zinc acetate ($Zn(OAc)_2$, 99,99%), OA (90%), ODE (90%), OLA (70%), ODA (90%), TOP, rhodamine 6G, TEOS, surfactant Brij L4 (M_n ~362) were purchased from Sigma-Aldrich (Bornem, Belgium). All organic solvents (ethanol, butanol, toluene, chloroform) and ammonium solution (25%) were purchased from Sigma-Aldrich (Bornem, Belgium) and were used without further purification. All other chemicals and solvents were of analytical grade. Ultrapure Milli Q water was used throughout.

5.2.2. Synthesis of core/multishell QDs

CdSe cores for QD^{550} and QD^{600} were prepared as described in section 4.2.2.

CdSe cores for QD^{630} were also prepared via a rapid hot-injection method but using different Se precursor. Briefly, 1 mmol of Se precursor solution (0.1 M Se in ODE) was injected into a three-neck flask contained 1mmol of Cd precursor solution (0.1 M CdO in OA and ODE) at 260 °C. Reaction was stopped after 30 min. To isolate CdSe QDs, addition of buthanol-ethanol

and centrifugation were done. After that the precipitate was dissolved in toluene and stored at 4 °C.

Green-emitting QDs (λ^{em}=550 nm, QD^{550}) were produced by means of the low-temperature shell growing process as described in (Beloglazova et al., 2012). Zn-precursor (0.1M $Zn(Ac)_2$ in OLA and ODE), S-precursor (0.1M S in ODE) and ODE was mixed in the atmosphere of Ar. Next, a 0.3 µmol toluene solution of CdSe was added to the mixture and the temperature was increased up to 140^0C for 2 h. To purify the CdSe/ZnS QDs from unreacted precursors, acetone was added to the CdSe/ZnS solution (V(QD solution):V(acetone)=1:2). The samples were left for 10 min and then centrifuged at 4000 rpm during 5 min. The precipitate was dissolved in a sufficient amount of toluene.

Core/shell red- and orange-emitting QDs were produced by means of the SILAR technique described in in Section 4.2.3. By means of this method, orange-emitting QDs with structure CdSe/2CdS/2CdZnS/2ZnS (λ^{em}=600 nm, QD^{600}) and red-emitting QDs with structure CdSe/3CdS/2ZnS (λ^{em}= 630 nm, QD^{630}) were synthesized (Figure 5.1).

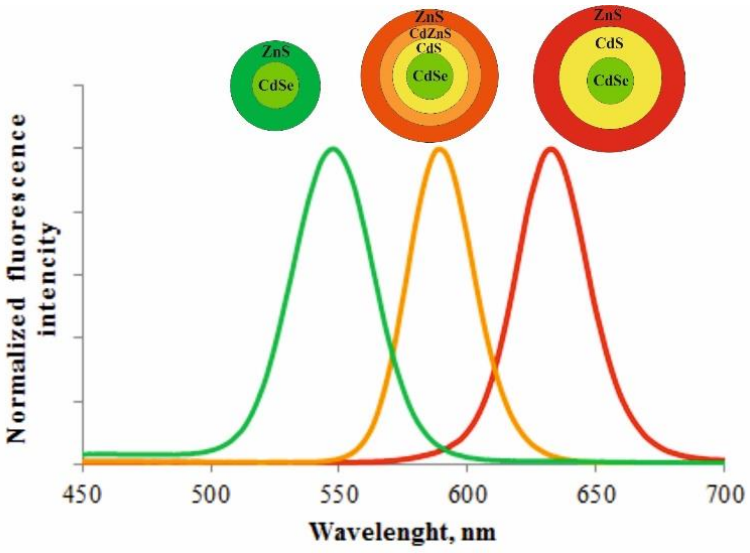

Figure 5.1. Emission spectra of the synthesized CdSe-based QDs with: ZnS shells (green line), CdS and ZnS shells (red line), and CdS and ZnS with an alloy CdZnS layer (orange line)

5.2.3. Synthesis of QD@SiO_2 NPs

The above mentioned QDs (QD^{550}, QD^{600} and QD^{630}) were encapsulated in silica NPs through the microemulsion process (Goftman et al., 2016). First, 1 mL of hexane, 0.32 mL Brij L4 as surfactant and 50 μL H_2O were mixed and let to stir for 30 min to form the microemulsion. Then, 1 nmol of QDs in chloroform was slowly added. 30 min later, 30 μL of TEOS was added, following by the addition of 10 μL NH_3 solution, which acts as the catalyst of the hydrolysis process. Subsequently, the reaction mixture was aged for 24 h at room temperature and the NPs were precipitated from the microemulsion using ethanol, centrifuged and the resultant precipitate of QD@SiO_2 particles was washed 3 times with hexane and at least 5 times with deionized water. Finally, aqueous dispersions of the composite particles were obtained via sonication.

5.2.4. Characterization techniques

For the relative QY estimation, the spectrally integrated emission of the QDs solutions was compared to the emission of a rhodamine 6G ethanol solution (QY=95% at excitation wavelength 490 nm) of identical optical density (~0.05) at the excitation wavelength (Grabolle et al., 2009). UV-vis absorption spectra of the QDs were measured by a Shimadzu 1800 spectrophotometer. PL spectra were recorded with a Cary Eclipse Fluorescence Spectrophotometer (Agilent Technologies).

5.3. RESULTS AND DISCUSSION

CdSe cores were prepared via a rapid hot-injection method in ODE using TOP as a stabilizer. To improve their PL intensity and stability, CdSe nanocrystals were covered with several shells of the wider band gap semiconductors, such as CdS and ZnS (Figure 5.1).

It is well known that ZnS is the best protecting shell for CdSe QDs because of the considerable differences in the values of the band gap energies (Protiere and Reiss, 2009). Low-temperature (120°C) synthesis was used to cover the CdSe cores directly with ZnS shells, using OA and OLA as stabilizers. This method allows increasing the QY of the QDs (by a factor of 10 on average), while the emission maximum does not significantly shift: 550 nm for the CdSe/ZnS QDs compared to 535 nm for the CdSe cores (table 5.1).

Table 5.1. Relative QY and emission maxima of the synthesized core and core-shell structures

	QY, %	**λ^{max}, nm**
CdSe	7	535
CdSe/ZnS	50	550
CdSe/CdS/CdZnS/ZnS	53	600
CdSe/CdS/ZnS	36	630

For efficient shell growing it is important to use semiconductors with similar parameters concerning their crystalline lattice. In the case of CdSe and ZnS semiconductors, these parameters are quite different. Thus it is preferable to introduce the additional middle shell (CdS or ZnSe) between the CdSe core and the ZnS outer shell to reduce strain inside the nanocrystal (Talapin et al., 2004). A high-temperature (230 ^{o}C) SILAR technique was used to cover the CdSe core with CdS and ZnS shells, using ODA as stabilizer. The difference between the band gaps of CdSe and CdS is not sufficient for a complete confinement of the electrons and holes inside the CdSe core, i.e. the hole is confined in the core but the electron is delocalized in the shell. Therefore, formation of an intermediate CdS shell around the CdSe cores results in a red shift of both the absorption and PL maxima (Figure 5.2). Due to blocking of electrons and holes inside the core, the PL intensity enhanced with each shell. Finally, the PL QY of core-shell particles reached at least 36% for CdSe/CdS/ZnS structure (table 5.1). QY of QDs based on CdSe-TOP cores was higher: for green CdSe/ZnS QDs it was 50%, and for orange CdSe/CdS/CdZnS/ZnS QDs it was 53%. As it was explained before, the alliy layer of CdZnS allows to protect luminescent core better.

The encapsulation of QDs in silica spheres can be achieved through two different methods. The first method is via Stöber synthesis, where the QDs act as seeds for silica growth in an ethanol/water mixture. Typically, this approach is applicable to initially hydrophilic QDs. This method yields single or multiple QDs per silica sphere, but the size and size dispersion of the QD/silica particles are not well-controlled.

The second method implies using a water-in-oil reverse microemulsion system, where small water droplets are stabilized by a non-ionic surfactant (e.g., NP-5, Igepal or Brij) in a continuous hydrophobic phase (e.g., cyclohexane, hexane or heptane). Hydrolysis and

condensation of the silica precursor (e.g., TEOS) take place in the water phase, resulting in highly monodisperse silica particles, even at small sizes (>25 nm).

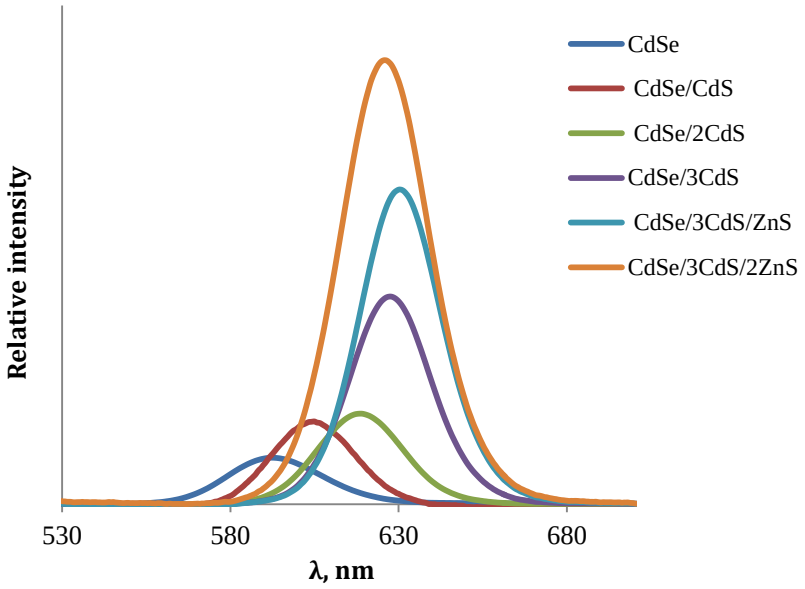

Figure 5.2. Emission spectra of CdSe cores with a varying number of CdS and ZnS shells (intensity is based on relative QY values)

The best possible mechanism of silanization in microemulsion assumes a ligand exchange: the initial hydrophobic ligands (TOP or OA) on the QD's surface are exchanged by partly hydrolyzed TEOS molecules. It results in quenching of the PL properties of the QDs, because the hydrolyzed molecule of TEOS can act as an efficient hole or electron acceptor, which introduces a new non-radiative decay pathway for the exciton (Koole et al., 2008). Also, the rate of the ligand exchange reaction dramatically affects the PL properties of the final silanized QDs. Thus, purity of TEOS affects the ligand exchange reaction rate, and, consequently, the QY of the silica coated QDs.

Long chain amines as OLA and ODA were used as a stabilizer, because they are found to be more suitable surfactants for the semiconductor nanocrystals (Talapin et al., 2004). This has been attributed to the close packing (theoretically, 100% surface coverage) of the ligands on the NP's surface and the etching of surface defects. Since ligand exchange is a key mechanism in the silanization process, it is important that the affinity of amino ligands to the QDs' surfaces allows a successful substitution with TEOS molecules. It was shown that if the

affinity of the initial ligands to the QD's surface is too high (when, for example, thiolated ligands are used as stabilizers), the possibility of ligand exchange is extremely low, which prohibits successful silica incorporation (Ren et al., 2014).

It is important to mention that the structure of the QDs also affects the PL properties of the QD@SiO_2 NPs. More specifically, the thinner the wider band gap of semiconductor shell, the higher the deterioration of the PL properties of silica covered NPs. The synthesized QD^{550} probably does not have a uniform ZnS shell to protect the CdSe core from oxidation, thus the PL properties of such QDs covered with silica shell quickly deteriorate. Even during one day of storage in a water solution, the QY immediately drops from an initial 50% down to 10% and keeps on decreasing with further storage. It may be safely assumed that the low temperature does not allow the ZnS lattice to properly build around the CdSe core, due to the considerable differences in lattice parameters.

In the meantime, the SILAR technology, owing to the high temperature of the shelling process and the intermediate CdS layer, allows better protection of the CdSe core and prevents a significant drop of the QY after silanization. The synthesized QD^{630}, with an initial QY of 36%, shows a QY of 22% after silica covering. In the case of QD^{600}, an alloy layer of CdZnS was added in between the CdS and ZnS shells. It was shown before (Zhang et al., 2008) that addition of such a layer between these shells allows retaining the original QY after the silanization process, which was confirmed by our results (table 5.2). QD^{600} with an intermediate CdZnS shell, synthesized according to the method presented in the experimental part, exhibits a relatively small QY drop from 53% to 43%, and it remains stable even after several months of storage.

Table 5.2. QYs of the synthesized QDs with different amount of shells, before and after silanization.

	QY, %		
	QDs in toluene	**QD@SiO_2 freshly prepared**	**QD@SiO_2 after 1 month of storage**
QD^{550} CdSe/ZnS	50	10	-
QD^{600} CdSe/CdS/CdZnS/ZnS	53	43	41
QD^{630} CdSe/CdS/ZnS	36	22	19

5.4. CONCLUSIONS

Green, orange and red emitting CdSe-based QDs were synthesized by varying the number and the material of the wider-band gap shells. In order to receive stable water solutions, all three of them were coated with silica shells by means of a reverse microemulsion method. The PL properties of the QDs were characterized before and after silanization. It was shown that the structure of the QD influences the QY of the silanized QDs: the more semiconductor shells protect the luminescent CdSe core of the QDs, the higher the QY remains after silanization.

CHAPTER 6. STABILITY OF POLYMER-COATED QUANTUM DOTS AFTER LYOPHILIZATION

Based on

Valentina V. Goftman, Anna V. Gaynbuch, Elizaveta V. Panfilova, Boris N. Khlebtsov, Irina Yu. Goryacheva **"Freeze-dried polymer-coated quantum dots for perspective biomedical application"**/ SPIE Proceeding 2015, V. 9448, №9. Saratov Fall Meeting: International Symposium on Optics & Biophotonics – 2014, Saratov, Russia.

ABSTRACT

Freeze-drying, also known as lyophilization, has been considered a convenient technique to improve the long-term stability of colloidal PL QDs for biomedical application. This contribution describes the synthesis of polymer-coated biocompatible CdSe-based core/shell QDs and discusses their optical and physical properties before and after freeze-drying. It is found that freeze-dried NPs can be stored for a long time under usual conditions and then can be easily redispersed in water at the desired concentration without any extra manipulations (sonication or heating).

6.1. INTRODUCTION

A tremendous amount of efforts has been devoted to the fabrication of biocompatible high quality QDs, applicable in biology and medicine. Commercial hydrophilic QDs are mostly available in a suspension colloid format. However, it is difficult to determine the exact concentration of QDs in a solution. Thus, in the context of clinical QDs applications, there is an obvious need for a powder alternative of fluorescence labels. The goal is to conceive a convenient technology to produce stable and water-soluble nanopowders, which after solubilization retain all physicochemical and optical properties of the initial functionalized colloidal QDs. Such powders could be stored for a longer time under usual conditions and could be easily dissolved at a desired concentration (Khlebtsov et al., 2012).

The quality of dried QDs mostly depends on the dehydration method. As all NPs, QDs show a strong tendency to agglomerate after being isolated from their colloidal suspensions. It leads to a red shift of both the absorption and emission spectra (Cao 2012). Freeze-drying is a mild and less damaging method, which allows obtaining stable NP powders, while retaining the physicochemical and optical properties of the initial colloidal particles.

However, general stability of QDs to the big extend depends on the structure of outer layer of ligands which provide stability in hydrophilic surrounding. It is important to know how structure of external molecules affects optical properties of QDs after lyophilization. Here we discuss the colloid stability and physical and optical properties of CdSe-based QDs covered with two different PEG contained amphiphilic polymers, before and after freeze-drying. Encapsulation of QDs with amphiphilic polymers is one of the most used approaches for QDs hydrophilization alongside with silanization, because the original hydrophobic ligands are not removed from the QDs surface, which ensures preservation of the initial brightness (Speranskaya et al., 2014).

Moreover, polymer coating allows modification of the outer hydrophilic layer. For example, it was proven that introduction of PEG chains into amphiphilic molecules leads to an improved colloidal stability of QDs over a wide pH range and it reduces the non-specific binding to biomolecules and carriers.

6.2. EXPERIMENTAL SECTION

6.2.1. Materials and methods

Poly(maleic anhydride-alt-1-octadecene) (PMAO, M ~ 30 000-50 000 g/mol), ethanol abs. (99,99%) were purchased from Sigma-Aldrich (Bornem, Belgium). Jeffamine M1000 (1000 g/mol) and Jeffamine ED2000 (2000 g/mol) were kindly provided by Huntsman (Belgium). Chloroform, butanol, toluene, acetone were purchased from Labtech company (Moscow, Russia).

The UV-vis absorption spectra of QDs were measured with a Shimadzu 1800 spectrophotometer (Kyoto, Japan). The PL spectra were recorded with a fiber-optic spectrofluorimeter AVALIGHT-LED-380 (Avantes, Apeldoorn, the Netherlands). The

hydrodynamic radius and ζ-potentials were measured with a Zetasizer Nano-ZS instrument (Malvern, U.K.).

6.2.2. Synthesis of QDs

Synthesis of core-shells QDs was performed according to the Section 4.2.2 and 5.2.2.

6.2.3. Amphiphilic polymer synthesis

For the amphiphilic polymer preparation, the PMAO polymer was conjugated with polyoxyethylene/polyoxypropylene block-copolymers, containing one primary amine group (Jeffamine M1000) or two primary amine groups (Jeffamine ED2000), using the method described in (Speranskaya et al., 2014). Amphiphilic polymers with carboxyl functional groups were synthesized by dissolving Jeffamine M1000 (2 g) in chloroform (~15 mL) and then added drop by drop to a flask containing 1 g of PMAO powder. PMAO was readily dissolved in the solution, the mixture was heated up to 60^{o}C under the inert atmosphere and left to stir overnight.

The synthesis of amphiphilic polymer with amine functional groups was done similarly by dissolving PMAO powder (0.25 g) in chloroform (10 mL), containing 0.25 g of Jeffamine M1000 to initiate the ring opening process, and then added in drops to Jeffamine ED2000 powder (2.5 g). Again, the mixture was left to stir overnight after heating up to 60^{o}C. A large excess of amine was used to avoid cross-linking of the polymer chains.

6.2.4. Encapsulation of QDs and their lyophilization

For encapsulation, the QDs and the synthesized amphiphilic polymer were mixed in chloroform and stirred overnight at room temperature (molar ratio of QD to polymer was ~1:40). Next, a 0.1M $NaHCO_3$ solution was added to the QD-polymer chloroform solution and the chloroform was slowly evaporated by a Bunsen's water-air-jet pump, resulting in a clear fluorescent water solution of QDs. Any excess of polymer was removed with centrifugation. Finally, the water-soluble QDs were transferred to a sterile bottle, frozen in liquid nitrogen, and freeze-dried overnight under vacuum.

6.3. RESULTS AND DISCUSSIONS

The great advantage of polymer encapsulation of QDs is that it allows retaining the initial PL intensity after the hydrophilization process. The hydrocarbon chains of the amphiphilic polymer attach to the stabilizing hydrophobic ligands (OLA) on the QDs surface using hydrophobic interactions, and the hydrophilic parts of the amphiphilic polymer are exposed to the solution and provide colloidal stability in aqueous solutions. Since the initial hydrophobic ligands remain attached to the QD's surface, it prevents damaging of the QD crystalline structure and, consequently, quenching of PL.

PMAO (Figure 6.1) is a widely used polymer for hydrophilization of QDs. Hydrophobic octadecene residues orient the polymer molecule around the nanocrystal, and the maleic anhydride rings open in the alkaline solution, resulting in the formation of hydrophilic carboxyl ions that can stabilize an aqueous QD solution by means of electrostatic repulsion.

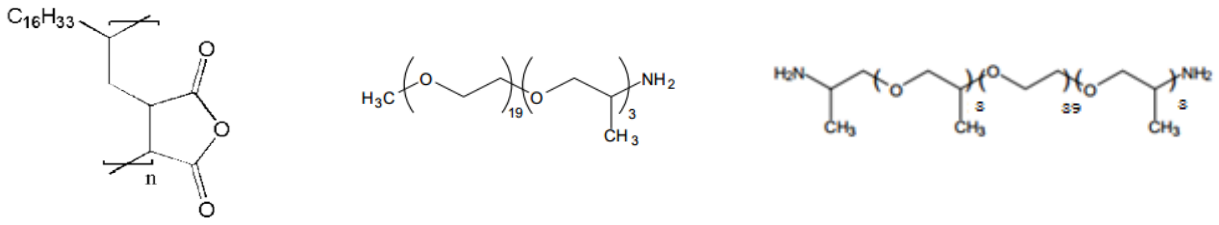

Poly(maleic anhydride-alt-1-octadecene)

Jeffamine M1000

Jeffamine ED 2000

Figure 6.1. Structures of polymers, used for the QDs hydrophilization: PMAO and Jeffamines with different structures and molecular weights

It is important to mention that the presence of PEG groups is preferred for potential bioapplicaiton of the QDs, as it minimizes non-specific interactions of the QDs with biological material and increases their buffer stability. In this work, we used analogues of PEG, i.e. commercially available polyetheramine Jeffamines (Figure 6.1). Their primary amine groups easily react with maleic anhydride groups at room temperature. We used Jeffamine M1000 to produce amphiphilic polymers and Jeffamine ED-2000 to vary charge and length of the PEG chain. We used JeffamineM1000 to produce amphiphilic polymers with carboxyl

functional groups and Jeffamine ED2000 to produce polymers with primary amine groups for further conjugation.

QDs with three different structures and, consequently, emission colors were synthesized varying number and composition of the wider band gap semiconductor shells (Figure 6.2). All three of them were transferred to the water solutions using co-polymers of PMAO with Jeffamines. After water solubilization there was no shift of the PL maxima and absorbance spectra, and the PL brightness of QDs covered with PMAO–Jeffamines amphiphilic polymers only slightly decreased after solubilization in water (table 6.1).

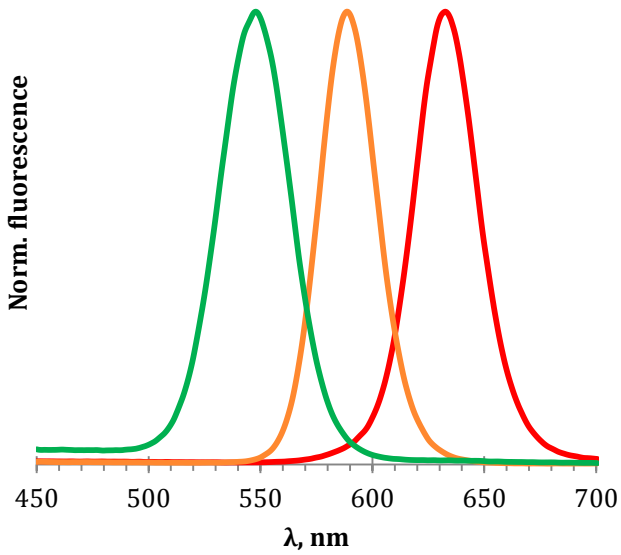

Figure 6.2. Emission spectra of polymer coated water-soluble QDs with different structures: CdSe/ZnS (green line), CdSe/CdS/CdZnS/ZnS (orange line) and CdSe/CdS/ZnS (red line). All spectra are normalized to the peak maximum

The prepared water-soluble QDs were freeze-dried and converted into a fluorescent powder. The fabricated powder of polymer-coated QDs can be easily dissolved in water after mild shaking without deterioration of optical properties (table 6.1). The shape of the absorption spectra and the exciton peak position did not differ after freeze-drying which indirectly testifies for the preservation of QDs size after lyophilization.

Table 6.1. Relative brightness of the QDs, covered with different PEG-polymers, and those, redispersed after freeze-drying. Numbers are based on the relative QY values

QD's structure	λ^{em}, nm	PL intensity, relative units			
		PMAO-Jeffamine M1000		PMAO-Jeffamine ED2000	
		initial	redispersed	initial	redispersed
CdSe/ZnS	547	1	0.92	1	0.88
CdSe/CdS/CdZnS/ZnS	589	1	0.92	1	0.86
CdSe/CdS/ZnS	629	1	0.94	1	0.86

It is interesting to mention that the structure of the PEG polymer affects the PL properties of the QDs after freeze drying (table 6.1). QDs modified with monoamine Jeffamine M1000 possess a sufficient negative surface charge (ζ-potential is -35 mV) and a shorter PEG chain (1000 g/mol), which explains the stability of the colloid before and after freeze-drying (table 6.2). In contrast, the end amino-group of Jeffamine ED2000 makes the ζ-potential of water-soluble QDs more neutral (-5 mV in average). Thus, the general stability of such QDs is lower, and lyophilization causes a more considerable drop of the PL properties.

Table 6.2. Zeta-potentials of the QDs, covered with different PEG-polymers, and those, redispersed after freeze-drying

QDs structure	λ^{em}, nm	ζ-potential, mV			
		PMAO-Jeffamine M1000		PMAO-Jeffamine ED2000	
		initial	redispersed	initial	redispersed
CdSe/ZnS	547	-34.2±4.7	-36.1±5.6	-4.9±4.4	-5.7±3.5
CdSe/CdS/CdZnS/ZnS	589	-33.7±4.8	-35.1±3.5	-3.7±2.5	-4.6±3.2
CdSe/CdS/ZnS	629	-39.9±5.7	-35.5±6.5	-3.7±2.5	-4.6±3.2

The size distribution was measured with Zetasizer Nano instrument (table 6.3). It should be emphasized that after double freeze-drying, due to the electrostatic repulsion of the PEG chains, QDs still did not aggregate and could be easily redispersed, albeit with further decreasing of their brightness.

Table 6.3. Hydrodynamic radii of QDs covered with PMAO-Jeffamine M1000 and redispersed from the powders after two consecutive freeze-drying steps, measured by dynamic light scattering

QDs structure	Hydrodynamic radius, nm		
	initial	1st freeze-drying	2nd freeze-drying
CdSe/ZnS	37±2	38±2	39±2
CdSe/CdS/CdZnS/ZnS	39±2	37±2	39±2
CdSe/CdS/ZnS	45±3	44±3	47±3

6.4. CONCLUSIONS

In summary, water-soluble QDs covered with amphiphilic polymers were synthesized and freeze-dried to obtain stable PL powders that retain all physicochemical and optical properties of the initial colloid solutions. Such powders can be stored for a long time under normal conditions and can be easily dissolved at a desired concentration in water or any aqua buffer solution. It was also shown, that the structure of the polymer shell affects the PL properties of QDs after lyophilization. E.g. zeta potentials, which basically are determined by the end functional group of the polymer, play a crucial role in NPs stability, especially after freeze-drying.

CHAPTER 7. HYDROPHILIC QUANTUM DOTS STABILITY AGAINST AN EXTERNAL LOW-STRENGTH ELECTRIC FIELD

Based on

Valentina V. Goftman, Vladislav A. Pankratov, Alexey V. Markin, Dries Vande Ginste, Sarah De Saeger, Irina Yu. Goryacheva **"Hydrophilic quantum dots stability against an external low-strength electric field"**, Applied Surface Science, 2016, 363, 259–263.

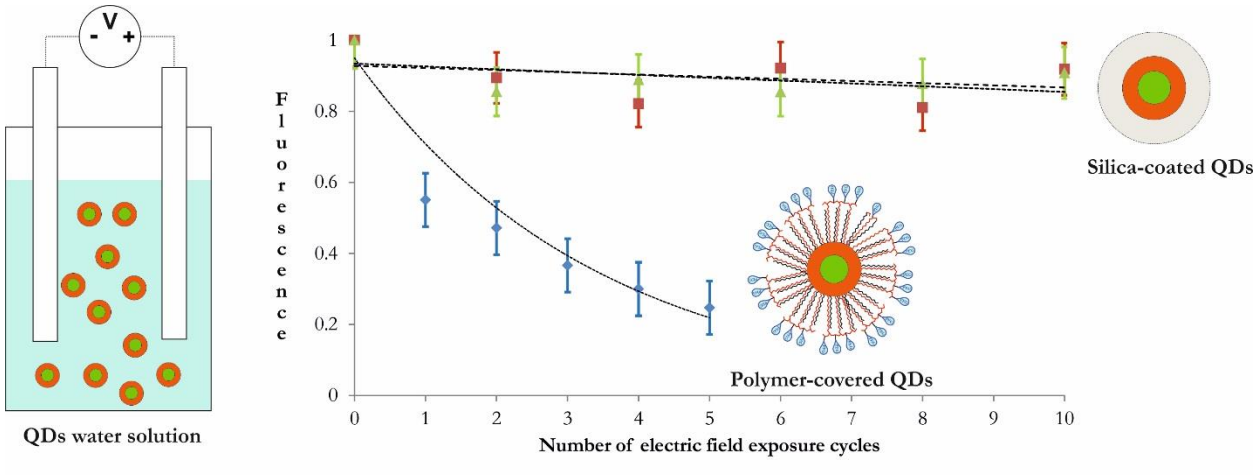

ABSTRACT

Since the stability of nanobiolabels plays a key role in their application, we thoroughly investigated how an external, low-strength electric field (EF) impacts on the PL properties of hydrophilic QDs. Two fundamentally different approaches were applied to make the QDs water-soluble, i.e. ligand exchange (namely silica covering) and encapsulation with an amphiphilic polymer. It is shown that, even under a low-strength EF, the polymer-coated QDs could lose 90% of their brightness because of the weak interaction between the QD's surface and the polymeric molecule. Silica-covered QDs, on the contrary, stay bright and stable owing to the covalently attached dense silica shell. These findings, which are clearly explained and

illustrated in this chapter, are of critical importance in the context of hydrophilic QDs' bioapplication.

7.1. INTRODUCTION

The stability of hydrophilic QDs against chemical, biochemical, and physical influences is especially important for their *in vitro* and *in vivo* applications**.** Some physical intracellular delivery strategies (e.g., electroporation) imply a rapid high-strength EF impulse in order to temporarily generate hydrophilic pores in the cell plasma membrane, necessary for the passive transportation of QDs into the cell (Zhang et al., 2006). Also, QDs are widely used as electrochemical sensors or for electrophoretic separation of labeled biomolecules, which implies a low-strength EF impact.

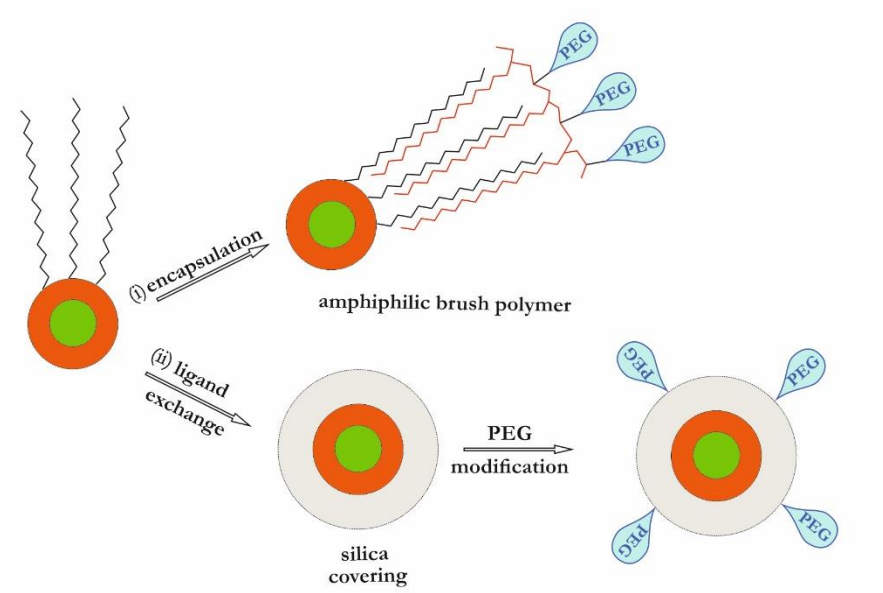

Figure 7.1. Scheme of the QDs hydrophilization techniques : (i) encapsulation in an amphiphilic brush polymer shell and (ii) silica covering with further PEG modification

It is interesting to investigate how different capping layers, meant to provide high stability and sufficient PL properties of QDs in a water solution, behave under adverse conditions, such as when being subjected to an EF. In this chapter, aqua solutions of the synthesized hydrophilic QDs were exposed to a low-strength EF and their PL properties were carefully

investigated. To compare different capping layers, hydrophobic core-shell CdSe/CdS/CdZnS/ZnS QDs (λ_{em}=600 nm) were transferred to a water solution using two of the most commonly used methods: (i) encapsulation in an amphiphilic brush polymer based on PMAO modified with PEG chains and (ii) silica covering, based on the ligand exchange technique.

7.2. EXPERIMENTS

7.2.1. Chemicals

Cadmium oxide (CdO, 99,99%), selenium powder (Se, 99,99%), sulfur powder (S, 99%), zinc acetate ($Zn(OAc)_2$, 99,99%), OA (90%), ODE (90%), OLA (70%), ODA (90%), TOP, rhodamine 6G, TEOS, surfactant Brij L4 (M_n~ 362), and PMAO (M ~ 30 000 - 50 000 g/mol) were purchased from Sigma-Aldrich (Bornem, Belgium). MPEGTMS was purchased from Gelest Inc. (USA). Jeffamine M1000 (1000 g/mol) was kindly provided by Huntsman (Belgium). All organic solvents (ethanol, butanol, toluene, chloroform) and ammonium solution (25%) were purchased from Sigma-Aldrich (Bornem, Belgium) and were used without further purification. All other chemicals and solvents were of analytical grade. Ultrapure Milli Q water was used throughout.

7.2.2. QDs synthesis

Synthesis of core-shells QDs was performed according to the Section 4.2.2 (Figure 7.2). By means of this method, QDs with structure CdSe/2CdS/2CdZnS/2ZnS (λ_{em}=600 nm,) were synthesized.

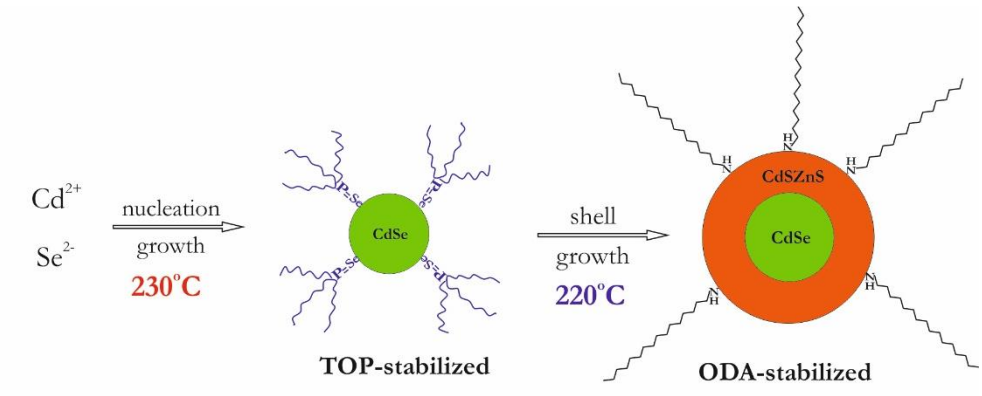

Figure 7.2. Scheme of the high-temperature colloid QDs' synthesis

7.2.3. Water-solubilization of QDs with amphiphilic polymer

The amphiphilic polymer was synthesized by dissolving JeffamineM1000 (2 g) in chloroform (15 mL) and then adding it drop by drop to a flask containing 1 g of PMAO powder, as described in (Speranskaya et al., 2014). Next, 60 nmol of QDs in chloroform was mixed with the synthesized PMAO-Jeffamine co-polymer (the molar ratio QD:polymer was 1:40) and left stirring for 24 h. To transfer the QDs to the aqueous media via the reverse phase evaporation approach, 10 mL of 0.1M $NaHCO_3$ buffer was added to the QD–polymer chloroform mixture. Afterwards, the chloroform was slowly evaporated by a rotary evaporator and a clear fluorescent solution was obtained.

7.2.4. Water-solubilization of QDs with silica covering

The above mentioned QDs were encapsulated in silica NPs through the water-in-oil microemulsion process as described in (Goftman et al., 2016). Briefly, a microemulsion, consisting of 1 mL hexane, 0.32 mL Brij L4 as surfactant and 50 µL H_2O, was prepared. Then, 1 nmol of QDs in chloroform was slowly added. 30 min later, 30 µL of TEOS was added, followed by adding 10 µL of NH_3 solution. Subsequently, the reaction mixture was aged for 24 h at room temperature resulting in QDs covered with silica shell (QD@SiO_2). PEG-terminated QD@SiO_2 were prepared next via addition of MPEGTMS (3 µL) to the microemulsion and stirring for another 24 h. After that, the NPs were separated from the solution and washed up via high-speed centrifugation (20 000 g). Finally, aqueous dispersions of the composite particles were obtained via sonication.

7.2.5. Electric field

The samples were subjected to an EF by using a Zetasizer Nano (Malvern, UK) in the mode for zeta potential (ZP) measurements. A universal dip cell for ZP measurement with palladium electrodes was used. For the measurements, first, 1 mL of the QD aqueous solution was placed into the polystyrene cuvette and the electrodes were dipped into the sample. Next, the EF treatments were carried out by cycles, varying from 1 to 10 cycles. Thereto, a combination of alternate and direct voltages was applied to the electrodes (Figure 7.3). As a potential difference between the electrodes of maximum 5 V was used in all measurements

and as the distance between the electrodes is about 5 mm, the EF strength was about 10 V/cm.

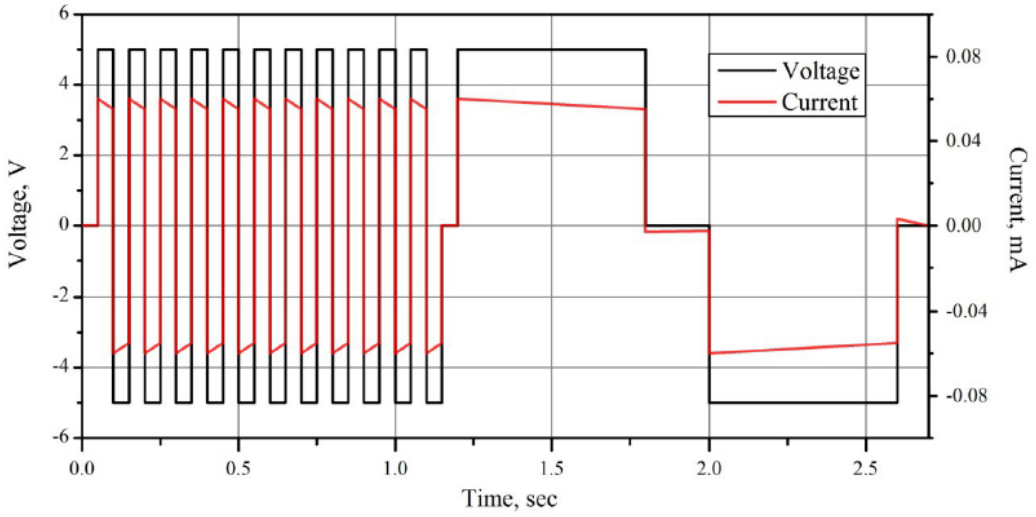

Figure 7.3. Voltage-time and current-time curves as applied to the universal dip cell's palladium electrodes to carry out one EF treatment cycle onto the QD aqueous solutions (Zetasizer Nano data)

The PL measurements of the hydrophilic QDs after EF treatments were performed by probing with a nano-laboratory Ntegra Spectra (NT-MDT, St. Petersburg, Russia), leveraging a 473 nm laser as excitation source. The PL measurements were performed after every cycle.

7.3. RESULTS AND DISCUSSION

7.3.1. Synthesis and characterization of the QDs

As stated above, CdSe cores were prepared via a rapid hot-injection method using TOP as a stabilizing ligand. To improve the PL intensity and stability, the CdSe nanocrystals were covered with an inorganic shell of the wider band-gap semiconductors CdS and ZnS. The synthesized QDs with the structure CdSe/CdS/CdZnS/ZnS showed a narrow symmetrical emission spectrum, more specifically, a FWHM of 30 nm with a maximum at λ=600 nm. The average size of the nanocrystals was 6 nm. TEM images of core–shell QDs, as well as the relative QY of the obtained QDs, are presented in Figure 7.4.

7.3.2. QDs hydrophilization

A polymer encapsulation preserves the initial ligands on the QDs' surface owing to the hydrophobic interaction between the ODE chains of the synthesized amphiphilic polymer and the ODA ligands on the QDs' surface (Figure 7.1). This covering process allows maintaining the initial PL properties, but the size and shape of obtained polymer shell is very sensitive to the changes in environment, e.g. pH range of water media. This fact complicates their molecular binding, delivery and migration in cells and tissues, and *in vivo* biodistribution (Smith and Nie, 2008).

However, covering with a silica shell, by means of the reverse microemulsion method, allows controlling the size (the average size is 27 nm) and maintaining PL properties (QY=43%) of the initial QDs (Figure 7.4), despite the initial ligands' exchange. PEG fragments (Figure 7.1) were added onto the QD@SiO_2 surface to increase the buffer stability of the NPs (Goftman et al., 2016). Thereby, the risk of agglomeration in biological fluids is remarkably reduced (Hezinger et al., 2008). Furthermore, this modification results in a reduced non-specific interaction of the obtained NPs with biomolecules.

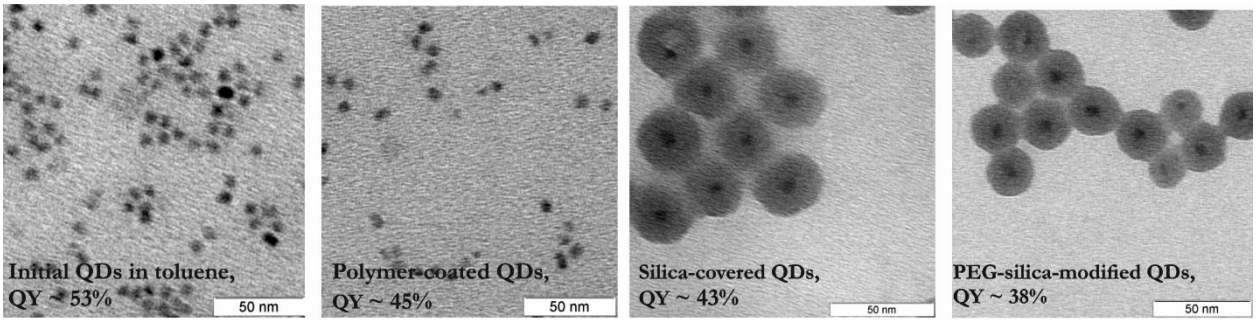

Figure 7.4. TEM images of the synthesized QDs (from the left to the right): initial hydrophobic in toluene, water solutions of polymer-coated, silica-covered and PEG-modified silica-covered QDs.

7.3.3. Impact of an external low-strength electric field on the QDs

The obtained water solutions of silica coated QDs and their PEG-terminated modifications, as well as polymer covered QDs, in a concentration of ~ 10^{-8} M, were exposed to a low-strength EF for a short time and the PL properties were investigated. The EF strength about 10 V/cm was chosen to model conditions approximate to the mentioned potential applications (for example, EF strength during electrophoresis reaches about 7 V/cm). Figure

7.5, the changes in the PL intensity of three different types of hydrophilic QDs as a function of the electrical field treatment cycles are presented. It is clearly observed that both silica-covered QD samples remain stable, whereas polymer-coated QDs lose their initial brightness with each cycle such that it was useless to expose it to the EF for more than 5 cycles.

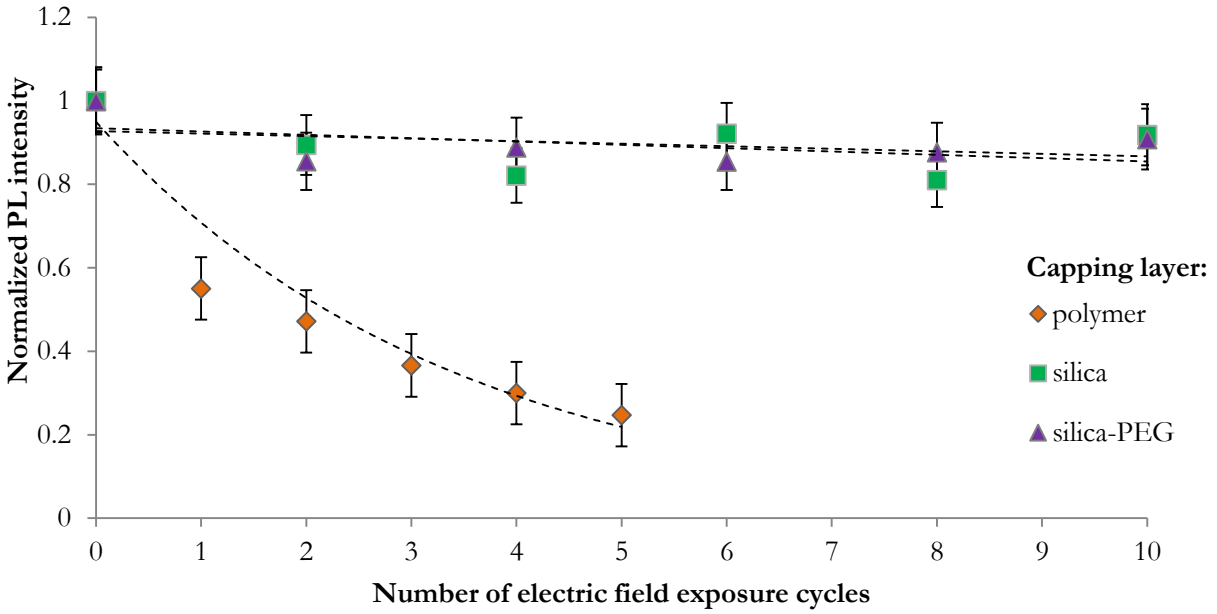

Figure 7.5. Changes in the PL intensity of hydrophilic QDs (encapsulated in polymer shell, covered with silica shell and with PEG-modified silica shell) as a function of the number of EF treatment cycles. c (QD) ~ 10^{-8} M. The data indicate the average of a threefold determination

Before explaining the observed behavior of Figure 7.5, it is interesting to mention that the influence of high-strength EF on the QDs has been widely studied for hydrophobic nanocrystals in solid matrices with a view to characterize the quantum-confined Stark effect, which causes reversible quenching of the PL and a shift of the emission maximum. According to literature (Gurinovich et al., 2012; Bozyigit et al., 2013), an EF of 10 V/cm is not strong enough to induce the Stark effect and would as such not impact on the PL properties (Miller et al., 1984). Nonetheless, we still observe quenching of the PL of the polymer-coated QDs when this weaker EF was applied. The reason for this effect could be weak hydrophobic interaction (<40 kJ/mol) between the amphiphilic polymer and the QD's surface. Moreover, the polymers' molecules possess a negative charge because of the remaining carboxylic groups on the PMAO chains, so that they could start to move towards the anode in the presence of the EF, albeit weak. This process destroys the homogeneity of the whole amphiphilic shell and it dramatically decreases the PL properties (dropping to 20% from its

initial value, Figure 7.5) because of the direct contact of the QDs with the strongly oxidative environment (water).

In contrast, a silica shell is covalently attached to the QD's surface and forms a rigid dense structure, which allows retaining 90% of its initial PL intensity, even after a longer impact of the EF (Figure 7.5). Also, addition of polymeric fragments, such as PEG chains, to the silica coated QDs does not affect their stability.

7.4. CONCLUSION

Stability comparison of hydrophilic QDs covered with different capping layers was performed. In particular, the influence of low-strength EF was investigated for amphiphilic polymer-coated and silica-covered CdSe-based QDs. It was shown that the hydrophilic shell affects the PL properties of the QDs under a low-strength EF. Hydrophobic forces, which bind the QD and the amphiphilic polymer molecule, are not strong enough to withstand the electrostatic attraction between the negatively charged polymer molecule and the anode. In contrast, the covalently bonded silica shell prevents any destruction and oxidation process under the influence of the EF and, as such, the NPs maintain their initial PL brightness. Thus, silica shells are clearly a preferable covering in the context of bioapplication of the QDs, because – besides their high uniform morphology, controllable size and biocompatibility – it allows protecting the QDs under the adverse physical conditions presented in this chapter.

CHAPTER 8. APPLICATION OF SYNTHESIZED LUMINESCENT BIOLABELS FOR MYCOTOXIN DETECTION

Based on

Valentina V. Goftman, Tangi Aubert, Dries Vande Ginste, Rik Van Deun, Natalia V. Beloglazova, Zeger Hens, Sarah De Saeger, Irina Yu. Goryacheva, **«Synthesis, modification, bioconjugation of silica coated fluorescent quantum dots and their application for mycotoxin detection»**, Biosensors and Bioelectronics, 2016, 79, 476–481.

and

Beloglazova N.V., Speranskaya E.S., Wu A., Wang Z., Sanders M., Goftman V.V., Zhang D., Goryacheva I.Y., De Saeger S. **"Novel multiplex fluorescent immunoassays based on quantum dot nanolabels for mycotoxins determination",** Biosensors and Bioelectronics 2014, 12 (62), 59-65.

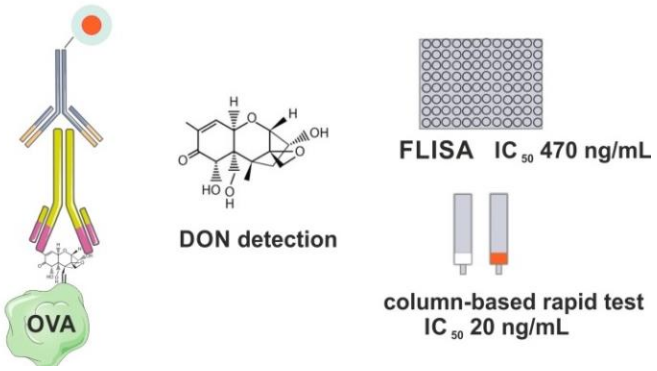

8.1. INTRODUCTION

Owing to simplicity and cheapness coupled to sensitivity and selectivity, immunoassays are preferably employed for the first level screening and survey studies on mycotoxin contamination (Goryacheva et al., 2007). The most common type of immunoassay for mycotoxin detection is enzyme-linked immunosorbent assay (ELISA). Currently, ELISA kits are commercially available for all regulated mycotoxins with the average price for single

analyte immunoassay kit of several hundred euros per one analyte (Sigma Aldrich). Enzyme labels offer high sensitivity, but also require an extra step of analysis, being addition of chromogenic substrate. Whereas PL labels use the emitted light as an analytical signal. This offers the opportunity to reduce the time of analysis while remaining the high sensitivity. Thus, FLISA is becoming more and more favored for mycotoxin detection, and QDs are turning out to be a very sensitive biolabel, due to their brightness and photostability.

It is important to mention, that within the wide range of FLISA design, direct and indirect formats can be distinguished. Direct competitive immunoassay implies absorption of specific antibodies on the solid surface. Next, fixed amount of labeled antigen is incubated in presence of sample solution (competition), and the labelled antigen – antibody complex is detected. Indirect immunoassay comprises adsorption of antigen on the solid surface, followed by addition of specific antibody together with the sample. The amount of bounded immunocomplexes is detected by addition of labeled secondary antibodies. Thereby, QDs can be coupled to the antigen molecule or to the secondary antibody. It is important to keep in mind that the conjugation path can influence the affinity of immunoreagents, therefore selection of linkers and optimization of method should be done.

In this chapter, luminescent conjugates based on QDs with different capping layers were used to develop direct and indirect FLISA formats for detection of deoxynivalenol (DON) mycotoxin.

DON is a natural-occurring mycotoxin mainly produced by *Fusarium graminearum*. It is also known as vomitoxin due to its strong emetic effects after consumption. DON contaminates important cereals such as oats, barley, wheat, corn and sorghum (Sobrova et al., 2010). Structurally, it is a polar organic compound, which belongs to the type B trichothecenes and its chemical name is 12,13-epoxy-3α,7α,15-trihydroxytrichothec-9-en-8-on (Figure 8.1). One of the most important physicochemical properties of DON is its ability to withstand high temperatures (no reduction of DON concentration is observed after 30 min processing at 170°C). Thus, DON is found in flour, bread, noodles, beer and malt. DON and its metabolites, although in a low concentration, are also found in eggs and milk.

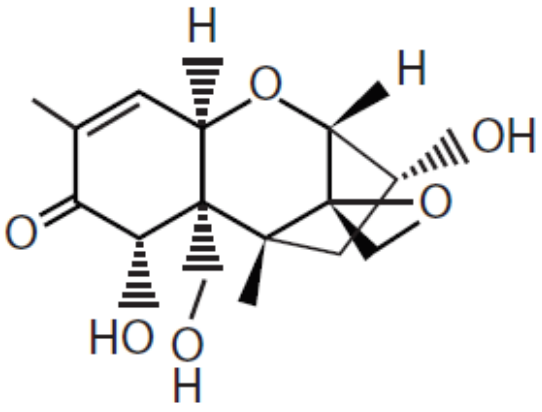

Figure 8.1. Chemical structure of DON

Owing to the prevalence of DON contaminated food and feed, immunochemical methods have become a convenient route for rapid evaluation of the product's safety. To detect DON, different formats of immunoassay were developed, using enzymes, gold NPs, fluorescent molecules and surface plasmon resonance structures as labels (Kolosova et al., 2008; Schneider et al., 2000; Kadota et al., 2010). QDs appeared to be novel PL labels for immunoassays for DON detection (Speranskaya et al., 2014; Beloglazova et al., 2014).

In order to obtain a PL label for indirect FLISA, the QD@SiO_2 NPs, modified with amino group, were conjugated with IgG. The synthesized QD conjugate was successfully applied as a novel label in a microtiter plate based immunoassay and a quantitative column-based rapid immunotest for DON detection.

In order to obtain a PL label for direct FLISA, the polymer coated QDs with available amino group were conjugated with DON-modified protein. The synthesized conjugate was successfully applied as a PL label in a microtiter plate based immunoassay for DON detection.

8.2. EXPERIMENTS

Throughout this chapter, the synthesized QD@SiO_2 NPs and polymer covered QDs were used. Synthesis protocols are given in Chapters 4, 6 and 7.

8.2.1. Chemicals

Rabbit anti-mouse IgG 2 g/L were purchased from Dako Denmark A/S (Glostrup, Denmark). Specific anti-DON monoclonal antibodies (MAb) as well as DON-OVA conjugates were prepared in-house (Sanders et al., 2014; Maragos and McCormick, 2010). DON, Tween 20 (Tween; polyoxyethylenesorbitan monolaurate), EDC, sNHS, NHS, BSA, albumin from chicken egg white (OVA), 4-(N-Maleimidomethyl)cyclohexane-1-carboxylic acid 3-sulfoN-hydroxysuccinimide ester sodium salt (sulfo-SMCC), 3-(2 pyridyldithio)propionic acid N-hydroxysuccinimide ester (SPDP), dithiothreitol, DMF, MES, casein sodium salt from bovine milk, skim milk powder, phosphate buffered saline tablets, carbonate bicarbonate buffered saline tablets, Greiner high and medium binding 96 well black plates and sealing film for 96-well multiwell plates were purchased from Sigma-Aldrich (Bornem, Belgium). Plastic tubes (Bond Elut reservoir, 1 mL) and polyethylene frits (¼ in. diameter) were supplied by Varian Belgium NV/SA (Sint-Katelijne-Waver, Belgium).

8.2.2. Conjugation of QD@SiO_2 NPs

QD@SiO_2-PEG-NH_2 NPs were conjugated with IgG by means of the method described in (Liu et al., 2007). After washing with DMF twice, 700 µL of NPs were mixed with 10% succinic anhydride in DMF (0.32 g succinic anhydride, 3 mL DMF). The reaction continued for 18 h under N_2 gas at 4 ^{o}C. Through this process, carboxyl groups were formed onto the NPs' surface. Next, the NPs dispersed in Milli-Q water were added to 0.2 mL 100 mM MES buffer, containing 0.01 g EDC and 0.015 g NHS and mixed for 5 min. Finally, 300 µL IgG (2 g/L) was introduced and mixed 2 h at 37 ^{o}C, followed by adding 1.4 mg BSA to reduce the effects of non-specific binding of the obtained conjugates. The prepared conjugates were kept at 4 °C

.

8.2.3. Indirect FLISA

The 96-well opaque black microtiter plates were coated with 100 µL/well of DON-OVA conjugate (5 µg/mL) in coating buffer (0.05 M sodium carbonate buffer, pH 9.6) by a 2 h incubation at 37 ^{o}C. The plates were covered with adhesive plate sealing films to prevent evaporation. Next, the plates were washed three times with PBS-Tween (0.05 %, v/v) followed by blocking with the blocking buffer (PBS containing 1% casein, w/v, 300 µL/well) for 1 h at 37 ^{o}C. After the blocking step, each plate was washed four times with PBS-Tween

(0.05 %, v/v, 300 µL/well). Different concentrations of DON standard solutions in PBS and primary mouse anti-DON antibody diluted with PBS (1:20,000, 100 µL/well) were added and the plates were incubated for 2 h at 37 °C. The plates were further washed three times with PBS-Tween (0.05 %, v/v). The QD@SiO_2-PEG-NH_2-IgG conjugate diluted with PBS (1:300) was added to each well (50 µL per well). The plates were then washed three times. The PL was measured using a Tecan Safire Multi-detection Microplate Reader.

8.2.4. Polyethylene frit-based indirect immunoassay

The frit-based column immunoassay procedure was described in previous publications (Beloglazova et al., 2013; Goftman et al., 2012). First, after degassing of the polyethylene frits by placing them in ethanol and ultrasonication for 10 min, they were inserted into the column. Carbonate buffer (1.5 mL, 0.1 M $NaHCO_3$, 0.1 M Na_2CO_3, pH 9.5) was then passed through the column. Absorption of the DON-OVA conjugates onto the frit was performed by adding 100 µL of the DON-OVA dissolved in carbonate buffer (dilution 1:1500) onto the column, followed by incubation for 5 min at room temperature. Each column was then washed with 1 mL of carbonate buffer. The frit surface was blocked with 100 µL of blocking solution (PBS-0.1% casein) for 5 min. Next, the frit was washed with 1 mL of PBS. Mixtures of different concentrations of DON standard solutions in PBS (50 µL) and primary mouse anti-DON antibody diluted with PBS (1:2000, 50 µL) were passed through the column, followed by a washing step with 1 mL of PBS. After that, 50 µL QD@SiO_2-PEG-NH_2-IgG conjugates was passed through the column followed by washing with 1 mL of PBS, containing 0.5% Tween. Finally, the frits' PL was measured using a fluorescence spectrophotometer equipped with a microplate reader.

The sigmoidal standard curves for both immunoassays were plotted in a semi-logarithmic scale, showing the relative PL intensity at 600 nm (λ^{ex} = 388 nm) *vs.* the logarithm of DON concentration. The limit of detection (LOD) of the developed methods was determined as the concentration at which the signal-to-noise ratio equals to 3.

8.2.5. Conjugation of polymer coated QDs with mycotoxins

For coupling of DON-OVA with NH_2-containinig QDs, thiolation of DON-OVA with SPDP was done. In parallel, sulfoSMCC was used to modify NH_2-containinig QDs. SPDP (100 nmol in ethanol) was added dropwise to DON-OVA solution (20 nmol in sodium phosphate, pH~7.5).

The reaction mixture was incubated for 30 min at RT under constant stirring, and after, excess of SPDP was removed by the protein concentrator tube. The residue was reconstituted in sodium acetate buffer (pH~4.5). For pyridine-2-thione release, dithiothreitol (250 nmol in water) was added dropwise to the modified protein conjugate. The reaction mixture was incubated for 30 min at RT under constant stirring, and then excess of dithiothreitol was removed by the protein concentrator tube. The modified conjugates were redissolved in sodium phosphate solution. In parallel, sulfo-SMCC (2 mg) was added dropwise to the QD solution (1 nmol). The reaction mixture was stirred for 1 h at RT. Excess of sulfo-SMCC was removed by gel-filtration. The modified QDs were added dropwise to the thiolated DON-OVA. Reaction was continued 2 hours under constant stirring at RT, afterwards, the mixture was completed by addition of 50 mM cysteine to block excess of maleimide-reactive groups. The obtained DON-NH_2-QDs were purified by gel-filtration.

8.2.6. Direct FLISA

The 96-well opaque black microtiter plates were coated with rabbit anti-mouse antibody (5 µg/mL; 100 µL/well) in 0.05 M sodium carbonate coating buffer (pH 9.6) by an overnight incubation at 4 °C. Afterwards the plates were washed three times with PBS containing 0.05 % (v/v) Tween 20 (PBST) and blocked with PBS containing 3% skim milk (w/v) for 1 h at 37 °C. The plates were washed two times with PBST. Further, the plates were incubated with specific anti-DON antibody (100 µL/well) for 2 h at 37 °C, and then washed three times with PBST. DON standard solution (in PBS) or diluted sample extract (50 µL/well) was added simultaneously with DON-QDs (dilution of DON-NH_2-QDs was 1/35). After 1 hour-incubation the plates were washed four times with PBST. The content of each well was re-dissolved in 100 µL of PBS and PL was measured using the Envision 2104 (Perkin Elmer).

8.3. RESULTS AND DISCUSSION

8.3.1. Application of QD@SiO_2-PEG-IgG conjugates for indirect immunoassay

QD@SiO_2-PEG-NH_2-IgG conjugates were used as PL labels in different kinds of immunoassay for detection of DON mycotoxin in indirect format of FLISA. The synthesized conjugate QD@SiO_2-PEG-IgG is a universal reagent for all monoclonal mouse antibodies, which opens

an opportunity to use it for the detection of different analytes, including multiplex detection of several different antigens. The developed FLISA method shows sufficient sensitivity (IC_{50} of 473 ng/mL) to meet requirements of current EU legislation 1881/2006/EC (Table 8.1), but it requires about 6 h to perform the analysis and usage of laboratory equipment at each stage.

Table 8.1. Current maximum limits for DON in food according to 1881/2006/EC and feed according to 2006/576/EC

Product	**Current maximum limit for DON, µg/kg**
FOOD	
Unprocessed cereals other than durum wheat, oats and maize	1 250
Unprocessed durum wheat and oats	1 750
Unprocessed maize with the exception of unprocessed maize intended to be processed by wet milling	1 750
Cereals intended for direct human consumption, cereal flour, bran and germ as end product marketed for direct human consumption	750
Pasta (dry)	750
Bread (including small bakery wares), pastries, biscuits, cereal snacks and breakfast cereals	500
Processed cereal-based foods and baby foods for infants and young children	200
FEED	
- Cereals and cereal products with the exception of maize by-products - Maize by-products	8 12
Complementary and complete feedstuffs with the exception of: - Complementary and complete feedstuffs for pigs - Complementary and complete feedstuffs for calves (< 4 months), lambs and kids	5 2 0.9

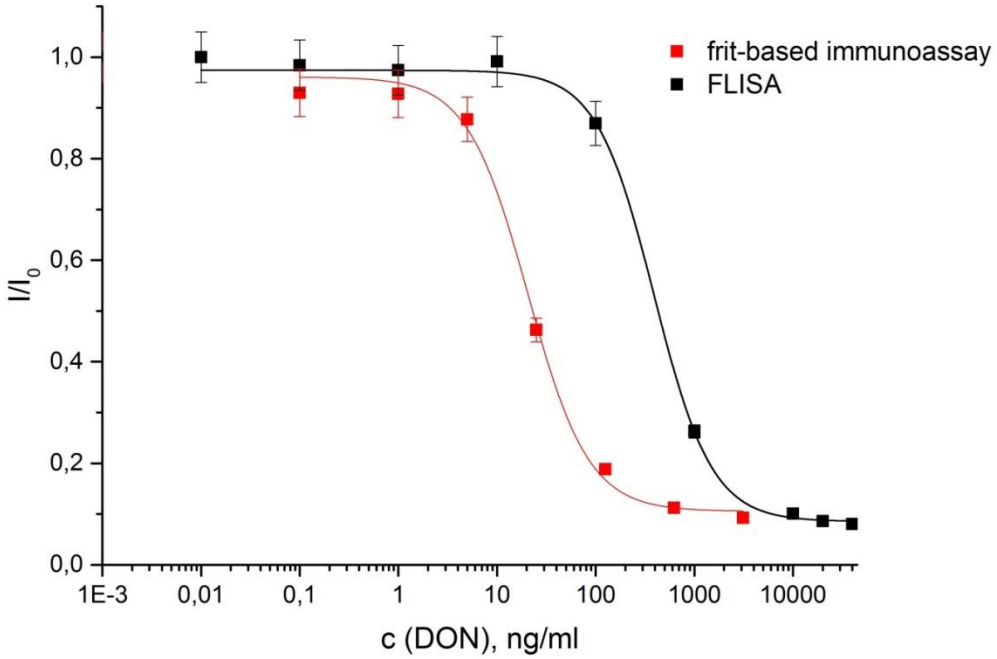

Figure 8.2. Calibration curves for the DON determination by the developed frit-based immunoassay and FLISA. The relative PL intensity was observed at λ^{ex} = 388 nm, λ^{em} = 600 nm. The data indicate the average of threefold determinations

To decrease time of analysis and also in order to obtain a rapid system for on-site detection, a novel polyethylene frit-based immunoassay for DON determination was also developed (device is presented at Figure 8.3).

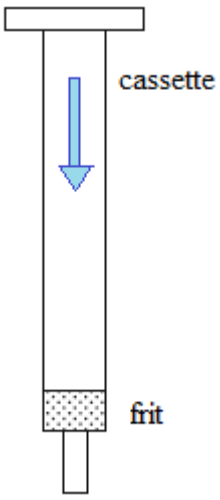

Figure 8.3. Test column for immunoassay

The analysis is performed in a column format: polyethylene frit is placed in a cassette and used as a carrier for immunoreagents. Analysis includes stages of consecutively passing of the sample solution

and the labeled conjugate. The sensitivity of the method can be varied by changing concentrations of the antibodies and the conjugate. The incorporation of antibodies on frit gives a possibility to concentrate mycotoxins analogously to the immunoaffinity columns; thus, the frit with immobilized antibodies simultaneously serves for separation, preconcentration, and determination. This column design has no limitation for volumes of liquid sample or extract, reagent and washing buffers. Besides reducing amount of analysis steps and, consequently, decreasing time of analysis, it also allows to use high extract volumes to improve assay sensitivity.

Both methods showed good precision, but the frit-based immunoassay allowed to decrease IC_{50} by a factor of 20 (IC_{50} for frit-based immunoassay was 20 ng/mL) (Figure 8.2). The total assay time for frit-based rapid test was only 1 h. An additional advantage of the frit-based assay is the possibility to work in a non-laboratory environment (in the case of availability of a handheld reader).

8.3.2. Application of polymer coated QDs conjugates for direct immunoassay

Polymer coated QDs were used as a label for direct FLISA for determination of DON. First the system was worked out on standard solutions of DON. Analytical characteristics of the method showed high sensitivity: LOD of 0.16 ng/mL, IC_{50} of 11 ng/mL.

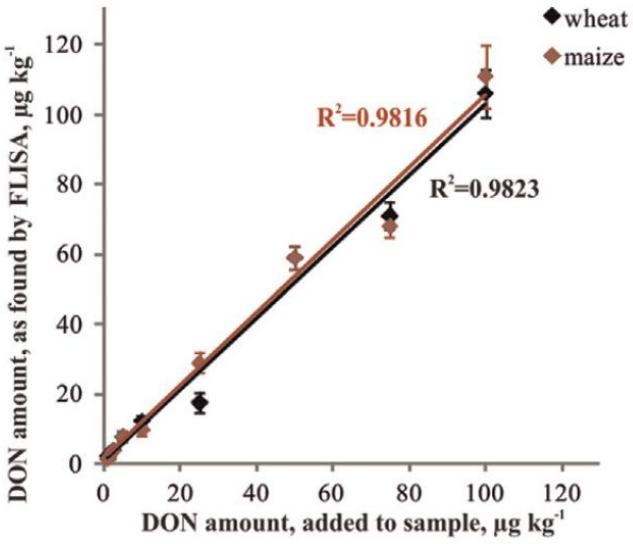

Figure 8.4. Linear regression using FLISA data for DON screening in artificially spiked wheat and maize samples (data indicate averages of fivefold determinations)

Validation of the developed immunoassays was performed using blank wheat and maize samples, spiked with DON at different concentrations. As a sample pretreatment, extraction with methanol/water (80/20 v/v) and further fivefold dilution of the extract was chosen. After extraction, the extract was usually standing for some minutes for sedimentation of particulate matter and afterwards the supernatant was collected and diluted with PBS. The described FLISA format performed good correlation between the added amounts of DON and the found concentrations (Figure 8.4).

Current EU legislation (1881/2006/EC) includes maximum limit for DON in unprocessed wheat and maize and the value is 1250 µg/kg. In this regard, naturally contaminated samples were analyzed with the developed FLISA method. A set of 19 wheat and 34 maize samples was used for validation of the developed analyses. As a confirmation technique liquid chromatography-tandem mass spectrometry (LC–MS/MS) was chosen (De Boevre et al., 2012). The comparison of results obtained by LC–MS/MS and FLISA is shown in Figure 8.5. A good agreement was demonstrated with the samples which were found to be contaminated, as determined with LC–MS/MS (R^2 =0.9902) (Figure 8.5).

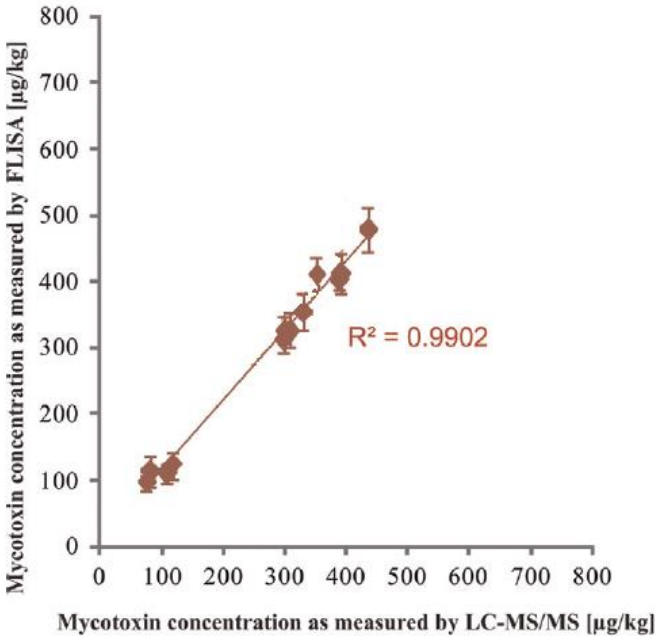

Figure 8.5. Linear regression equations derived using FLISA and LC–MS/MS data for DON screening in naturally-contaminated cereal samples

8.4. CONCLUSIONS

In this chapter it was shown, that QDs are promising labels for mycotoxin screening using immunoassay. Polymer coated and silica covered QDs were applied for direct and indirect FLISA for DON detection in microtiter plate as well as polyethylene frit-based format. Both synthesized PL labels show high sensitivity, satisfying the legislation norms. Although the direct format suggests higher sensitivity, the indirect format operates with a more universal label, available for application in multi-analysis.

PART 3. CONCLUSIONS AND FUTURE RESEARCH

CHAPTER 9. FINAL DISCUSSION AND GENERAL CONCLUSIONS

QDs are semiconductor nanocrystals with unique optical properties, which nowadays are of a great significance as PL labels in diverse biomedical applications. To constitute sensitive biolabels, QDs have to meet the following requirements: (i) high brightness (QY) and photostability, independent of their environment, (ii) solubility in aqueous buffers (including physiological solutions) and stability under relevant conditions (iii) availabillity of functional groups on their surface for the potential bioconjugation and a low non-specific sorption of biomolecules, (iv) manufacturability with a reproducible quality.

To comply with these demands, first, an appropriate synthesis protocol should be established. Colloid synthesis of CdSe QDs is very well developed. In this work, the synthesis of CdSe based core-shell QDs was performed, using different stabilizing ligands, i.e. TOP and OA, and varying the material and thickness of the wider band gap semiconductors, being CdS, alloy CdZnS and ZnS. Important to note, that usage of different ion precursors allows to diversify quality if the obtained QDs. Thus cheap and stable precursors were used in order to develop an easy and reproducible way to synthesize high quality QDs. These synthesis routes allow manufacturing QDs with a high QY (~ 50%) and with a controllable wavelength of emission maxima.

There are two well-known common approaches for making QDs biocompatible: (i) ligand exchange, i.e. the substitution of native hydrophobic ligands for hydrophilic ones, and (ii) covering with amphiphilic molecules, a technique also known as encapsulation. In the framework of this dissertation, both approaches were applied (more specifically by using silica precursors and amphiphilc polymers respectively) in order to obtain sensitive luminescent label for immunoassay. Reporter immunochemical systems with luminescent detection are now widely used in research and clinical diagnostics because they provide high sensitivity and are capable of simultaneous use of multiple labels with different spectral characteristics (multiplexing). In some cases, the sensitivity of luminescent labels is comparable with that of enzymatic labels, but the assay procedure is essentially simpler.

The most important advantage of polymer encapsulation of QDs is that the initial PL intensity is retained after the hydrophilization process. Covering with amphiphilic molecules was performed by employing a synthesized co-polymer of PMAO and Jeffamine polymers. PMAO is widely used for NPs hydrophilization, because it has active maleic ring, available for further modification. Jeffamine polymers are low-cost analogues of PEG, they are commercially available and presented on the market in diverse adaptations, thus it not only adds stability to the QDs through PEG fragments. Pertinent variation of the Jeffamine polymer structure allowed choosing the appropriate functional group on the QDs' surface. In particular, QDs with 3 different emission colors were covered with amphiphilic polymer without loss of brightness. Polymer coating preserves 90% of the initial brightness of the QDs (Table 9.1). This combination of polymers was firstly applied for CdSe QDs in 2014 in our group (Speranskaya et al., 2014).

Table 9.1. Quantum Yields of QDs with different structures after covering with PMAO-Jeffamine M1000 co-polymer and silica shell

QY (%)	**in toluene**	**in water**	
		Polymer	**Silica**
QD^{550} CdSe/ZnS	50	45	10
QD^{600} CdSe/CdS/CdZnS/ZnS	53	46	43
QD^{630} CdSe/CdS/ZnS	36	32	22

Silanization of QDs was performed by leveraging the microemulsion method, which implies ligand exchange with silane molecules, such as TEOS, to form nucleation sites on the QD surface, and followed by a condensation step yielding formation of the silica shell. According to the literature, silanization of CdSe core - shell QDs synthesized with SILAR technique, usually leads to decreasing of the QY (Aubert et al., 2014). The developed approach, presented in this dissertation, allows maintaining PL properties, controlling the size of the synthesized water-soluble silica-coated QDs and varying the functional groups for further bioconjugation (namely, carboxyl-, amino-, epoxy- groups). Also, a high buffer stability of the NPs was achieved using PEG derivatives of silanes. Additionally, the PL properties of the QDs with different structures and emission colors were characterized before and after

silanization. It was shown that silanization is a convenient route towards the synthesis of water-soluble, stable, bright QD-based labels with different emission colors, yielding a promising outlook for multiplex analysis.

To assess the stability of the synthesized PL biolabels, their optical properties were investigated under adverse conditions. For instance, polymer coated QDs were freeze dried in order to obtain PL nanopowders that are easy to dissolve in any desirable concentration. It was shown, that the structure of the polymer shell affects the PL properties of QDs after lyophilization. For example, zeta potentials, which are predominantly determined by the polymer structure, play a crucial role in NPs' stability.

Moreover, the influence of low-strength EF on amphiphilic polymer-coated and silica-covered CdSe-based QDs was investigated. For the first time this parameter was investigated in QDs solutions and at low EF strength, since normally influence of EF is studied for QDs in polymeric matrixes and at significantly higher voltage. It was shown that the hydrophilic shell affects the PL properties of the QDs under a low-strength EF. The hydrophobic forces, which bind the QD and the amphiphilic polymer molecule, are not strong enough to withstand the electrostatic attraction between the negatively charged polymer molecule and the anode. In contrast, the covalently bonded silica shell prevents any destruction and oxidation process under the influence of the EF and, as such, the NPs maintain their initial PL brightness.

Consequently, two types of QD-based biolabels were synthesized and characterized in order to obtain sensitive PL labels for immunoassay analysis. Having a great experience in development immunochemical methods for toxins detection, in 2011 our scientific group published an article, where enzyme label was compared with QDs and gold nanoparticles (Beloglazova et al., 2011). For the first time was shown that QDs possess the same sensitivity as enzyme label, while allowing reducing time of analysis, since it doesn't require addition of substrate. After that, QD-based label considered to be a good alternative to the traditional enzyme label for immunoassay. Following years of our experiments showed that QDs are even more sensitive that traditional labels (Beloglazova et al., 2012; Beloglazova et al., 2014; Speranskaya et al., 2014).

Nevertheless, silica-coated QDs had been never applied as a luminescent labels for immunoassay for mycotoxin detection. In this regard, silica-coated QDs, modified with

diverse functional groups were efficiently conjugated with antibodies, using different activation and bioconjugation reactions. Stability and ability to be coupled with antibodies was investigated. According to our knowledge, for the first time silica-based QD conjugates were successfully applied as a novel label in a microtiter plate based FLISA and a quantitative column-based rapid immunotest for DON detection.

Polymer coated QDs were applied as PL biolabels in FLISA format for detection of mycotoxin DON. Naturally contaminated samples of wheat and maize were analyzed using the developed method and the results considerably correlate with LC/MS-MS analysis. The developed immunoassays show sensitivity high enough to detect DON at the legislation levels in food and feed.

In summary, it may be stated that the novel synthesis routes and newly developed QD-based biolabels, presented in this work, are applicable in the content of detection of mycotoxins and other analytes of interest and also pave a way for future application not only in academic, but also in commercial domains, as elaborated in the next chapter.

CHAPTER 10. BROADER INTERNATIONAL CONTEXT AND FUTURE RESEARCH

Suitable labels form the core of luminescence sensing and imaging. One of the most challenging tasks is to find a technology to produce highly sensitive biocompatible labels. Today, nanotechnology has proven to be a powerful tool to obtain such labels, with many desirable properties. In particular, QDs possess very unique optical properties, making them suitable for production of labels. This fact is also reflected in the existence of an enormous amount of recently published studies on QD-based labels.

Nowadays, there are many international scientific groups that devote their research to QDs. For instance, one of the most renowned groups, and historically the first, is Bawendi's group from Massachusetts Institute of Technology (MIT), USA. They are performing cutting-edge experiments in several subdomains of QD research simultaneously. In particular, they focus on the development of new synthesis routes and new materials for QDs, on their application for biosensing (*in vivo* and *in vitro)* and chemical sensing, on the QD spectroscopy, as well as on designing and manufacturing photovoltaic and photodetector devices.

The Physics and Chemistry of Nanostructures Group of Ghent University, Belgium, is also one of the leading groups in QDs research in the world. Besides new synthesis routes and new materials development, these scientists are working on the application of QDs as biolables, and for usage in solar cells, IR cameras, LED displays, lasers, switches, sources, modulators, etc. Every year this group publishes tens of articles in high-ranking scientific journals, such as *Nature Materials, ACS Nano*, *Nano Letters*, *Advanced Materials, and Langmuir*.

The research presented in this dissertation, and other work performed by the research groups involved, have further opened the perspective of using QDs in immunoassay for food quality control. Specifically, the presented techniques unlock the possibility for the production and application of sensitive immunosensors for mycotoxin determination. On a global scale, the significance of this is indisputable, as mycotoxins, being highly toxic substances, poison 25% of the world's crop.

Taking into account that chromatography is the “golden standard” of mycotoxin analysis, the Center for Analytical Chemistry of the University of Natural Resources and Applied Life Sciences,Vienna, Austria, is one of the most influential laboratories in the domain of mycotoxin research. The main focus of this research group is the development of modern LC-MS based analytical methods for the study of selected natural toxins and their metabolites in plants and foods.

The Laboratory of Food Analysis of Ghent University, Belgium, is part of the multidisciplinary MYTOX research group, established as a collaboration between Ghent University, Hogeschool Gent and the Food2Know organization. This consortium deals with all kinds of aspects of mycotoxins and toxigenic mould issues. Annual conferences and symposiums, organized by MYTOX, allow disseminating and exchanging state-of-the-art knowledge between scientists from all over the world. The knowledge and expertise as well as the advanced and very sensitive LC equipment of the Laboratory of Food Analysis attracts many international researchers and stimulates new international collaborations and projects.

The development of rapid immunoassays for mycotoxin detection has been always a priority for the Laboratory of Food Analysis. Sensitive immunotests for in-field analysis were yet developed both for single mycotoxin and for multi-mycotoxins detection. Some of these methods are patented. Diverse labels were applied, including enzymes and colloid gold NPs. Finally, in 2012, one of the very first articles about QDs-based rapid test for mycotoxin detection was published by this group. As shown in the Table 3.1., at the moment, less than 20 articles about QD-based immunofluorescent methods exist.

In this regard, the further development of QD-based rapid tests is very important, since such tests can considerably decrease the time of analysis, and, consequently, the amount of contaminated food on the market. The possible commercialization of the developed approaches (e.g. FLISA) is feasible, especially taking into account the fact that immunoassay kits (like ELISA, for example) are nowadays widely spread, also for food diagnostic. Moreover, test methods of analysis, such as immunochromatographic strips or columns, facilitate the industrialization of the novel techniques.

When looking at future perspectives, and given the increasingly severe restrictions imposed by toxicity legislation norms, the development of QDs based on non-toxic materials is extremely essential. Thereto, the elimination of the Cd ions from QDs is a necessity and

constitutes a critical topic of investigation. The research group, in which the present work was carried out, has expertise in the synthesis of $CuInS_2$ QDs. This material not only allows reducing the toxicity of QDs, but it also covers the window of optical transparency for living tissues. This in turn opens unlimited possibilities for *in vitro* and *in vivo* application of PL QDs for diagnostic and treatment. Some characteristics of $CuInS_2$ QDs, such as toxicity for blood cells and temperature depending optical properties for their application as nanothermometers during cancer treatment, have already been investigated. These results are very promising and provide a starting point for further advancement in this domain. Another possible Cd-free material for QDs production is InP, that combines emission characteristics that come close to CdSe QDs with a reduced toxicity.

Whereas in this work we apply QDs as labels, starting from a solutions, for completeness we need to mention QDs have also already found application in a solid state. One example is for control of charge separation. The structuring of QD solids can add highly desirable functionalities. A suitable size gradient can lead to enhanced and unidirectional energy transfer, which competes with undesired processes such as charge trapping and multi-exciton annihilation. Mainly, these conductive properties of QDs are currently being investigated in order to create high-efficiency solar cells.

To summarize, QDs are remarkable and unique NPs that have already found advanced application in very diverse domains and that still have a great potential to be further developed and leveraged for other goals, in engineering, bioscience, medicine, pharmacy, etc. We will for sure continue our research on the bioapplication of QDs in order to keep providing a bright future for our bright NPs.

REFERENCES

REFERENCES

A

Abe, S., Capek, R.K., De Geyter, B., Hens, Z., 2012. Tuning the Postfocused Size of Colloidal Nanocrystals by the Reaction Rate: From Theory to Application. ACS Nano 6 (1), 42–53.

Adamczak, M., Hoel, H.J., Gaudernack, G., Barnasz, J., Szczepanowich, K., Warszynski, P., 2012. Poluelectrolute multilayer capsules with quantum dots for biomedical application. Colloid Surf. 90, 211–216.

Anfossi, L., Giovannoli, C., Baggiani., C., 2016. Mycotoxin detection. Current Opinion in Biotechnology 37, 120–126.

Aubert, T., Soenen, S.J., Wassmuth, D., Cirillo, M., Van Deun, R., Braeckmans, K., Hens, Z., 2014. Bright and Stable CdSe/CdS@SiO2 Nanoparticles Suitable for Long-Term Cell Labeling. ACS Appl. Mater. Interfaces 6 (14), 11714–11723.

B

Bagwe, R.P., Hilliard,L.R., Tan, W., 2006. Surface Modification of Silica Nanoparticles to Reduce Aggregation and Nonspecific Binding. Langmuir 22, 4357-4362.

Baker, D.R., Kamat, P.V., 2010. Tuning the emission of CdSe quantum dots by controlled trap enhancement. Langmuir 26 (13), 11272–11276.

Bangham, A.D., Standish, M.M., Watkins, J.C., 1965. Diffusion of univalent ions across the lamellae of swollen phospholipids. J. Mol. Biol. 13,238-252.

Beloglazova, N. V., Shmelin, P.S., Speranskaya, E.S.., Lucas, B., Helmbrecht, C., Knopp, D., Niessner, R., De Saeger, S., Goryacheva, I.Yu., 2013. Quantum Dot Loaded Liposomes as Fluorescent Labels for Immunoassay. Anal. Chem. 85, 7197–7204.

Beloglazova, N. V., Speranskaya, E. S., Wu, A., Wang, Z., Sanders, M., Goftman, V. V., Zhang, D., Goryacheva, I. Yu., De Saeger, S., 2014. Novel multiplex fluorescent immunoassays based on quantum dot nanolabels for mycotoxins determination. Biosensors and Bioelectronics 61, 59-65.

Beloglazova, N.V., Goryacheva, O.A., Speranskaya, E.S., Aubert, T., Shmelin, P.S., Kurbangaleev, V.R., Goryacheva, I.Yu., DeSaeger, S., 2015. Silica-coated liposomes loaded with quantum dots as labels for multiplex fluorescent immunoassay. Talanta 134, 120–125.

Beloglazova, N.V., Speranskaya, E.S., De Saeger, S., Hens, Z., Abé, S., Goryacheva, I.Yu., 2012. Quantum dot based rapid tests for zearalenone detection. Analytical and Bioanalytical Chemistry 403(10), 3013-3024.

Biju, V., Itoh, T., Ishikawa, M., 2010. Delivering quantum dots to cells: bioconjugated quantum dots for targeted and nonspecific extracellular and intracellular imaging. Chem Soc. Rev. 39(8), 3031-56.

Bozyigit, D., Yarema, O., Wood, V., 2013. Origins of low quantum efficiencies in quantum dot LEDs. Adv. Funct. Mater., 3024-3029.

Brazhnik, K., Sokolova, Z., Baryshnikova, M., Bilan, R., Efimov, A., Nabiev, I., Sukhanova, A., 20215. Quantum dot-based lab-on-a-bead system for multiplexed detection of free and total prostate-specific antigens in clinical human serum samples. Nanomedicine: Nanotechnology Biology and Medicine 11, 1065–1075.

Breus, V. V., 2008. Design, Synthesis and Characterization of Biocompatible Quantum Dots for Application in Biophysics. Dissertation, Faculty of Natural Sciences, University of Ulm.

Bruchez, M. Jr., Moronne, M., Gin, P., Weiss, S., Alivisatos, A.P., 1998. Semiconductor nanocrystals as fluorescent biological labels. Science 281 (5385), 2013-2016.

Brus, L., 1986. Electronic wave functions in semiconductor clusters: experiment and theory. J. Phys. Chem. 90, 2555–2560.

C

Cao, Y.-C., 2012. Preparation of thermally stable well-dispersed water-soluble CdTe quantum dots in montmorillonite clay host media. Journal of Colloid and Interface Science 368, 139-143.

Capek, R. K., Moreels, I., Lambert, K., De Muynck, D., Zhao, Q., Van Tomme, A., Vanhaecke, F., Hens, Z., 2010. Optical Properties of Zincblende Cadmium Selenide Quantum Dots. The Journal of Physical Chemistry C 114, 6371–6376.

CAST, 2003. Council for Agricultural Science and Technology. Mycotoxins: Risks in plant, animal and human systems. Task force report R139.

Chan, W. C. W. , Nie. S., 1998. Quantum dot bioconjugates for ultrasensitive nonisotopic detection. Science, 281(5385), 2016-2018.

Chen, N., He, Y., Su, Y., Li, X., Huang, Q., Wang, H., Zhang, X., Tai, R., Fan, C., 2012. The cytotoxicity of cadmium-based quantum dots. Biomaterials 33, 1238-1244.

Chen, O., Zhao, J., Chauhan, V.P., Cui, J., Wong, C., Harris, D.K., Wei, H., Han, H.-S., Fukumura, D., Jain, R.K., Bawendi, M.G., 2013. Compact high-quality CdSe-CdS core-shell nanocrystals with narrow emission linewidths and suppressed blinking. Nature Materials 12, 445-451.

Chen, S.-C., Yao, J., Durst, R.A., 2006. Liposome encapsulation of fluorescent nanoparticles: Quantum dots and silica nanoparticles. Journal of Nanoparticle Research 8, 1033–1038.

Chen, Y., Jiang, B., Xiang, Y., Chai, Y., Yuan, R., 2011. Aptamer-based highly sensitive electrochemiluminescent detection of thrombin via nanoparticle layer-by-layer assembled amplification labels. Chem. Commun. 47, 7758–7760.

Cheng, Z., Thorek, D.L.J., Tsourkas, A., 2010. Gadolinium-conjugated dendrimer nanoclusters as a tumor-targeted T1 magnetic resonance imaging contrast agent. Angew. Chem. Int. Ed. 49, 346–350.

Chu, M., Sun, Y., Xu, S., 2008. Silica-coated quantum dots fluorescent spheres synthesized using a quaternary 'water-in-oil' microemulsion system. J. Nanopart. Res. 10, 613–624.

Costas-Mora, I., Romero, V., Lavilla, I., Bendicho, C., 2014. An overview of recent advances in the application of quantum dots as luminescent probes to inorganic-trace analysis. Trends in Analytical Chemistry 57, 64–72.

D

Dabbousi, B. O., Rodriguez-Viejo, J., Mikulec, F.V., Heine, J. R., Mattoussi, H., Ober, R., Jensen, K. F., Bawendi, M.G., 1997. (CdSe)ZnS Core–Shell Quantum Dots: Synthesis and Characterization of a Size Series of Highly Luminescent Nanocrystallites. J. Phys. Chem. B 101 (46), 9463–9475.

Darbandi, M., Urban, G., Krüger, M., 2010. A facile synthesis method to silica coated CdSe/ZnS nanocomposites with tuneable size and optical properties. Journal of Colloid and Interface Science 351, 30–34.

De Boevre, M., Di Mavungu, J.D., Maene, P., Audenaert, K., Deforce, D., Haesaert, G., Eeckhout, M., Callebaut, A., Berthiller, F., Van Peteghem, C., De Saeger, S., 2012. Food Addit. Contam. 29, 819–835.

de Mello, J. C., Wittmann, H. F., Friend, R. H., 1997. An improved experimental determination of external photoluminescence quantum efficiency. Adv. Mater. 9, 230-232.

De Nolf, K., Capek, R.K., Abe, S., Sluydts, M., Jang, Y., Martins, J.C., Cottenier, S., Lifshitz, E., Hens, Z., 2015. Controlling the Size of Hot Injection Made Nanocrystals by Manipulating the Diffusion Coefficient of the Solute. Am. Chem. Soc. 137 (7), 2495–2505.

Decher, G., 1997. Fuzzy nanoassemblies: toward layered polymeric multicomposites. Science 277, 1232–1237.

Delehanty, J.B., Susumu, K., Manthe, R.L., Algar, W.R., Medintz, I.L., 2012. Active cellular sensing with quantum dots: Transitioning from research tool to reality; a review. Analytica Chimica Acta 750 (2012), 63–81.

Di Nardo, F., Anfossi, L., Giovannoli, C., Passini, C., Goftman, V.V.., Goryacheva, I.Yu., Baggiani, C., 2016. A fluorescent immunochromatographic strip test using quantum dots for fumonisins detection. Talanta 150, 463–468.

Dubois, F., Mahler, B., Dubertret, B., Doris, E., Mioskowski, C., 2007. A versatile strategy for quantum dot ligand exchange. J. Am. Chem. Soc. 129(3), 482-483.

F

Friedrich, M., Nozadze, R., Gan, Q., Zelman-Femiak, M., Ermolayev, V., Wagner, T.U., Harms, G.S., 2009. Detection of single quantum dots in model organisms with sheet illumination microscopy. Biochemical and Biophysical Research Communications 390 (3), 722–727.

Frigerio, C., Ribeiro, D.S., Rodrigues, S.S., Abreu, V.L., Barbosa, J.A., Prior, J.A., Marques, K.L., Santos, J.L., 2012. Application of quantum dots as analytical tools in automated chemical analysis: a review. Anal Chim Acta 20 (735), 9-22.

Gao, J., Chen, K., Luong, R., Bouley, D.M., Mao, H., Qiao, T., Gambhir, S.S., Cheng, Z., 2012. A novel clinically translatable fluorescent nanoparticle for targeted molecular imaging of tumors in living subjects. Nano Lett. 12(1), 281-286.

Gao, X., Cui, Y., Levenson, R.M., Chung, L.W.K, Nie, S., 2004. In vivo cancer targeting and imaging with semiconductor quantum dots. Nature Biotechnology 22, 969 – 976.

Generalova, A.N., Oleinikov, V.A., Zarifullina, M.M., Lankina, E.V., Sizova, S.V., Artemyev, M.V., 2011. Optical sensing quantum dot-labeled polyacrolein particles prepared by layer-by-layer deposition technique. J. Colloid Interface Sci. 357, 265–272.

Geraldo, D.A., Duran-Lara, E.F., Aguayo, D., Cachau, R.E., Tapia, J., Esparza, R., Yacaman, M.J., Gonzalez-Nilo, F.D., Santos, L.S., 2011. Supramolecular complexes of quantum dots and a polyamidoamine (PAMAM)-folate derivative for molecular imaging of cancer cells. Anal. Bioanal. Chem. 400, 483–492.

Gerion, D., Pinaud, F., Williams, S.C., Parak, W.J., Zanchet, D., Weiss, S., Alivisatos, A.P., 2001. Synthesis and properties of biocompatible water-soluble silica-coated CdSe/ZnS semiconductor quantum dots. J. Phys. Chem. B 105 (37), 8861–8871.

Geszke-Moritz, M., Moritz, M., 2013. Quantum dots as versatile probes in medical sciences: Synthesis, modification and properties. Materials Science and Engineering C 33, 1008–1021.

Goftman, V. V., Beloglazova, N. V., Njumbe Ediage, E., De Saeger, S., Dietrich, R., Martlbauer, E., Goryacheva, I.Yu.,2012. Rapid immunochemical tests for qualitative and quantitative determination of T-2 and HT-2 toxins. Anal. Methods 4, 4244-4249.

Goftman, V.V., Aubert, T., Vande Ginste, D., Van Deun, R., Beloglazova, N.V., Hens, Z., De Saeger, S., Goryacheva, I.Yu., 2016. Synthesis, modification, bioconjugation and application of silica coated fluorescent quantum dots. Biosensors and Bioelectronics 79, 476–481

Gong, K., Zeng, Y., Kelley, D.F., 2013. Extinction Coefficients, Oscillator Strengths, and Radiative Lifetimes of CdSe, CdTe, and CdTe/CdSe Nanocrystals. J. Phys. Chem. C 117 (39), 20268–20279

Goryacheva, I. Yu., Speranskaya, E. S., Goftman, V. V., Tang, D., De Saeger, S., 2015. Synthesis and bioanalytical applications of nanostructures multiloaded with quantum dots. Trends in Analytical Chemistry 66, 53–62.

Goryacheva, I.Yu., Lenain, P., De Saeger, S., 2013. Nanosized labels for rapid immunotests. Trends in Analytical Chemistry 46, 30 - 43.

Goryacheva, I. Y., De Saeger, S., Eremin, S.A., Van Peteghem, C., 2007. Immunochemical methods for rapid mycotoxin detection: Evolution from single to multiple analyte screening: A review. Food Additives & Contaminants 24 (10), 1169 – 1183.

Grabolle, M., Spieles, M., Lesnyak, V., Gaponik, N., Eychmüller, A., Resch-Genger, U., 2009. Determination of the Fluorescence Quantum Yield of Quantum Dots: Suitable Procedures and Achievable Uncertainties. Analytical Chemistry 81 (15), 6285–6294.

Grayson, S.M., Frechet, J.M.J., 2001. Convergent dendrons and dendrimers: from synthesis to applications. Chem. Rev. 101, 3819–3867.

Green, M., 2010. The nature of quantum dot capping ligands. Journal of Materials Chemistry 20, 5797–5809.

Green, M., 2014. Semiconductor Quantum Dots : Organometallic and Inorganic Synthesis. Cambridge, GBR: Royal Society of Chemistry.

Guerrero-Martınez, A., Perez-Juste, J., Liz-Marzan, L. M., 2010. Recent Progress on Silica Coating of Nanoparticles and Related Nanomaterials. Adv. Mater. 22, 1182–1195.

Gurinovich, L.I., Artemyev, M.V., Stupak, A.P., Prislopskii, S.Ya., Zhukovsky, S.V., Gaponenko, S.V., 2012. Quenching of photoluminescence in cadmium selenide nanocrystals in external electric fields for different excitation photon energies. J. Appl. Spectrosc. 79 (1), 95-103.

H

Hermanson, G. T., 2008. Bioconjugation techniques, second ed. Elsevier Inc., Rockford.

Hezinger, A.F.E., Tesmar, J., Gopferich, A., 2008. Polymer coating of quantum dots – A powerful tool toward diagnostics and sensorics. European Journal of Pharmaceutics and Biopharmaceutics 68, 138–152.

Higuchi, Y., Wu, C., Chang, K.L., Irie, K., Kawakami, S., Yamashita, F., 2011. Polyamidoamine dendrimer-conjugated quantum dots for efficient labeling of primary cultured mesenchymal stem cells. Biomaterials 32, 6676–6682.

Hines, M. A., Guyot-Sionnest, Ph., 1996. Synthesis and Characterization of Strongly Luminescing ZnS-Capped CdSe Nanocrystals. J. Phys. Chem. 100, 468-471.

Hlavacek, A., Sedlmeier, A., Skladal, P., Gorris, H.H., 2014. Electrophoretic characterization and purification of silica-coated photon-upconverting nanoparticles and their bioconjugates. ACS Appl. Mater. Interfaces 6, 6930–6935.

Hsu, J.-C., Huang, C.-C., Ou, K.-L., Lu, N., Mai, F.-D., Chen, J.-K., Chang, J.-Y., 2011. Silica nanohybrids integrated with CuInS2/ZnS quantum dots and magnetite nanocrystals: multifunctional agents for dual-modality imaging and drug delivery. J. Mater. Chem. 21, 19257-19266.

Huan, X., Zhan, F., Lee, S., Swierczewska, M., Kiesewetter, D.O., Lang, L., Zhang, G., Zhu, L., Gao, H., Choi, H.S., Niu, G., Chen, X., 2012. Long-term multimodal imaging of tumor draining sentinel lymph nodes using mesoporous silica-based nanoprobes. Biomaterials 33, 4370-4378.

Huang, J., Kovalenko, M.V., Talapin, D.V., 2010. Alkyl chains of surface ligands affect polytypism of CdSe nanocrystals and play an important role in the synthesis of anisotropic nanoheterostructures. J. Am. Chem. Soc. 132 (45), 15866–15868.

Hurley, M.T., Wang, Z., Mahle, A., Rabin, D., Liu, Q., English, D.S., Zachariah, M.R., Stein, D., DeShong, P., 2013. Synthesis, characterization, and application of antibody functionalized fluorescent silica nanoparticles. Adv. Funct. Mater. 23, 3335–3343.

I

Isnaeni, Jin, L.-H., Cho, Y.-H., 2013. Silica encapsulation of toluene soluble quantum dots with high photostability. Journal of Colloid and Interface Science 395, 45–49.

J

Jaiswal, J.K., Mattoussi, H., Mauro, J.M., Simon, S.M., 2003. Long-term multiple color imaging of live cells using quantum dot bioconjugates. Nat. Biotechnol. 21(1), 47-51.

Jamieson, T., Bakhshi, R., Petrova, D., Pocock, R., Imani, M., Seifalian, A.M., 2007. Biological applications of quantum dots. Biomaterials 28(31), 4717-4732.

Jiang, T., Yin, N., Liu, L., Song, J., Huang, Q., Zhu, L., Xu, X., 2014. A Au nanoflower@SiO2@CdTe/CdS/ZnS quantum dot multi-functional nanoprobe for photothermal treatment and cellular imaging. RSC Adv. 4, 23630-23636.

Jie, G., Yuan, J., Zhang, J., 2012. Quantum dots-based multifunctional dendritic superstructure for amplified electrochemiluminescence detection of ATP. Biosens. Bioelectron. 31, 69–76.

Jing, P., Zheng, J., Ikezawa, M., Liu, X., Lv, S., Kong, X., Zhao, J., Masumoto, Y., 2009. Temperature-Dependent Photoluminescence of CdSe-Core CdS/CdZnS/ZnS-Multishell Quantum Dots. J. Phys. Chem. C 113, 13545–13550.

Jokerst, J.V., Lobovkina, T., Zare, R.N., Gambhir, S.S., 2011. Nanoparticle PEGylation for imaging and therapy. Nanomedicine 6(4), 715–728.

K

Kadota, T., Takezawa, Y., Hirano, S., Tajima, O., Maragos, C.M., Nakajima, T., Tanaka, T., Kamata, Y., Sugita-Konishi, Y., 2010. Rapid detection of nivalenol and deoxynivalenol in wheat using surface plasmon resonance immunoassay. Analytica Chimica Acta 673, 173–178.

Khlebtsov, B.N., Panfilova, E.V., Terentyuk, G.S., Maksimova, I.L., Ivanov, A.V., Khlebtsov, N.G., 2012. Plasmonic nanopowders for photothermal therapy of tumors. Langmuir 28 (24), 8994-9002.

Kirchner, C., Liedl, T., Kudera, S., Pellegrino, T., Muoz Javier, A., Gaub, H.E., Stlzle, S., Fertig, N., Parak, W.G., 2005. Cytotoxicity of colloidal CdSe and CdSe/ZnS nanoparticles. Nano Lett. 5(2), 331-338.

Knopp, D., Tang, D., Niessner, R., 2009. Review: Bioanalytical applications of biomolecule-functionalized nanometer-sized doped silica particles. Anal. Chim. Acta 647, 14-30.

Kobayashi, H., Hama, Y., Koyama, Y., Barrett, T., Regino, C. A. S., Urano, Y., Choyke, P.L., 2007. Simultaneous multicolor imaging of five different lymphatic basins using quantum dots. Nano Letters 7(6), 1711-1716.

Kobayashi, Y., Matsudo, H., Nakagawa, T., Kubota, Y., Gonda, K., Ohuchi, N., 2013. In-vivo fluorescence imaging technique using colloid solution of multiple quantum dots/silica/poly(ethylene glycol) nanoparticles. J. Sol-Gel Sci. Technol. 66, 31–37.

Kolosova, A,Yu., Sibandab, L., Dumoulin, F., Lewis, J., Duveiller, E., Van Peteghem, C., De Saeger, S., 2008. Lateral-flow colloidal gold-based immunoassay for the rapid detection of deoxynivalenol with two indicator ranges. Analytica Chimica Acta 616, 235–244.

Koole, R., van Schooneveld, M. M., Hilhorst, J., de Mello Donegá, C., Hart, D. C., van Blaaderen, A., Vanmaekelbergh, D., Meijerink, A., 2008. On the Incorporation Mechanism of Hydrophobic Quantum Dots in Silica Spheres by a Reverse Microemulsion Method. Chem. Mater. 20, 2503–2512.

Kosaka, N., Mitsunaga, M., Choyke, P. L., Kobayashi, H., 2013. *In vivo* real-time lymphatic draining using quantum-dot optical imaging in mice. Contrast Media & Molecular Imaging 8(1), 96-100.

L

Lees, E.E., Nguyen, T.-L., Clayton, A.H.A., Mulvaney, P., 2009. The Preparation of Colloidally Stable, Water-Soluble, Biocompatible, Semiconductor Nanocrystals with a Small Hydrodynamic Diameter. ACS Nano 3, 1121-1128.

Li, H., Mu, Y., Lu, J., Wei, W., Wan, Y., Liu, S., 2014. Target-cell-specific fluorescence silica nanoprobes for imaging and theranostics of cancer cells. Anal. Chem. 86 (7), 3602−3609.

Li, J.J., Wang, Y.A., Guo, W., Keay, J.C., Mishima, T.D., Johnson, M.B., Peng, X., 2003. Large-Scale Synthesis of Nearly Monodisperse CdSe/CdS Core/Shell Nanocrystals Using Air-Stable Reagents via Successive Ion Layer Adsorption and Reaction. J. Am. Chem. Soc. 125 (41), 12567−12575.

Liu, S., Zhang, H.-L., Liu, T.-C., Liu, B., Cao, Y.-Ch., Huang, Zh.-L., Zhao, Y.-D., Luo, Q.-M., 2007. Optimization of the methods for introduction of amine groups onto the silica nanoparticle surface. Journal of Biomedical Materials Research Part A 80A (3), 752–757.

Liu, W., Choi, H.S., Zimmer, J.P., Tanaka, E., Frangioni, J.V., Bawendi, M., 2007. Compact Cysteine-Coated CdSe(ZnCdS) quantum dots for *in vivo* applications. J. Am. Chem. Soc. 129(47), 14530-14531.

Luo, G., Long, J., Zhang, B., Liu, C., Ji, S., Xu, J., Yu, X., Ni, Q., 2012. Quantum dots in cancer therapy. Expert Opin. Drug Deliv. 9(1), 47-58.

M

Ma, Q., Nakane, Y., Mori, Y., Hasegawa, M., Yoshioka, Y., Watanabe, T.M., Gondad, K., Ohuchi, N., Jina, T., 2012. Multilayered, core/shell nanoprobes based on magnetic ferric oxide particles and quantum dots for multimodality imaging of breast cancer tumors. Biomaterials 33, 8486-8494.

Maragos, C., 2009. Fluorescence polarization immunoassay of mycotoxins: A review. Toxins 1, 196–207.

Maragos, C. M., McCormick, S. P., 2010. Monoclonal Antibodies for the Mycotoxins Deoxynivalenol and 3-Acetyl-Deoxynivalenol. Food and Agricultural Immunology 12 (3), 181-192.

Marroquín-Cardona, A.G., Johnson, N.M., Phillips, T.D., Hayes, A.W., 2014. Mycotoxins in a changing global environment – A review. Food and Chemical Toxicology 69, 220–230.

Mattoussi, H., Mauro, J.M., Goldman, E.R., Green, T.M., Anderson, G.P., Sundar, V.C., Bawendi, M.G., 2001. Bioconjugation of highly luminescent colloidal CdSe–ZnS quantum dots with an engineered two-domain recombinant protein. Physica status solidi (b) 224 (1), 277–283.

Michalet, X., Pinaud, F. F., Bentolila, L. A., Tsay, J. M., Doose, S., Li, J. J., Sundaresan, G., Wu, A. M., Gambhir, S. S., Weiss, S., 2005. Quantum Dots for Live Cells, *in vivo* Imaging, and Diagnostics. Science 307(5709), 538-544.

Miller, D.A.B., Chemla, D.S., Damen, T.C., 1984. Band-edge electroabsorption in quantum well structures: the quantum-confined Stark effect. Phys. Rev. Lett. 53 (22), 2173-2176.

Mitchell, G.P., Mirkin, C.A., Letsinger, R.L., 1999. Programmed assembly of DNA functionalized quantum dots. J. Am. Chem. Soc. 121(35), 8122-8123.

Montón, H., Nogués, C., Rossinyol, E., Castell, O., Roldán, M., 2009. QDs versus Alexa: reality of promising tools for immunocytochemistry. Journal of Nanobiotechnology 7 (4), 1-10.

Murphy, C. J. and Coffer, J. L., 2002. Quantum Dots: A Primer. Applied Spectroscopy 56 (1), 16A-27A.

Murray, C. B., Kagan, C. R., Bawendi, M. G., 2000. Synthesis and characterization of monodisperse nanocrystals and close-packed nanocrystal assemblies. Annu. Rev. Mater. Sci. 30, 545–610.

Murray, C. B., Norris, D. J., Bawendi, M. G., 1993. Synthesis and characterization of nearly monodisperse CdE (E = sulfur, selenium, tellurium) semiconductor nanocrystallites. Am. Chem. Soc. 115 (19), 8706–8715.

N

Nirmal, M., Norris, D.J., Kuno, M., Bawendi, M.G., Efros, A.L., Rosen, M., 1995. Observation of the "Dark exciton" in CdSe quantum dots. Phys. Rev. Lett. 75, 3728-3731.

P

Palaniappan, K., Hackney, S.A., Liu, J., 2004. Supramolecular control of complexation-induced fluorescence change of water-soluble, β-cyclodextrin-modified CdS quantum dots. Chem. Commun., 23, 2704-2705.

Pathak, S., Choi, S.-K., Arnheim, N., Thompson, M.E., 2001. Hydroxylated quantum dots as luminescent probes for in situ hybridization. J. Am. Chem. Soc. 123(17), 4103-4104

Peraica, M., Radic, B., Lucic, A., Pavlovic, M., 1999. Toxic effects of mycotoxins in humans. Bull World Health Organ. 77(9), 754–766.

Petryayeva, E., Algar, W.R., Medintz, I.L., 2013. Quantum dots in bioanalysis: a review of applications across various platforms for fluorescence spectroscopy and imaging. Appl Spectrosc. 67(3), 215-252.

Pichaandi, J., Abel, K.A., Johnson, N.J.J., Van Veggel, F.C.J.M., 2013. Long-Term Colloidal Stability and Photoluminescence Retention of Lead-Based Quantum Dots in Saline Buffers and Biological Media through Surface Modification. Chemistry of Materials 25, 2035-2044.

Protiere, M., Reiss, P., 2006. Facile synthesis of monodisperse ZnS capped CdS nanocrystals exhibiting efficient blue emission. Nanoscale Res. Lett. 1, 62–67.

Q

Qhobosheane, M., Santra, S., Zhang, P., Tan, W., 2001. Biochemically functionalized silica nanoparticles. Analyst 126, 1274–1278.

Qu, L., Peng, Z.A., Peng, X., 2001. Alternative Routes toward High Quality CdSe Nanocrystals. Nano Letters 1 (6), 333–337.

Querner, C., Reiss, P., Bleuse, J., Pron, A., 2004. Chelating ligands for nanocrystals' surface functionalization. J. Am. Chem. Soc. 126(37), 11574-11582.

R

Reiss, P., Protière, M., Li, L., 2009. Core/Shell Semiconductor Nanocrystals. Small 5(2), 154-168.

Ren, M., Xu, H., Huang, X., Kuang, M., Xiong, Y., Xu, H., Xu, Y., Chen, H., Wang, A., 2014. Immunochromatographic assay for ultrasensitive detection of aflatoxin b1 in maize by highly luminescent quantum dot beads. ACS Appl. Mater. Interfaces 6, 2011−2017.

Resch-Genger, U., Grabolle, M., Cavaliere-Jaricot, S., Nitschke, R., Nann, T., 2008. Quantum dots versus organic dyes as fluorescent labels. Nature Methods 5, 763 – 775.

Rosenthal, S.J., Chang, J.C., Kovtun, O., McBride, J.R., Tomlinson, I.D., 2011. Biocompatible Quantum Dots for Biological Applications. Chem. Biol. 18(1), 10-24.

Ruedas-Rama, M. J., Walters, J. D., Orte, A., Hall, E. H., 2012. Fluorescent nanoparticles for intracellular sensing: a review. Analytica Chimica Acta 751, 1-23.

Sanders, M., Guo, Y., Iyer, A., García, R.Y., Galvita, A., Heyerick, A., Deforce, D., Risseeuw, M.D.P., Van Calenbergh, S., Bracke, M., Eremin, S., Madder, A., De Saeger, S., 2014. An immunogen synthesis strategy for the development of specific anti-deoxynivalenol monoclonal antibodies. Food additives and contaminants part A-chemistry analysis control exposure & risk assessment 31 (10), 1751–1759.

Schneider, L., Pichler, H., Krska, R., 2000. An enzyme linked immunoassay for the determination of deoxynivalenol in wheat based on chicken egg yolk antibodies. Fresenius J Anal Chem 367, 98–100.

Smith, A.M., Nie, S., 2008. Minimizing the Hydrodynamic Size of Quantum Dots with Multifunctional Multidentate Polymer Ligands. J. Am. Chem. Soc. 130, 11278–11279.

Smith, W.E., Brownell, J., White, C.C., Afsharineja, Z., Tsai, J., Hu, X., Polyak, S.J., Gao, X., Kavanagh, T.J., Eaton, D.L., 2012. *In vitro* toxicity assessment of amphiphillic polymer-coated CdSe/ZnS quantum dots in two human liver cell models. ACS Nano 6(11), 9475-9484.

Sobrova, P., Adam, V., Vasatkova, A., Beklova, M., Zeman, L., Kizek, R., 2010. Deoxynivalenol and its toxicity. Interdisc Toxicol. 3(3), 94–99.

Speranskaya, E.S., Beloglazova, N.V., Abé, S., Aubert, T., Smet, P.F., Poelman, D., Goryacheva, I.Yu., De Saeger, S., Hens, Z., 2014. Hydrophilic, bright $CuInS_2$ quantum dots as Cd-free fluorescent labels in quantitative immunoassay. Langmuir 30, 7567–7575.

Speranskaya, E.S., Beloglazova, N.V., Lenain, P., De Saeger, S., Wang, Zh., Zhang, S., Hens, Z., Knopp, D., Niessner, R., Potapkin, D.V., Goryacheva, I.Yu., 2014. Polymer-coated fluorescent CdSe-based quantum dots for application in immunoassay. Biosensors and Bioelectronics 53, 225–231.

Srinivasan, C., Lee, J., Papadimitrakopoulos, F., Silbart, L.K., Zhao, M., Burgess, D.J., 2006. Labeling and Intracellular Tracking of Functionally Active Plasmid DNA with Semiconductor Quantum Dots. Molecular Therapy 14, 192–201.

Subila, K. B., Kishore Kumar, G., Shivaprasad, S.M., George Thomas, K., 2013. Luminescence Properties of CdSe Quantum Dots: Role of Crystal Structure and Surface Composition. J. Phys. Chem. Lett. 4, 2774−2779.

Sukhanova, A., Venteo, L., Devy, J., Artemyev, M., Oleinikov, V., Pluot, M., Nabiev, J., 2002. Highly stable fluorescent nanocrystals as a novel class of labels for immunohistochemical analysis of paraffin-embedded tissue sections. Lab Invest. 82(9), 1259-1261.

Sukhorukov, G.B., Donath, E., Lichtenfeld, H., Knippel, H., Knippel, M., Budde, A.,1998. Layer-by-layer self-assembly of polyelectrolytes on colloidal particles. Colloids Surf. A 137, 253–266.

Suzuki, Y., 2012. Exploring transduction mechanisms of protein transduction domains (PTDs) in living cells utilizing single-quantum dot tracking (SQT) technology. Sensors 12, 549-572.

T

Talapin, D.V., Mekis, I., Götzinger , S., Kornowski, A., Benson, O., Weller, H., 2004. CdSe/CdS/ZnS and CdSe/ZnSe/ZnS Core−Shell−Shell Nanocrystals. J. Phys. Chem. B 108 (49), 18826–18831.

Talapin, D.V., Rogach, A.L., Kornowski, A., Haase, M., Weller., H., 2001. Highly luminescent monodisperse CdSe and CdSe/ZnS nanocrystals synthesized in a hexadecylamine−trioctylphosphine oxide−trioctylphospine mixture. Nano Letters 1 (4), 207–211.

Turner, N.V., Bramhmbhatt, H., Szabo-Vezse, M., Poma, A., Coker, R., Piletsky, S.A., 2015. Analytical methods for determination of mycotoxins: An update (2009–2014). Analytica Chimica Acta 901, 12-33.

V

Valizadeh, A., Mikaeili, H., Samiei, M., Farkhani, S.M., Zarghami, N., Kouhi, M., Akbarzadeh, A., Davaran, S., 2012. Quantum dots: synthesis, bioapplications, and toxicity. Nanoscale Research Letters 7, 480-494.

Velappan N., Clements J., C. Kiss, Valero-Aracama R., Pavlik P., Bradbury A.R.M., 2008. Fluorescence linked immunosorbant assays using microtiter plates Journal of Immunological Methods 336 (2), 135–141.

Vibin, M., Vinayakan, R., John, A., Raji, V., Rejiya, C.S., Vinesh, N.S., Abraham, A., 2011. Cytotoxicity and fluorescence studies of silica-coated CdSe quantum dots for bioimaging applications. J. Nanopart. Res. 13 (6), 2587-2596.

Vu, T. Q., Lam, W. Y., Hatch, E. W., Lidke, D. S., 2015. Quantum dots for quantitative imaging: from single molecules to tissue. Cell Tissue Research 360, 71–86.

W

Wang, B., Wang, Q., Cai, Z., Ma, M., 2015. Simultaneous, rapid and sensitive detection of three food-borne pathogenic bacteria using multicolor quantum dot probes based on multiplex fluoroimmunoassay in food samples. LWT-Food Science and Technology 61, 368-376.

Wang, D., Qian, J., Cai, F., He, S., Han, S., Mu, Y., 2012. 'Green'-synthesized near-infrared PbS quantum dots with silica–PEG dual-layer coating: ultrastable and biocompatible optical probes for *in vivo* animal imaging. Nanotechnology 23, 245701.

Wang, J., Shah, Z.H., Zhang, S., Lu, R., 2014. Silica-based nanocomposites via reverse microemulsions: classifications, preparations, and applications. Nanoscale 6, 4418-4437.

Wang, J., Xu, J., Goodman, M.D., Chen, Y.,Cai, M., Shinar, J., Lin, Z., 2008. A simple biphasic route to water soluble dithiocarbamate functionalized quantum dots. J. Mater. Chem. 18(27), 3270-3274.

Wang, L., Chen, W., Ma, W., Liu, L., Ma, W., Zhao, Y., Zhu, Y., Xu, L., Kuang, H., Xu, C., 2011. Fluorescent strip sensor for rapid determination of toxins. Chem. Commun. 47, 1574–1576

Wang, S., Li, C., Yang, P., Ando, M., Murase, N., 2012. Silica encapsulation of highly luminescent hydrophobic quantum dots by two-step microemulsion method. Colloids and Surfaces A: Physicochem. Eng. Aspects 395, 24– 31.

Wang, X., Niessner, R., Knopp, D., 2010. Magnetic bead-based fluorescence immunoassay for aflatoxin B1 in food using biofunctionalized rhodamine B-doped silica nanoparticles. Analyst 135, 2661–2667.

Wang, Y., Hu, R., Lin, G., Roy, I., Yong, K.-T., 2013. Functionalized Quantum Dots for Biosensing and Bioimaging and Concerns on Toxicity. ACS Appl. Mater. Interfaces 5, 2786–2799.

Wang, Z., Li, H., Li, C.,Yu, Q., Shen, J., De Saeger, S., 2013. Development and application of a quantitative fluorescence-based immunochromatographic assay for fumonisin B1 in maize. Anal. Bioanal. Chem. 405, 7795–7802.

Washington, A.L., Foley, M.E., Cheong, S., Quffa, L., Breshike, C.J., Watt, J., Tilley, R.D., Strouse, G.F., 2012. Ostwald's Rule of Stages and Its Role in CdSe Quantum Dot Crystallization. J. Am. Chem. Soc. 134 (41), 17046–17052

Wolcott, A., Gerion, D., Visconte, M.,Sun, J., Schwartzberg, A., Chen, S., Zhang, J.Z., 2006. Silica-coated CdTe quantum dots functionalized with thiols for bioconjugation to IgG proteins. J. Phys. Chem. B 110 (11), 5779-5789.

Wu, S.H., Mou, C.Y., Lin, H.P., 2013. Synthesis of mesoporous silica nanoparticles. Chem. Soc. Rev. 42, 3862-3875.

Wu, X., Liu, H., Liu, J., Haley, K.N., Treadway, J.A., Larson, J.P., Ge, N., Peale, F., Bruchez, M.P., 2002. Immunofluorescent labeling of cancer marker Her2 and other cellular targets with semiconductor quantum dots. Nature Biotechnology 21, 41 – 46.

X

Xia, H.-X., Yang, X.-Q., Song, J.-T., Chen, J., Zhang, M.-Z., Yan, D.-M., Zhang, L., Qin, M.-Y., Bai, L.-Y., Zhao, Y.-D., Ma, Z.-Y., 2014. Folic acid-conjugated silica-coated gold nanorods and quantum dots for dual-modality CT and fluorescence imaging and photothermal therapy. J. Mater. Chem. 2, 1945-1953.

Xiang, Y., Zhang, H., Jiang, B., Chai, Y., Yuan, R., 2011. Quantum dot layer-by-layer assemblies as signal amplification labels for ultrasensitive electronic detection of uropathogens. Anal. Chem. 83, 4302–4306.

Xie, R., Kolb, U., Li, J., Basché, T., Mews, A., 2005. Synthesis and Characterization of Highly Luminescent CdSe–Core CdS/Zn0.5Cd0.5S/ZnS Multishell Nanocrystals. J. Am. Chem. Soc. 127 (20), 7480–7488.

Xu, W., Xiong, Y., Lai, W., Xu, Y., Li, C., Xie, M., 2014. A homogeneous immunosensor for AFB1 detection based on FRET between different-sized quantum dots. Biosensors and Bioelectronics 56, 144–150.

Y

Ye, L., Yong, K.-T., Liu, L., Roy, I., Hu, R., Zhu, J., Cai, H., Law, W.-C., Liu, J., Wang, K., Liu, J., Liu, Y., Hu, Y., Zhang, X., Swihart, M.T., Prasad, P.N., 2012. A pilot study in non-human primates shows no adverse response to intravenous injection of quantum dots. Nature Nanotechnology 7, 453–458.

Yong, K.-T., Law, W.-C., Hu, R., Ye, L., Liu, L., Swiharte, M. T., Prasad, P. N., 2013. Nanotoxicity assessment of quantum dots: from cellular to primate studies. Chem. Soc. Rev. 42, 1236-1250.

Yu, W.W., Chang, E., Falkner, J.C., Zhang, J., Al-Somali, A.M., Sayes, C.M., Johns, J., Drezek, R., Colvin, V.L., 2007. Forming biocompatible and nonaggregated nanocrystals in water using amphiphilic polymers. J. Am. Chem. Soc. 129 (10), 2871–2879.

Z

Zekavati, R., Safi, S., Jamal Hashemi, S., Rahmani-Cherati, T., Tabatabaei, M., Mohsenifar, A., Bayat, M., 2013. Highly sensitive FRET-based fluorescence immunoassay for aflatoxin B1 using cadmium telluride quantum dots. Microchim. Acta 180, 1217–1223.

Zeng, W.-J., Peng, C.-W., Yuan, J.-P., Cui, R., Li, Y., 2015. Quantum dot-based multiplexed imaging in malignant ascites: a new model for malignant ascites classification. International Journal of Nanomedicine 10, 1759–1768.

Zeng, X., Gao, H., Pan, D., Sun, Y., Cao, J., Wu, Z., Pan, Z., 2015. Highly sensitive electrochemical determination of Alfatoxin B1 using quantum dots-assembled amplification labels. Sensors 15, 20648-20658.

Zeng, Y., Tang, C., Wang, H., Jiang, J., Tian, M., Shen, G., Yu, R., 2008. A novel density-tunable nanocomposites of CdTe quantum dots linked to dendrimer-tethered multi-wall carbon nanotubes. Spectrochim. Acta [A.] 70, 966–972.

Zhang, B., Gong, X., Hao, L., Cheng, J., Han, Y., Chang, J., 2008. A novel method to enhance quantum yield of silica-coated quantum dots for biodetection. Nanotechnology 19(46), 465604-465612.

Zhang, B., Tang, D., Goryacheva, I.Yu., Niessner, R., Knopp, D., 2013. Anodic-stripping voltammetric immunoassay for ultrasensitive detection of low-abundance proteins using quantum dot aggregated hollow microspheres. Chem. Eur. J. 19, 2496–2503.

Zhang, L.W., Bäumer, W., Monteiro-Riviere, N.A., 2011. Cellular uptake mechanisms and toxicity of quantum dots in dendritic cells. Nanomedicine 6(5), 777-791.

Zhang, Y., 2011. Surface functionalization of quantum dots for biotechnological applications. Dissertation, Iowa State University.

Zhang, Y., So, M. K., Rao, J., 2006. Protease-Modulated Cellular Uptake of Quantum Dots. Nano Lett. 6, 1988–1992.

Zhang, Y-W., Tiwari, M. K., Jeya, M., Lee, J-K., 2011. Covalent immobilization of recombinant Rhizobium etli CFN42 xylitol dehydrogenase onto modified silica nanoparticles. Appl. Microbiol. Biotechnol. 90, 499–507.

Zhang, Z., Li, Y., Li, P., Zhang, Q., Zhang, W., Hu, X.,Ding, X., 2014. Monoclonal antibody-quantum dots CdTe conjugate-based fluoroimmunoassay for the determination of aflatoxin B1 in peanuts. Food Chem. 146, 314–319.

Zrazhevskiy, P., Sena, M., Gao, X., 2010. Designing multifunctional quantum dots for bioimaging, detection, and drug delivery. Chem. Soc. Rev. 39, 4326-4354.

SUMMARY

SUMMARY

Quantum dots (QDs) are semiconductor nanocrystals with unique optical properties, which nowadays are of great significance as photoluminescence (PL) labels in diverse biomedical applications. Thereby, Part 1 provides the necessary theoretical background on QDs in context of development of sensitive PL labels for mycotoxin detection and food quality control. In Chapter 1, basic introductory information on QDs synthesis and optical properties is given. A survey of hydrophilization techniques is outlined in Chapter 2, including synthesis of biocompatible enhanced labels. This dissertation is entitled "Quantum dots as PL labels for mycotoxin detection", thus a review on the application of QDs in immunoassays for mycotoxin detection is presented in Chapter 3.

Part 2 is devoted to experimental work, which was done in order to synthesize, characterize and apply the PL QD-based label for immunoassay to determine mycotoxins. In this regard, two well-known approaches for making QDs biocompatible have been involved: (i) ligand exchange, i.e. the substitution of native hydrophobic ligands for hydrophilic ones, i.e. silica precursors; and (ii) covering with amphiphilic molecules, i.e. amphiphlic polymers.

Silanization of QDs was performed by leveraging the microemulsion method, which implies ligand exchange with silane molecules, such as TEOS, to form nucleation sites on the QD surface, and followed by a condensation step yielding formation of the silica shell (Chapter 4). It was shown that silanization is a convenient route towards the synthesis of water-soluble, stable, bright QD-based labels with different emission colors, yielding a promising outlook for multiplex analysis (Chapter 5).

Covering with amphiphilic molecules was performed by employing a synthesized co-polymer of PMAO and Jeffamine polymers (Chapter 6). QDs with 3 different emission colors were covered with amphiphilic polymer without loss of brightness. Pertinent variation of the Jeffamine polymer structure allowed choosing the appropriate functional group on the QDs' surface.

To assess the stability of the synthesized PL biolabels, their optical properties were investigated under adverse conditions. For instance, polymer coated QDs were freeze dried in order to obtain PL nanopowders that are easy to dissolve in any desirable concentration.

Moreover, the influence of low-strength electric field (EF) on amphiphilic polymer-coated and silica-covered CdSe-based QDs was investigated (Chapter 7). It was shown that the hydrophilic shell affects the PL properties of the QDs under a low-strength EF.

Consequently, two types of QD-based biolabels were synthesized and characterized in order to obtain sensitive PL labels for immunoassay analysis. Silica-coated QDs, modified with diverse functional groups were efficiently conjugated with antibodies, using different activation and bioconjugation reactions. The synthesized QD conjugate was successfully applied as a novel label in a microtiter plate based immunoassay and a quantitative column-based rapid immunotest for DON detection.

Polymer coated QDs were applied as PL biolabels in fluorescent labelled immunosorbent assay (FLISA) format for detection of mycotoxin deoxynivalenol. Naturally contaminated samples of wheat and maize were analyzed using the developed method and the results considerably correlate with liquid chromatography-tandem mass spectrometry (LC/MS-MS) analysis.

Part 3 summarizes the work by providing a general discussion and conclusions, and it also extends the possibilities for future research and broadens its international context.

SAMENVATTING

SAMENVATTING

Quantum dots (QDs) zijn halfgeleider nanokristallen met unieke optische eigenschappen, die een zeer belangrijke rol spelen als fotoluminescent label in een waaier van biomedische toepassingen. Deel 1 geeft de theoretische achtergrond aangaande het ontwikkelen van gevoelige fotoluminescente labels voor de detectie van mycotoxines en kwaliteitscontrole in de voedingssector. In Hoofdstuk 1 wordt een inleiding gegeven omtrent de QD synthese en hun optische eigenschappen. Een overzicht van de bestaande hydrofilisatie technieken wordt beschreven in Hoofdstuk 2, waaronder de synthese van biocompatibele labels. Dit doctoraatsproefschrift is getiteld "Quantum dots as photoluminescent labels for mycotoxin detection", waarbij ook een overzicht gegeven wordt over de applicatie van QDs in immunoassays voor mycotoxine detectie (Hoofdstuk 3).

Deel 2 omvat het experimentele werk dat gedaan werd om de fotoluminescente QD labels te synthetiseren, karakteriseren en vervolgens te gebruiken voor de ontwikkeling van een immunoassay voor de detectie van mycotoxines. Om de QDs biocompatibel te maken werden twee welgekende technieken gebruikt: (i) ligand uitwisseling, waarbij de oorspronkelijke liganden vervangen worden door hydrofiele silica precursoren, en (ii) coaten met amfifiele moleculen nl. amfifiele polymeren.

Silaneren van de QDs werd uitgevoerd d.m.v. de micro-emulsie methode. Hierbij vindt er ligand uitwisseling met silaan moleculen, zoals TEOS, plaats. Dit geeft aanleiding tot nucleatie plaatsen op het oppervlak van de QDs, wat na een condensatie stap resulteert in een silica coating (Hoofdstuk 4). Het is aangetoond dat silaneren een geschikte methode is voor de synthese van wateroplosbare, stabiele en heldere QD gebaseerde labels die verschillende kleuren kunnen emitteren. Dit laatste is veelbelovend voor multiplex analyse (Hoofstuk 5).

Het coaten met amfifiele moleculen werd uitgevoerd door gebruik te maken van het gesynthetiseerde copolymeer PMOA en Jeffamine polymeren (Hoofdstuk 6). QDs die 3 verschillende kleuren emitteren werden gecoat met amfifiel polymeer zonder verlies van helderheid. Variatie in de structuur van Jeffamine liet toe de geschikte functionele groep op het QD oppervlak te incorporeren.

Om de stabiliteit van de gesynthetiseerde fotoluminescente labels na te gaan, werden hun optische eigenschappen onderzocht door hun bloot te stellen aan nadelige condities. Zo

werden polymer gecoate QDs gevriesdroogd om fotoluminescente nanopoeders te bekomen, die makkelijk in een gewenste concentratie op te lossen zijn.

Verder werd de invloed van een laag elektrische veldsterkte op de polymeer -en silica gecoate CdSe QDs onderzocht (Hoofdstuk 7). Hierbij werd aangetoond dat de hydrofiele coating de fotoluminescente eigenschappen van de QDs onder invloed van een lage veldsterkte beïnvloed.

Bijgevolg werden twee types QD gebaseerde biolabels gesynthetiseerd en gekarakteriseerd om zo'n gevoelig mogelijke fotoluminescente labels te bekomen voor immunoassay analyse. Silica gecoate QDs, die gemodificeerd werden met verschillende functionele groepen werden efficiënt geconjugeerd met antilichamen d. m. v. verschillende activatie en bioconjugatie strategieën. Het gesynthetiseerde QD conjugaat werd succesvol gebruikt als label in een microplaat gebaseerde immunoassay en een kwantitatieve kolom gebaseerde immunotest voor de detectie van deoxynivalenol (DON).

Polymeer gecoate QDs werden gebruikt als fotoluminescent biolabel in een 'fluorescent labelled immunosorbent assay' (FLISA) voor de detectie van het mycotoxine DON. Natuurlijk gecontamineerde tarwe en maïs stalen werden geanalyseerd door de ontwikkelde FLISA-methode en de resultaten vertoonden een goede correlatie met de resultaten verkregen via 'liquid chromatography tandem mass spectrometry' (LC/MS-MS) analyse.

Deel 3 is een samenvatting van het werk, samen met een algemene discussie en conclusie. Verder wordt dieper ingegaan op de toekomst -en bredere internationale perspectieven van het werk.

ABOUT THE AUTHOR

ABOUT THE AUTHOR

Valentina Goftman was born in Saratov (Russian Federation) on July 16th, 1989. In September 2006, her university education was started at Saratov State University (SSU) and in 2010 she graduated as a Bachelor in Chemistry, followed by a Master degree in Chemistry (diploma with only excellent marks; GPA 5 out of 5) in 2012. Her master's thesis "Synthesis and optical properties of quantum dots based on CdSe" was supervised by prof. Irina Yu. Goryacheva. Shortly after obtaining her Master degree, she was admitted to the Doctoral Program in Analytical chemistry in SSU. In parallel, a Joint PhD project in collaboration with prof. Sarah De Saeger (Laboratory of Food Analysis, Faculty of Pharmaceutical Sciences, Ghent University) was successfully submitted and fully supported by the Special Research Fund, Ghent University (Joint PhD programme) project №01SF3012, giving to Valentina the opportunity to work in both Universities. Results of her research were published in a number of peer reviewed scientific journals and were presented during several national and international conferences.

A1 PEER-REVIEWED PUBLICATIONS

1. V.V. Goftman, T. Aubert, D. Vande Ginste, R. Van Deun, N.V. Beloglazova, Z. Hens, S. De Saeger, I.Yu. Goryacheva. **"Synthesis, modification, bioconjugation of silica coated fluorescent quantum dots and their application for mycotoxin detection"**, *Biosensors and Bioelectronics*, *2016, 79, 476–481.*

2. V.V.Goftman, V.A. Pankratov, A.V. Markin, D. Vande Ginste, S. De Saeger, I.Yu. Goryacheva. **"Hydrophilic quantum dots stability against an external low-strength electric field"**, *Applied Surface Science, 2016, 363, 259–263.*

3. F. Di Nardo , L. Anfossi, C. Giovannoli, C. Passini, V.V. Goftman, I.Y. Goryacheva, C. Baggiani **"A fluorescent immunochromatographic strip test using Quantum Dots for fumonisins detection"**, *Talanta 2016, 150, 463–468.*

4. I.Yu. Goryacheva, E.S. Speranskaya, V.V. Goftman, D. Tang, S. De Saeger "**Synthesis and bioanalytical applications of nanostructures multiloaded with quantum dots**", *Trends in Analytical Chemistry 2015, 66, 53–62.*

5. N.V. Beloglazova, E.S. Speranskaya, A. Wu, Z. Wang, M. Sanders, V.V. Goftman, D. Zhang, I.Yu. Goryacheva, S. De Saeger. **"Novel multiplex fluorescent immunoassays based on quantum dot nanolabels for mycotoxins determination***", Biosensors and Bioelectronics 2014, 12 (62), 59-65.*

6. V.V. Goftman, N.V. Beloglazova, E. Njumbe Ediage, S. De Saeger, R. Dietrich, E. Märtlbauer, I.Yu. Goryacheva. **"Tests for qualitative and quantitative determination of T-2 and HT-2 toxins"**, *Analytical methods 2012, 4, 4244 - 4249.*

PUBLICATIONS IN PROCEEDINGS OF INTERNATIOINAL CONFERENCES

1. Valentina V. Goftman, Anna V. Gaynbuch, Elizaveta V. Panfilova, Boris N. Khlebtsov, Irina Yu. Goryacheva "Freeze-dried polymer-coated quantum dots for perspective biomedical application"/ SPIE Proceeding 2015, V. 9448, №9.

2. Valentina V. Goftman, Alexey V. Markin, Sarah De Saeger, Irina Yu. Goryacheva "Multicolored silica coated CdSe core/shell quantum dots" SPIE Proceeding 2016, V. 9917, №16.

3. Alexander A. Skaptsov , Valentina V. Goftman , Viktor V. Galushka , Alexey V. Markin, Vyacheslav I. Kochubey, Irina Yu. Goryacheva "Thermosensitivity of nanothermometer: CdSe/ZnS vs. $CuInS_2$/ZnS" SPIE Proceeding 2016, V. 9917, №12.

4. Anastasya S. Novikova, Valentina V. Goftman, Irina Yu. Goryacheva "Synthesis of cadmium-free quantum dots based on $CuInS_2$ nanocrystals" SPIE Proceeding 2016, V. 9917, №14.

ORAL PRESENTATIONS

1. XVII International Conference on Quantum Dots, 10-11 December 2015, London, Great Britain. Valentina V. Goftman, Vladislav A. Pankratov, Alexey V. Markin, Tangi Aubert, Zeger Hens, Sarah De Saeger, Irina Yu. Goryacheva **"Impact of Electric Field on the Optical Properties of Hydrophilic Quantum Dots".**

2. Saratov Fall Meeting: International Symposium on Optics & Biophotonics, 23-26 September 2014, Saratov, Russia. Valentina V. Goftman, Anna V. Tretiakova, Sarah De Saeger, Irina Yu. Goryacheva **"Silica-coated CdSe based quantum dots with high buffer stability"**.

3. Vth International workshop on "Nanoparticles, nanostructured coatings and microcontainers: technology, properties, applications" 9-12 May 2014, Ghent, Belgium. Valentina V. Goftman, Irina Yu. Goryacheva **"Synthesis of silica-coated core-shell quantum dots".**

4. Saratov Fall Meeting: International Symposium on Optics & Biophotonics, 25-28 September 2013, Saratov, Russia. Valentina V. Goftman, Irina Yu. Goryacheva **"Synthesis of SiO_2-coated CdSe/CdS/ZnS quantum dots nanohybrids"**.

POSTER PRESENTATIONS

1. Biosensors 2016: 26th Anniversary World Congress on Biosensors, 25-27 May 2016, Gothenburg, Sweden. Valentina V. Goftman, Irina Yu. Goryacheva, Sarah De Saeger "**Quantum dot-based luminescent nanobiolabels: synthesis and bioapplication"**

2. 5th International Symposium on Mycotoxins and Toxigenic Moulds: Challenges and Perspectives, Ghent, Belgium 11 May 2016. Valentina V. Goftman, Irina Yu. Goryacheva, Sarah De Saeger **"Development of immunochemical test for mycotoxin detection using luminescent nanobiolabel".**

3. 35th Mycotoxin Workshop, 22-24 May 2013, Gent, Belgium**.** Valentina V. Goftman, Elena S. Speranskaya, Sarah De Saeger, Zeger Hens, Irina Yu. Goryacheva

"Synthesis of multicolored labels based on CdSe quantum dots for immunochemical mycotoxin detection".

4. International congress "Biotechnology: State of the Art and Prospects of Development", 19-22 March, 2013, Moscow, Russia. Valentina V. Goftman, Elena S. Speranskaya, Irina Yu. Goryacheva **"Hydrophilization of Quantum Dots and their application as biolabels".** Poster was awarded a medal on the Young Researcher's Contest.

FOLLOWED COURCES

Advanced Academic English writing skills (2016) at University Language Center, Ghent University, Belgium

Translational Biomedical *In Vivo* Imaging (2015) at Ghent University, Belgium

Advanced Academic English: Conference Skills (Presentation Skills in English) (2015) at University Language Center, Ghent University, Belgium

18th International School for Junior Scientists and Students on Optics, Laser Physics & Biophotonics September 22 – 26, 2014 Saratov, Russia

17th International School for Junior Scientists and Students on Optics, Laser Physics & Biophotonics September 24 – 27, 2013 Saratov, Russia

TUTORSHIP STUDENT'S THESIS

Tretiakova Anna (2014) "**Silanization as one of approaches to quantum dots hydrophilization"**, Chemistry Institute, Saratov State University, Russia.

Vostrikova Anna (2014) "**Hydroplilization of quantum dots by using amphiphilic polymers and organosilanes**", Chemistry Institute, Saratov State University, Russia.

Pankratov Vlad (2015) "**Stability of quantum dots against an external electric field"**, Chemistry Institute, Saratov State University, Russia.

LIST OF FIGURES

LIST OF FIGURES

Figure 1.1. A simplified energy level diagram for metals, semiconductors and insulators (Murphy and Coffer, 2002). **11**

Figure 1.2. Absorption spectrum of CdSe quantum dots (Breus 2008). **12**

Figure 1.3. Dependence of emission maxima on the material and size of QDs (Michalet et al., 2005). **14**

Figure 1.4. Photostability profile of PL intensity changes of QDs conjugates under laser radiation (Monton et al., 2009; Srinivasan et al., 2006) **15**

Figure 1.5. Two possible core-shell structures of CdSe-based quantum dots. Reprinted from (Petryayeva et al., 2013) **16**

Figure 1.6. The stages of nucleation and growth for the preparation of monodisperse (Murray et al., 2000). **18**

Figure 1.7. Schematic representation of the elemental distribution in zincblende and wurtzite CdSe QDs (Subila et al., 2013). **19**

Figure 1.8. The most frequently used coordinating ligands for CdSe core synthesis **20**

Figure 2.1. Routes for water-solubilization of hydrophobic QDs. (Zrazhevskiy et al., 2010) **24**

Figure 2.2. Ligand exchange between dodecylamine and 3-mercaptopropionic acid (Baker and Kamat, 2010). **25**

Figure 2.3. QDs in LBL technology for drug delivery **30**

Figure 2.4. Basic structure of dendrimers **31**

Figure 2.5. Preparation scheme of multi-label dendrimer-covered quantum dots (QDs). **32**

Figure 3.1. Structures of common mycotoxins **36**

Figure 3.2. Comparing chromatographic-based and immunochemical-based methods for mycotoxin detection (Anfossi et al., 2016). **37**

Figure 4.1. Reverse microemulsion synthesis of silica coatedQDs (QD@SiO_2) **49**

Figure 4.2. Characteristics of the synthesized CdSe/2CdS/2CdZnS/2ZnS QDs **50**

Figure 4.3. TEM images of the obtained QDs covered with silica shell **52**

Figure 4.4. Gel electrophoresis of the obtained QD@SiO_2-PEG nanoparticles and their conjugates with IgG. **53**

Figure 4.5. pH stability comparison of the synthesized QD@SiO_2-NH_2 and QD@SiO_2-PEG-NH_2. **55**

Figure 5.1. Emission spectra of the synthesized CdSe-based QDs **59**

Figure 5.2. Emission spectra of CdSe cores with a varying number of CdS and ZnS shells **62**

Figure 6.1. Structures of polymers, used for the QDs hydrophilization **68**

Figure 6.2. Emission spectra of polymer coated water-soluble QDs with different structures **69**

Figure 7.1. Scheme of the QDs hydrophilization techniques **74**

Figure 7.2. Scheme of the high-temperature colloid quantum dots' synthesis. **75**

Figure 7.3. Voltage-time and current-time curves as applied to the universal dip cell's palladium electrodes to carry out one EF treatment cycle onto the QD aqueous solutions (Zetasizer Nano data). **77**

Figure 7.4. TEM images of the synthesized QDs **78**

Figure 7.5. Changes in the fluorescent intensity of hydrophilic QDs as a function of the number of EF treatment cycles. **79**

Figure 8.1. Chemical structure of DON **83**

Figure 8.2. Calibration curves for the DON determination by the developed frit-based immunoassay and FLISA. **88**

Figure 8.3. Test column for immunoassay **88**

Figure 8.4. Linear regression using FLISA data for the DON screening in artificially spiked wheat and maize samples (data indicate averages of fivefold determinations). **89**

Figure 8.5. Linear regression equations derived using FLISA and LC–MS/MS data for DON screening in naturally-contaminated cereal samples **90**

LIST OF TABLES

LIST OF TABLES

Table 1.1. Crystalline structure constants of a series of semiconductors **21**

Table 3.1. Existing immunofluorescent methods for mycotoxin detection **40**

Table 4.1. QYs of synthesized QD@SiO_2 NPs in comparison to the QY of initially uncovered hydrophobic QDs **51**

Table 4.2. ζ-potential measurements in water solutions of QD@SiO_2 and modified with the indicated precursors **52**

Table 5.1. Relative QY and emission maxima of the synthesized core and core-shell structures **61**

Table 5.2. QYs of the synthesized QDs with different amount of shells, before and after silanization. **63**

Table 6.1. Relative brightness of the QDs, covered with different PEG-polymers, and those, redispersed after freeze-drying. **70**

Table 6.2. Zeta-potentials of the QDs, covered with different PEG-polymers, and those, redispersed after freeze-drying. **70**

Table 6.3. Hydrodynamic radii of QDs covered with PMAO-Jeffamine M1000 and redispersed from the powders after two consecutive freeze-dryings, measured by dynamic light scattering method **71**

Table 8.1. Current maximum limits for DON in food according to 1881/2006/EC and feed according to 2006/576/EC **87**

Table 9.1. Quantum Yields of QDs with different structures after covering with PMAO-Jeffamine M1000 co-polymer and silica shell **96**